ON THE SPECTRA OF CERTAIN DIATOMIC HYDRIDE AND DEUTERIDE MOLECULES

- by -

Frank Lawrence Whittaker, B.Sc., A.R.C.S.

A thesis submitted for the
degree of Doctor of Philosophy in the
University of London

----oOo----

November 1967

Physics Department,
Imperial College of Science and Technology,
London, S.W.7.

ABSTRACT

A heavy-current positive-column discharge through helium containing traces of nitrogen and hydrogen (or deuterium) gives intense emission spectra of NH, ND, NH^+ and ND^+. Rotational analyses have been made of thirty bands in the regions 2450-3020Å and 4300-5590Å from photographs taken in a 21ft. concave grating spectrograph.

In NH^+, Feast's analysis of bands at $\lambda\lambda$ 2886, 2730 has been revised, and new analyses of $^2\Sigma^+ - {}^2\Pi$ bands at $\lambda\lambda$ 2965, 2812, 2683 and 2599, a $^2\Delta - {}^2\Pi$ band at λ 4348, and $^2\Sigma^- - {}^2\Pi$ bands at $\lambda\lambda$ 5348 and 4628 are presented. Similarities to CH are noted, and the molecular states are correlated with those of the united atom and the dissociation products. Morse potential curves have been drawn on the assumption that $D_0^{\circ}(NH^+) = 4.65$ eV. New bands of ND^+ have been found at $\lambda\lambda$ 5096, 4593, 4357($^2\Sigma^- - {}^2\Pi$), 4334($^2\Delta - {}^2\Pi$), 2878, 2817, 2760, 2715 and 2657 ($^2\Sigma^+ - {}^2\Pi$). Perturbations in the $^2\Pi$ state and the predicted spacing of terms derived from the $\sigma\pi^2$ electron configuration provide strong evidence that $^2\Pi_r$ is the ground state of NH^+, being 332 cm^{-1} below a $^4\Sigma^-$ state. The principal constants

of NH^+ (in cm^{-1}) are:

	T_o	ω_e	B_e	A_o
$c^2\Sigma^+$	34538	2162.66	13.2735	
$B^2\Delta$	22912	(2269)	13.5295(B_o)	-3.538
$A^2\Sigma^-$	21544	(1669)	11.461	
$a^4\Sigma^-$	332	2680	14.95	
$X^2\Pi$	0	2988	15.620	78.2

The NH bands at $\lambda\lambda$ 2530, 2683, 2516 ($d^1\Sigma^+ - c^1\Pi$) and λ 4502 ($c^1\Pi - b^1\Sigma^+$) have been observed at high dispersion for the first time, together with a new band at λ 5254. In ND, two new systems have been studied: the (0,0), (0,1), (1,1), (1,2) and (2,2) bands of $d^1\Sigma^+ - c^1\Pi$ and the (0,0) and (0,1) bands of $c^1\Pi - b^1\Sigma^+$.

In general, the band constants agree with the simple isotope theory.

CONTENTS

CHAPTER 1 : INTRODUCTION

1.1 Band Spectra

The molecules whose spectra form the subject of this thesis are the diatomic hydrides and deuterides of nitrogen, namely NH, ND, NH^+ and ND^+ (where the symbol D represents a deuterium atom, ${}_1H^2$). As these are relatively light molecules, with small moments of inertia, it is usually possible to resolve completely the "fine structure" of the bands and so deduce many molecular constants. It will therefore be convenient to summarize the various contributions to the energy of a heteronuclear diatomic molecule, together with the symbols used to characterize the states. The results quoted are in basic agreement both with wave mechanics and with the experimental results for the wide range of diatomic molecules so far studied. The notation used is, unless otherwise stated, the same as that in the book by Herzberg (1950).

1.1.1 Electronic states

For most purposes the energy of a diatomic molecule can be regarded as separable into three parts - the energy of the electrons, the vibrational energy of the nuclei about the equilibrium position and the rotational energy of the nuclei about the centre of gravity of the system:

$$E = E_e + E_v + E_r \qquad (1.1).$$

This expression is usually divided by Planck's constant, h,

and the velocity of light c (in vacuo) so as to give the energy in wave number units, which are usually expressed in waves per cm (or cm^{-1}):

$$T = \frac{E}{hc} = T_e + G(v) + F(J) \qquad (1.2)$$

Each stable molecular state must have a minimum value for its potential energy at some value of the distance, r, between the nuclei. This minimum value is the electronic energy, T_e, and the 'equilibrium' value of r for which it occurs is called r_e. Each electronic state is further characterized by quantum numbers corresponding to the orbital and spin angular momenta found in atoms. The molecule may be regarded as the result either of bringing together two separate atoms or of splitting a large atom into two fragments. In either case a resultant angular momentum $L\acute{h}$ can be found, and this precesses about the inter-nuclear axis under the influence of a strong axial electric field. Only the component $(M_L\acute{h})$ of $L\acute{h}$ in the field direction is a constant of the motion, and M_L can take the values L, L-1, L-2, ___ -L. If the molecular rotation is neglected, terms with equal $|M_L|$ have the same energy, so a molecular quantum number, Λ, is defined by

$$\Lambda = |M_L| \qquad (1.3).$$

The electronic state is called $\Sigma, \Pi, \Delta, \Phi$ according as $\Lambda = 0,1,2,3$.

As in the case of atoms, the spins of the electrons form a resultant represented by a quantum

number S, and the multiplicity, 2S+1, of a state is written as a left superscript to the value of Λ. (Thus $^3\Pi$ represents a state with Λ=1 and S=1). If $\Lambda \neq 0$ there is an internal magnetic field in the direction of the inter-nuclear axis which is often strong enough to make S precess about the field direction with a constant component $M_S\hbar$. For molecules M_S is called Σ, so that Σ has the values S, S-1, S-2, ___ -S.

When both Λ and Σ are defined, the quantum number Ω of the resultant electronic angular momentum about the inter-nuclear axis is given by

$$\Omega = | \Lambda + \Sigma | \qquad (1.4)$$

and the electronic energy of the state is given to a first approximation by

$$T_e = T_o + A\Lambda\Sigma \qquad (1.5)$$

where T_o is the term value when spin is neglected and A is the spin-orbit coupling constant. When A is positive the state is said to be 'normal' or 'regular'; when A is negative the state is 'inverted'. The value of Ω is added as a subscript to the term symbol so that, for example, a $^2\Pi$ state has the two components $^2\Pi_{\frac{1}{2}}$ and $^2\Pi_{3/2}$.

1.1.2 Vibration and Rotation

All stable molecules are rotating and vibrating; and to a good approximation we may consider each of these motions to have its own discrete energy

levels. The vibrational energy function, G(v), has the energy levels of an anharmonic oscillator and is written

$$G(v) = \omega_e(v+\tfrac{1}{2}) - \omega_e x_e (v+\tfrac{1}{2})^2 + \omega_e y_e (v+\tfrac{1}{2})^3 \quad \text{---} \quad (1.6)$$

where v is the vibrational quantum number and ω_e, $\omega_e x_e$, $\omega_e y_e$ are called vibrational constants. As shown in Figure 1.1 there is a finite number of discrete vibrational levels; at energies corresponding to the hatched area of the figure the molecule dissociates. If each vibrational quantum, G(v+1) - G(v), is denoted by $\Delta\, G(v+\tfrac{1}{2})$ then the dissociation energy, D_o, measured from G(0), is given by

$$D_o = \sum_v \Delta\, G(v+\tfrac{1}{2}) \qquad (1.7)$$

If the dissociation energy is measured from the bottom of the potential curve it is denoted by D_e. As $r \to \infty$ the energy tends towards that of the separated atoms; as $r \to o$ the energy becomes approximately that of the "united atom".

The rotational energy levels, a few of which are shown in Figure 1.1 as short horizontal lines, are much closer together than the vibrational ones, and their energy is a function of the rotational quantum number J. However, some allowance has usually to be made for the fact that the molecule is rotating and vibrating at the same time, and the model of a "vibrating rotator" is found to reproduce most experimental observations satisfactorily. The rotational energy is then written

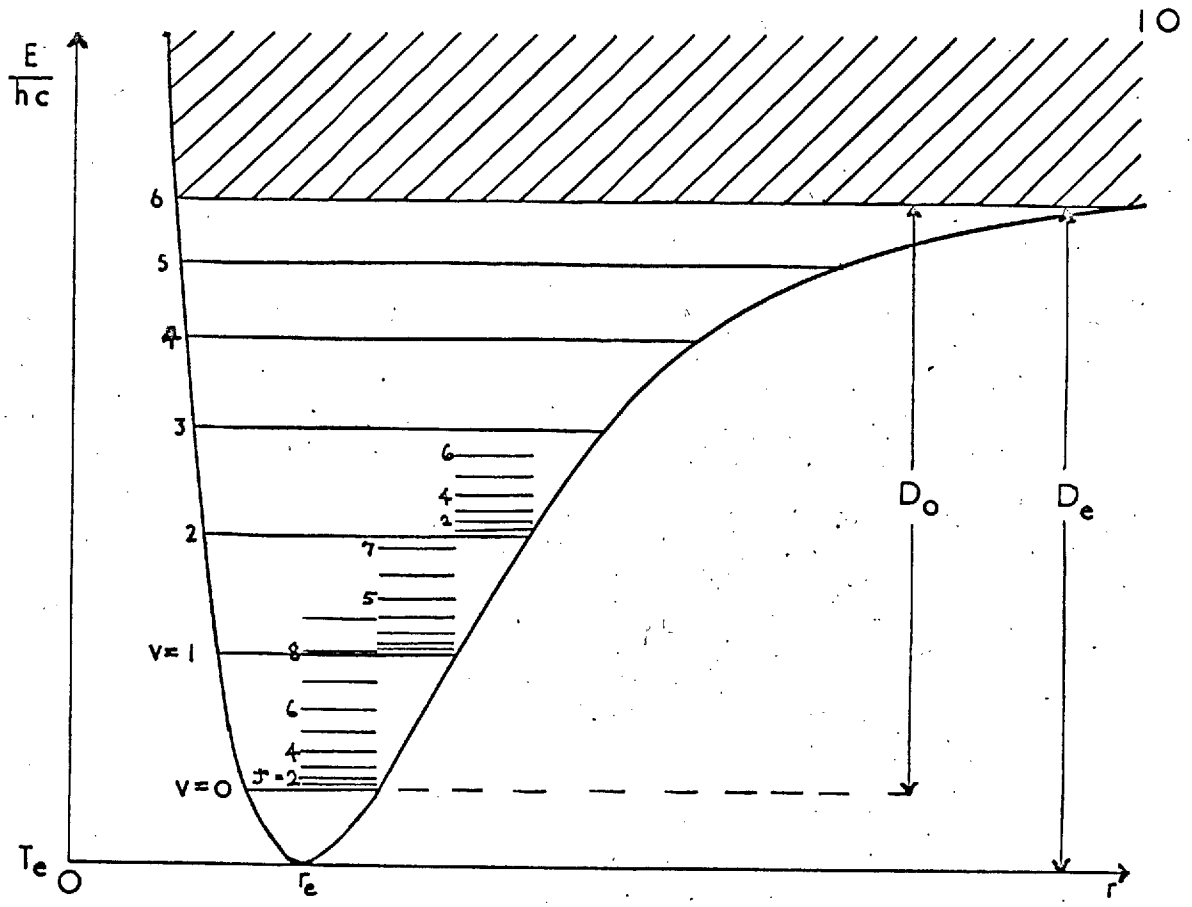

Figure 1.1: Potential Energy curve for a stable state of a diatomic molecule

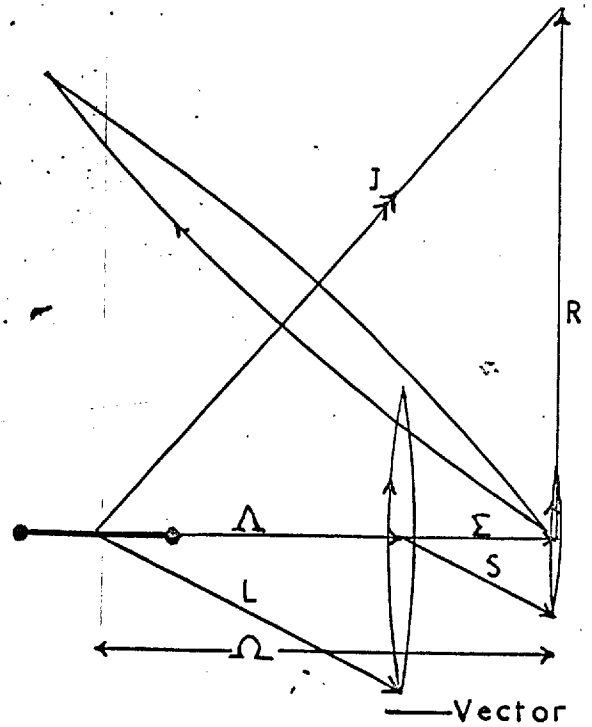

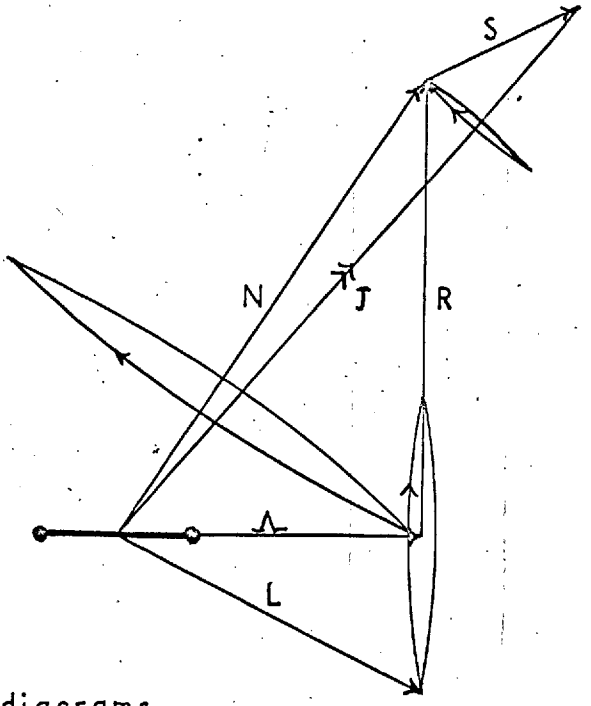

Vector diagrams

Figure 1.2: Hund's case (a)

Figure 1.3: Hund's case (b)

$$F_v(J) = B_v\, J(J+1) - D_v\, J^2(J+1)^2 + H_v\, J^3(J+1)^3 \quad (1.8)$$

where $B_v = B_e - \alpha_e\,(v+\frac{1}{2}) + \gamma_e(v+\frac{1}{2})^2$ (1.9)

and $D_v = D_e + \beta_e\,(v+\frac{1}{2})$ (1.10).

B_e is related to the moment of inertia, I_e, about the centre of gravity (when $r = r_e$) by the equation

$$B_e = \frac{h}{8\pi^2 c I_e} \quad (1.11)$$

while the terms in D_v and H_v allow for the expansion of the molecule as the rotational speed is increased.

The mutual influence of the rotational and electronic motions is also important, and two kinds of coupling are frequently approximated in practice, namely, Hund's cases (a) and (b). A vector diagram for Hund's case (a) is shown in Figure 1.2. The electronic motion is strongly coupled to the line joining the nuclei and the quantum numbers Λ, Σ and Ω are defined as in section 1.1.1. $\Omega\hbar$ combines with the angular momentum $R\hbar$ of the nuclear rotation to form the resultant angular momentum $J^{\frac{1}{2}}\,(J+1)^{\frac{1}{2}}\hbar$ for the whole molecule. The rotational energy in a given vibrational level v is given by

$$F_v(J) = B_v(J(J+1) - \Omega^2) - D_v J^2(J+1)^2 + \_\_\_ \quad (1.12)$$

where $J = \Omega,\ \Omega+1,\ \Omega+2$ ___ . In case (a) the separation of the multiplet components ($^2\Pi_{\frac{1}{2}}$, $^2\Pi_{3/2}$ say) is relatively large.

Hund's case (b) is shown in Figure 1.3. The coupling between S and the inter-nuclear axis is here very weak and $\Lambda\hbar$ and $R\hbar$ combine to give a resultant

$N^{\frac{1}{2}}(N+1)^{\frac{1}{2}}\hbar$, which is the total angular momentum without spin. The vector N combines with S to give the total angular momentum (including spin) of $J^{\frac{1}{2}}(J+1)^{\frac{1}{2}}\hbar$, but the rotational energy is determined chiefly by N. Thus, apart from a small splitting of the sub-states of different spin, the rotational energy is given by

$$F_v(N) = B_v(N(N+1) - \Lambda^2) - D_v N^2(N+1)^2 + \ldots \quad (1.13)$$

with $N = \Lambda, \Lambda + 1, \Lambda + 2 \ldots$.

Hund's case (b) holds for all Σ states and singlet states, but most multiplet Π and Δ states have couplings which are intermediate between cases (a) and (b). Energy formulae have been calculated for such cases and will be given in a later chapter. (It should be noted that the symbol N has been used here in place of Herzberg's K. N was recommended by Jenkins (1953), approved by the Joint Commission for Spectroscopy, and has since been widely adopted).

It will be recalled from section 1.1.1 that if molecular rotation is neglected, terms with equal $|M_L|$ have the same energy. States with $\Lambda \neq 0$ are therefore degenerate, while Σ states ($M_L = 0$) are non-degenerate. Therefore, since any plane containing the inter-nuclear axis is a plane of symmetry, the electronic eigenfunction ψ_e of a Σ state either remains unchanged or changes sign when reflected in any plane passing through both nuclei. If the sign changes, the state is said to be a Σ^- state; otherwise it is a Σ^+ state. The rotational levels themselves also have

a parity property, being called positive or negative according as the <u>total</u> eigenfunction, ψ, remains the same or changes sign when reflected at the origin. To a first approximation we may write

$$\psi = \psi_e \frac{1}{r} \psi_v \psi_r \qquad (1.14)$$

where the vibrational eigenfunction $\frac{1}{r}\psi_v$ depends only on $|r|$ and always remains unchanged on reflection at the origin, and where the rotational eigenfunction ψ_r changes sign if N is odd but remains unchanged if N is even. It follows that for Σ^+ states levels with even N have positive parity and levels with odd N have negative parity while for Σ^- states levels with odd N have positive parity and levels with even N have negative parity.

When the molecular rotation is included, the degeneracy in states with $\Lambda \neq 0$ is removed and the rotational levels of each multiplet component are split into two components of slightly different energy. The components of this <u>Λ-type doubling</u> form two rotational term series of opposite parity; the levels which behave like the levels in a Σ^+ state are called c levels and those which behave like the levels in a Σ^- state are called d levels. (This is the convention of Herzberg (1950); for Π states the labelling is the opposite to that proposed by Mulliken (1931)).

1.1.3 The formation of bands

A system of bands in the visible or ultraviolet region of the spectrum corresponds to the allowed frequency transitions between the vibrational and rotational energy levels of two electronic states. The quantum numbers of levels in the electronic state with the higher energy are marked with a single prime (') and those of levels in the lower state are marked with a double prime (").

For transitions accompanied by electric dipole radiation, the following selection rules hold (with varying degrees of rigour):

$$\Delta J = J' - J'' = 0, \pm 1, \text{ but } J = 0 \not\leftrightarrow J=0 \quad (1.15)$$

$$\text{parity: } + \rightleftharpoons - \; ; \; + \not\rightleftharpoons + \; ; \; - \not\rightleftharpoons - \quad (1.16)$$

$$\Delta \Lambda = 0, \pm 1 \text{ , but } \Sigma^+ \not\leftrightarrow \Sigma^- \quad (1.17)$$

$$\Delta S = 0 \quad (1.18)$$

$$\Delta v = \text{any integer} \quad (1.19)$$

$$\text{for case (a) } \Delta \Sigma = 0 \quad (1.20)$$

$$\text{for case (b) } \Delta N = 0 \pm 1, \text{ but } \Delta N \neq 0 \text{ for } \Sigma \rightarrow \Sigma \quad (1.21)$$

Within a particular band (symbolised as (v',v")) there are series of lines known as branches, which have gradually varying intensities. Branches with $\Delta J = -1, 0, 1$ are labelled P, Q and R respectively, and particular lines are indicated by the value of J" (e.g. R(4), Q(6)). In multiplet bands there are often "satellite" branches for which ΔJ and ΔN differ; in such cases ΔN is given as a superscript (e.g. ^{Q}R).

Because of the selection rules and restrictions such as $N \geq \Lambda$, $J \geq \Omega$, there are characteristic patterns of 'missing' lines for particular kinds of transition. The frequency for which $F'(J) = F''(J) = 0$ is called the origin of the band (written ν_0) and is used in finding the vibrational constants.

1.1.4 The isotope effect

For all but the lightest molecules, the electronic energy T_e of a given state and the form of the potential curve remain unchanged when an isotope of different mass is substituted for one of the atoms. However, the vibrational and rotational levels are altered through the change in the reduced mass μ, the levels of the heavier isotope being closer together. As we are concerned only with hydrides and deuterides, the superscript D will be used here to distinguish quantities relating to the heavier isotope. If the term values of the vibrating rotator are expressed in the form

$$T_{v,J} = \sum_{l,j} Y_{lj}(v+\tfrac{1}{2})^l \, (J(J+1))^j \qquad (1.22)$$

then according to the Bohr theory (see Dunham (1932)), the isotopic constants can be related in the simple form

$$\frac{Y^D_{lj}}{Y_{lj}} = \left(\frac{\mu}{\mu^D}\right)^{(l + 2j)/2} \qquad (1.23)$$

As the quantity $(\mu/\mu^D)^{\frac{1}{2}}$ is usually written as ρ,

equation (1.23) reduces to

$$\frac{Y^D_{\ell j}}{Y_{\ell j}} = \rho^{\ell + 2j} \qquad (1.24)$$

Table 1.1 shows which powers of ρ are appropriate for the constants usually measured, together with numerical values, based on the Chemical Scale of atomic masses ($M_H = 1.007856$, $M_D = 2.014182$, $M_N = 14.00740$), for the isotopes studied here.

Table 1.1 : Ratios of band constants according to the Isotope Effect.

Constants	Power of ρ	Value for ND/NH & ND^+/NH^+
$\omega_e(Y_{10})$	ρ	0.730695
$\omega_e x_e(Y_{20})$, $B_e(Y_{01})$	ρ^2	0.533915
$\omega_e y_e(Y_{30})$, $\alpha_e(Y_{11})$	ρ^3	0.39013
$D_e(Y_{02})$, $\gamma_e(Y_{21})$	ρ^4	0.28507
$\beta_e(Y_{12})$	ρ^5	0.2083
$H_e(Y_{03})$	ρ^6	0.1522

Dunham (1932) - who introduced the notation of (1.22) - showed that the finer interaction of vibration and rotation leads to corrections of the order of B_e^2/ω_e^2 in both the interpretation of the observed constants and equation (1.24). For NH and ND these corrections are a few parts in 10^5 and could only be calculated if a large number of small constants were accurately known. Other deviations from the simple isotope theory (Herzberg, P.164) are very small and will be ignored here as the isotope effect will be

used chiefly as a means of interpreting the spectra.

1.1.5 Rotational Perturbations

It often happens that for a given molecule a rotational term series of one electronic state (say X) lies at similar energies to a rotational term series of another electronic state (say Y). Under certain conditions, rotational levels of approximately equal energy perturb each other. Such a case is shown in Figure 1.4 where the two levels with J=4 repel each other - perturbations being always in a repulsive sense - by equal amounts, to take up the energies shown by dotted lines. The regular courses of the branches in observed bands are disturbed accordingly. The selection rules for the quantum numbers and symmetry properties of perturbed and perturbing states were first derived by Kronig (1928) and are:

$$\Delta J\ (=J_x - J_y) = 0 \qquad (1.25)$$

$$\Delta \Lambda = 0, \pm 1 \qquad (1.26)$$

$$\text{parity} : + \leftrightarrow + \ ; \ - \leftrightarrow - \ ; \ + \not\leftrightarrow - \qquad (1.27)$$

$$\Delta S = 0 \qquad (1.28)$$

When $\Delta S = 0$ and both states are pure case (b), then $\Delta K = 0$; but $\Delta S = 0$ holds only approximately and many perturbations between states of different multiplicity are known.

Since a perturbed level represents a mixture of the eigenfunctions of the unperturbed levels, it has

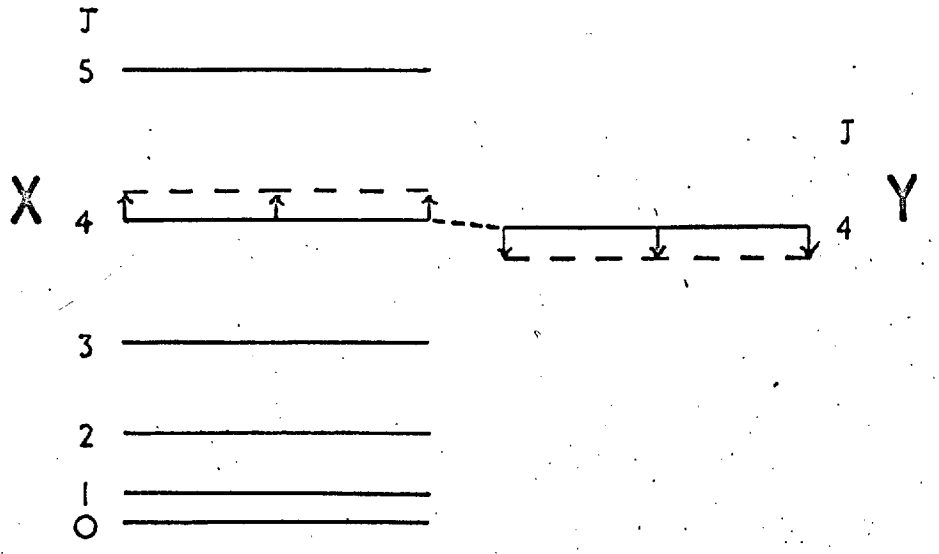

Figure 1.4: A rotational perturbation

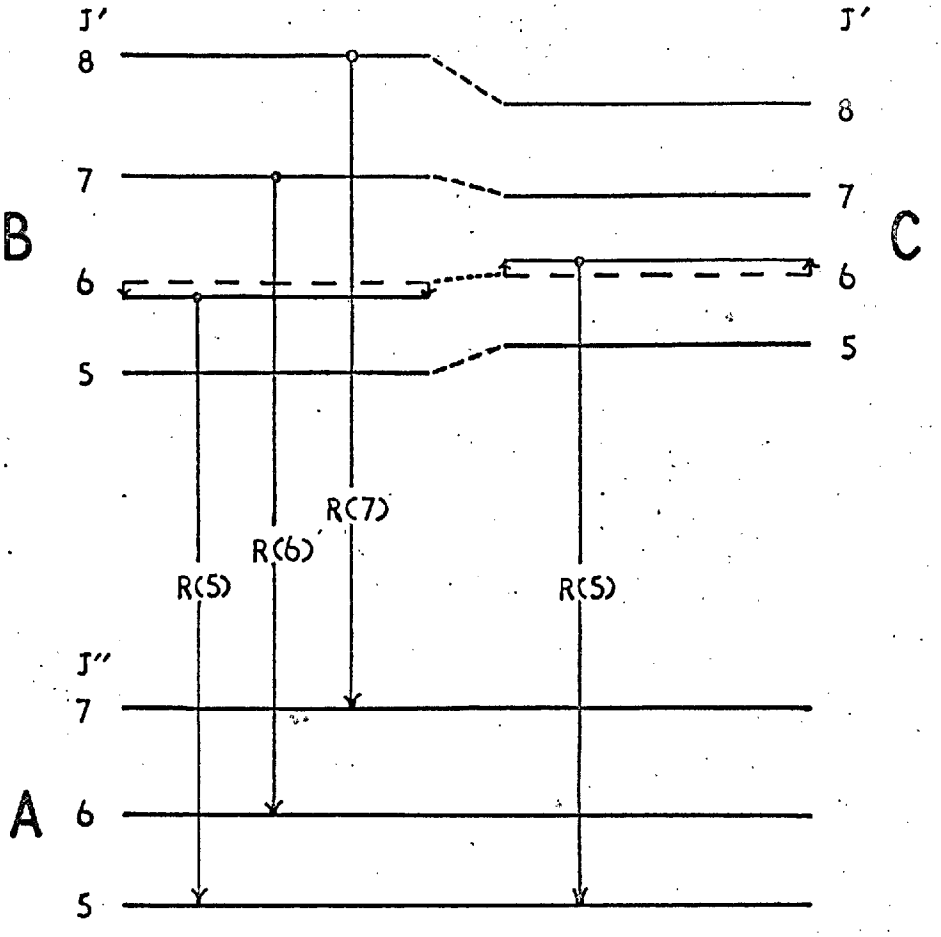

Figure 1.5: An extra line occurring because of a rotational perturbation

some of the properties of both electronic states concerned, so "extra" lines are sometimes observed. For example, in Figure 1.5 there are two lines near the expected position of R(5) in the B-A system.

1.2 The spectra of NH and ND

NH is one of the most important diatomic radicals; its spectra have been observed in solar absorption, in carbon stars and in emission from comets. In the laboratory, all the stable states predicted from the low-energy atomic states of N and H have been observed and are shown in table 1.2.

Table 1.2 The observed electronic states of NH

State	Observed transitions	Wavelength of (0,0) band
$d^1\Sigma^+$	d → c	λ 2530
$c^1\Pi$	d → c	λ2530
	c → b	λ4502
	c → a	λ3240
$A^3\Pi_i$	A ↔ X	λ3360
$b^1\Sigma^+$	c → b	λ4502
$a^1\Delta$	c → a	λ3240
$X^3\Sigma^-$(ground state)	A ↔ X	λ3360

1.2.1 The $A^3\Pi_i - X^3\Sigma^-$ system

The triplet system is by far the most intense and occurs as a frequent impurity in laboratory sources.

It was first mentioned by Eder in 1893 (quoted by Gleu (1926)) and was known to early workers as the 'β band of ammonia' - as opposed to the 'α band', which was a many-line spectrum in the visible region, now known to be carried by NH_2 (Dressler and Ramsay (1959)). The first astrophysical identification was in the solar spectrum by Fowler and Gregory (1919), who also photographed the system in the ammonia-oxygen flame, the flame of moist cyanogen burning in oxygen and the copper arc in ammonia. The appearance is dominated by the intense Q branches, the lines of which are piled up together at λ3360 ((0,0) band) and λ3370 ((1,1) band). Because of the similarity of the internuclear distances and vibrational frequencies in the A and X states, bands of other sequences are relatively weak (Herzberg, P.198); nevertheless Gleu (1926) obtained several other bands on a low dispersion spectrogram of the chemi-luminescence of $N_3Cl + HN_3$.

The first rotational analysis of the (0,0) and (1,1) bands was by Funke (1935, 1936), who obtained emission spectra from a high pressure arc burning in ammonia and absorption spectra by absorption in an ammonia-coalgas flame - essentially high temperature sources. Dixon (1959) observed the (0,0) and (1,0) bands in absorption by Flash Photolysis of isocyanic acid vapour (HNCO). The molecules were at room temperature, so Dixon found 25 of the possible 27

branches of the (0,0) band at low values of J whereas Funke had found only 11 branches. It was found that Funke's assignments - particularly those for the (0,0) band - needed correction.

For ND, Kopp et al (1965) have analysed the (0,0) and (1,1) bands from high dispersion emission spectra of a hollow cathode discharge through flowing heavy ammonia. This was a high temperature source and no satellite branches were observed. Their numbering of the main Q branches was uncertain but has been confirmed by Shimauchi (1966), who used a hollow cathode discharge through nitrogen, hydrogen and helium. Shimauchi has also observed five of the satellite branches.

A number of the weaker bands of both isotopes were observed by Pannetier and his collaborators (see for example Guenebaut (1955), Pannetier et al (1955)) during the explosive decomposition of hydrogen and deuterium azide (N_3H, N_3D). Some 8000 explosions were needed for a low dispersion spectrogram, and an approximate value (3.8eV) for the dissociation energy of the ground state was deduced from measurements of the band heads. An accurate value (3.21 $\pm$ 0.16 eV) of the dissociation energy of NH, based on the intensity of the (0,0) band photographed in absorption through a shock tube, has recently been given by Seal and Gaydon (1966).

1.2.2 The $c^1\Pi - a^1\Delta$ system

c - a is the strongest of the singlet systems and the (0,0) band (λ3240 for NH, λ3235 for ND) overlaps the triplet system in all emission sources with sufficient energy (effectively, all except flames). The λ3240 band was analysed from high dispersion spectra by Pearse (1933) and Dieke and Blue (1934), using heavy-current discharges through hydrogen containing a small proportion of nitrogen. Shimauchi (1964) has also studied this band from a hollow cathode discharge through nitrogen and hydrogen diluted with helium. The (0,1) and (1,0) bands of NH have only been studied at low dispersion (medium quartz) by Nakamura and Shidei (1935), using a Geissler discharge in ammonia.

For ND the λ3235 band was analysed by Dieke and Blue and by Shimauchi, and the (1,0) and (0,1) bands were studied under low dispersion by Florent and Leach (1952). Quite the best paper on ND, however, is that by Hanson et al (1965) who obtained the (1,0), (0,0) and (0,1) bands at a reciprocal dispersion of 0.36 Å/mm from a hollow cathode discharge through heavy ammonia.

The energy difference between $a^1\Delta$ and the ground state is uncertain, as no intercombination systems have been observed, and estimates have to be based on extrapolated dissociation energies for the singlet states. In spite of the fact that $a^1\Delta$ is an excited state, Babcock (1945) identified the λ3240 band of NH in

absorption in the solar spectrum.

1.2.3. The $d^1\Sigma^+ - c^1\Pi$ and $c^1\Pi - b^1\Sigma^+$ systems.

These systems are much weaker than c-a; furthermore $d^1\Sigma^+$ is very highly excited, being some 10eV above the ground state. During the present work, primarily concerned with NH^+ (as section 1.3 will show), a source has been developed which produces these systems with an intensity much greater than that reported hitherto. The opportunity has therefore been taken to photograph these systems at high dispersion, to analyse new bands for both isotopes and to calculate more accurate molecular constants.

The d-c system of NH (λ2530) was discovered by Hori (1929), using a 40kV transformer discharge in a mixture of nitrogen and hydrogen between a wire and a cup-shaped electrode containing sodium or lithium. He correctly assigned the band to NH, but misnumbered the branches. This was probably because

1) the c-a system had not been analysed, so the combination differences for c were not known
2) the R branch would be very weak on his spectrogram
3) he was not aware that the first 10(say) members of the Q branch were not resolved.

The correct assignments were made by Lunt, Pearse and Smith (1936) using the spectrum of a hollow cathode discharge in rapidly streaming ammonia, photographed with

a large quartz spectrograph. Narasimham and Krishnamurty (1966) have recently analysed the (1,1) and (0,1) bands of NH at a reciprocal dispersion of 2.6Å/mm (comparable to that of Lunt et al) from a mildly condensed transformer discharge through flowing ammonia.

The $b^1\Sigma^+$ state was predicted by Mulliken (1932) from the possible electron configurations in NH, and Lunt, Pearse and Smith (1935a) analysed the (0,0) band of the c-b system (at λ4502), using their hollow cathode discharge in flowing ammonia. No other work has been published for NH, but a low dispersion analysis of the (0,0) ND band is mentioned in a note by Chauvin and Leach (1950). Babcock (1945) identified the λ4502 band in the solar absorption spectrum.

1.3 NH^+

The spectrum of NH^+ deserves attention for two reasons: firstly, because NH^+ is isoelectronic with CH and therefore of spectroscopic interest, and secondly, because it is likely to be found in astrophysical sources. The ionized radicals CO^+, N_2^+, CO_2^+ and CH^+ have already been found in cometary spectra, and CH^+ is also known from absorption by interstellar matter. Swings (1951) has roundly written: "The spectra of the singly ionized molecules probably present in interstellar space or in comets, or both, such as NH^+, C_2^+ and CN^+ should be studied."

Yet to date only a brief note (Lunt, Pearse and Smith (1935b)) and one paper (Feast (1951)) have appeared on the subject. Lunt et al, discussing their spectra of NH obtained in a hollow-cathode discharge through flowing ammonia, state "In addition we have obtained four weaker bands at λλ 2730, 2835, 2885 and 2980 which appear to be due to the ion NH^+". Feast used a similar source, with a very rapid flow of ammonia and low currents (0.1 amp), and photographed bands at λλ 2885, 2725, 2825 and 2614, degraded to the red. Using a large quartz (Hilger E.478) spectrograph, exposures of 12 hours and 30 hours were necessary for good spectrograms of the 2885Å and 2725Å bands, which he analysed and classified as the (0,0) and (1,0) bands of the NH^+ $^2\Sigma^+ - ^2\Pi_r$ system corresponding to the CH system at λ3143. The 2825Å and 2614Å bands were too weak for rotational analysis, but he thought these were the (2,1) and (2,0) bands of the same system. Feast did not find the λ 2980 band of Lunt et al, and thought that it might have been part of the λ2885 band, separated from the main part by the (2,0) sequence of the N_2 Second Positive system at 2977Å. A weak violet-degraded band at 2684Å was also found, and this is the (0,1) band of the NH d-c system (Narasimham and Krishnamurty (1966)).

Feast's analysis shows that the $^2\Pi$ state is strongly perturbed by a $^4\Sigma^-$ state with a vibrational

level only 331cm^{-1} above $^2\Pi$(v=o). Since the vibrational numbering of the $^4\Sigma^-$ state is unknown, either of these electronic states could be the ground state of NH^+. Since the ionization potential of hydrogen is less than that of nitrogen, the lowest pair of dissociation products is $N(^4S_u) + H^+(^1S_g)$ which can give rise only to $^4\Sigma^-$, as can the lowest level of the united atom, $O^+(^4S_u)$. The lowest electron configuration is $K(2s\sigma)^2\ (2p\sigma)^2\ 2p\pi$, and this gives rise to the $^2\Pi_r$ state, which is correlated with the first excited state of both the united atom, $O^+(^2D_u)$, and the dissociation products, $N^+(^3P_g) + H\ (^2S_g)$. Thus the molecular orbital method predicts a $^2\Pi_r$ ground state, whereas the united atom method - known to be a good approximation for light diatomic hydrides - predicts a $^4\Sigma^-$ ground state. Feast suggested that highly excited quartet levels might combine with $^4\Sigma^-$ to give a vacuum-ultraviolet emission spectrum, and that a study of perturbations in such bands might identify the ground state with certainty.

The above system is the analogue of the λ3143 system of CH ; but CH has two more systems, $^2\Sigma^- - ^2\Pi$ at λ3900 and $^2\Delta - ^2\Pi$ at λ4300, whose analogues would be more convenient for astrophysical observation. Feast did not find these systems, but pointed out that $^2\Sigma^-$ may be unstable in NH^+ as it has low stability (D_o = 2300 cm^{-1}) in CH.

As a result of these considerations, the main purposes of the present work are

1) to observe new band spectra of NH^+
2) to observe the band spectra of ND^+, and so derive more information about both molecules, and
3) to attempt to identify the ground state of NH^+.

CHAPTER 2 : EXPERIMENTAL METHODS

2.1 The work of C. B. Sharma

During experiments to find the effects of the presence of helium on the intensity of NH bands under a wide range of physical conditions, C. B. Sharma (1959) discovered that the two NH^+ bands analysed by Feast appeared with considerable intensity in a positive column discharge through a mixture of nitrogen and hydrogen when "excess" of helium was added. Sharma photographed the λ 2885 and λ2725 bands in the first order of a 21 ft. concave grating (reciprocal dispersion 1.30Å/mm) using exposures of one hour and two hours respectively. He re-measured the bands but did not extend the analysis, as the λ2825 and λ2614 bands were too weak, and longer exposures resulted only in the increase of the background continuum.

As this positive column source appeared to be markedly more intense than the hollow cathode used by Feast, the present investigation was begun with an attempt to reproduce and improve the excitation conditions found by Sharma, and in particular to obtain intense spectrograms of the (2, 0) and (2, 1) bands of the NH^+ $^2\Sigma^+ - {}^2\Pi$ system. No attempt was made to find the (0, 1) band as this will be overlapped by the strong NH triplet and c-a systems.

2.2 Apparatus

A general view of the apparatus is shown in

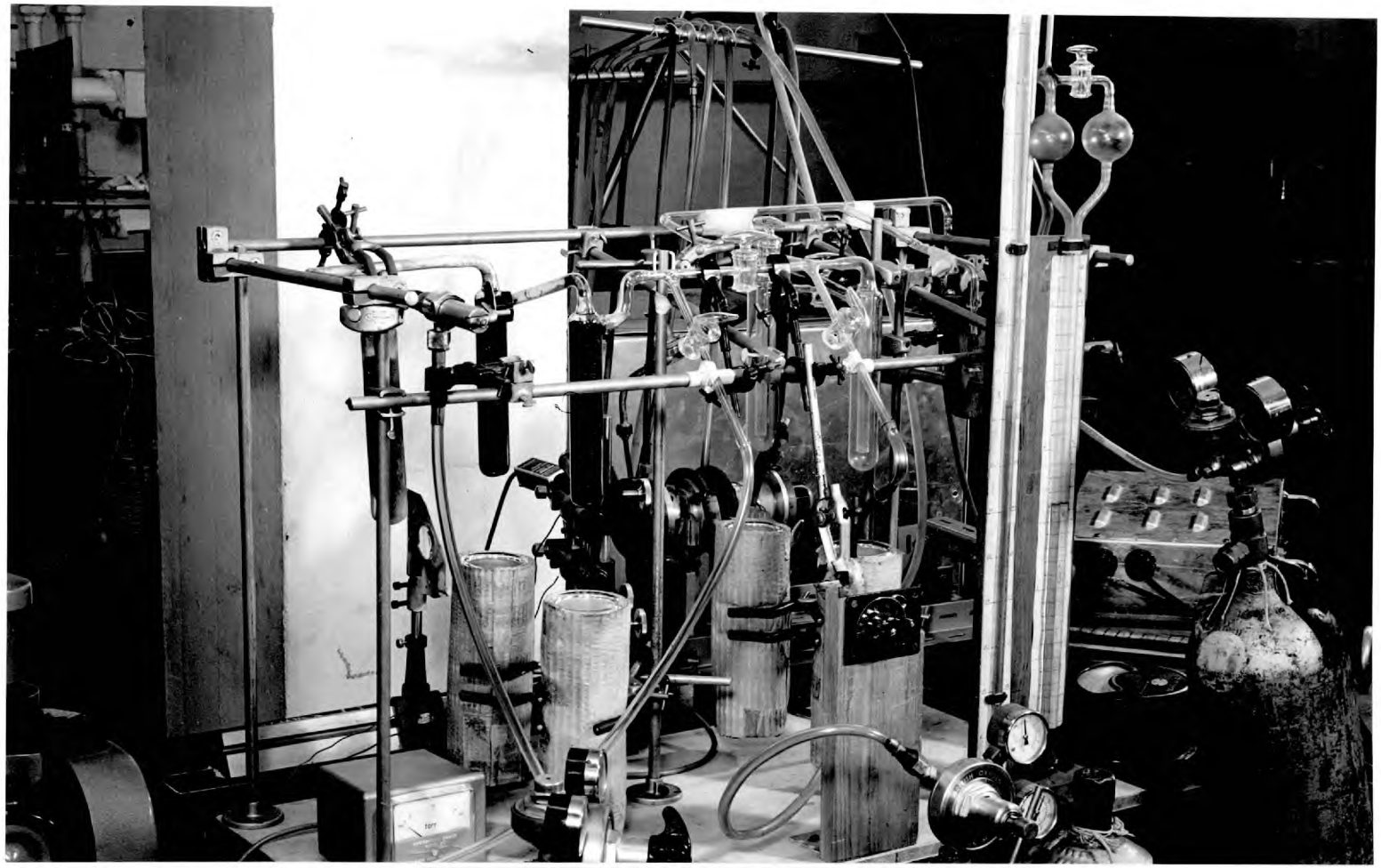

PLATE 1: GENERAL VIEW OF APPARATUS

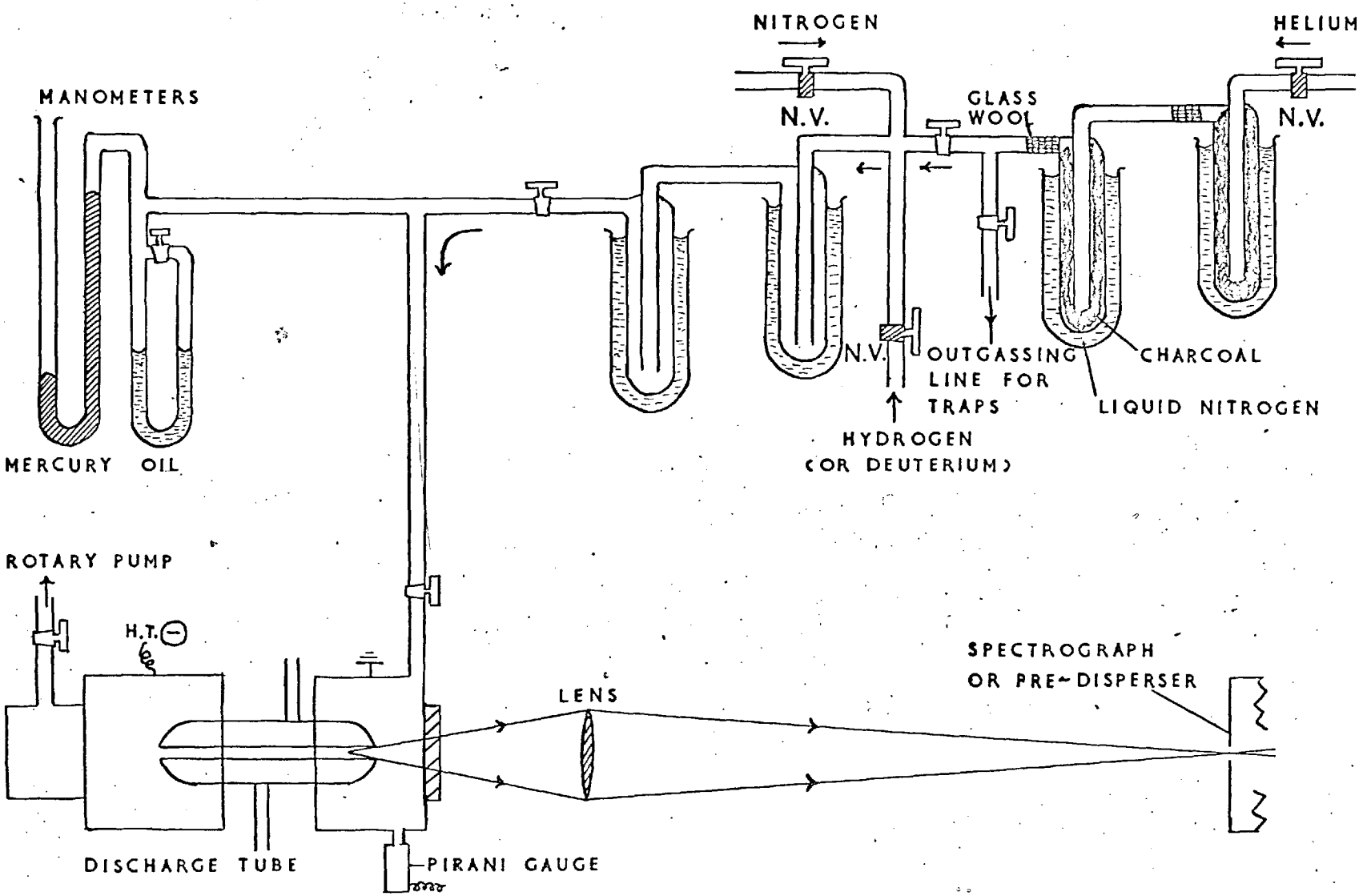

Figure 2.1: Schematic diagram of apparatus

Plate 1 and the scheme of it can be followed from Figure 2.1. Impurities in the mineral helium were removed by absorption in the charcoal traps and impurities of high freezing point were removed from the other gases by two liquid nitrogen traps. The nitrogen was of "oxygen-free" grade, the deuterium was 99.8% pure (from a cylinder) and the hydrogen was of the usual commercial grade. Each gas was admitted through a fine-control needle valve (N.V.) and the pressures were measured with the following instruments:

Pirani gauge ... 10^{-3} torr to 5.10^{-1} torr

oil manometer .. differences of 2.10^{-1} torr to 20 torr

mercury manometer ..more than 10 torr.

The gases were continuously pumped through the discharge tube by a small rotary pump. All the spectra were observed in emission, and the power for the discharge tube was taken from d.c. motor generators capable of delivering up to 4000V at 2.5A. The output voltage was controlled by a variable transformer supplying the field windings, and a bank of resistors (1000 Ω when cold) was connected in series with the tube to limit the current.

2.3 Positive Column discharges

The type of discharge tube used by Sharma was that described by Hunter and Pearse (1936). It has a water-cooled capillary of fused quartz onto each end of which is sealed a pyrex tube containing a hollow,

cylindrical electrode made of aluminium. When viewed end-on, such a tube is suitable for the production of the ultraviolet continuum of hydrogen, since there is a high current density in the capillary. One of these discharge tubes was available in the laboratory and was used in preliminary experiments with a medium quartz spectrograph. Unfortunately the tube was badly made and suffered continually from leaks, so that the γ bands of NO appeared in the ultraviolet. Furthermore, since the electrodes are not cooled, the area surrounding the cathode became very hot when the current was as much as 0.5A.

It was already clear that the NH bands would be more intense at higher current densities, so a modern development of the tube was tried. This is the "hydrogen" tube described by Clarke and Garton (1959) which, as Figure 2.2 shows, has water-cooled electrodes and O-ring vacuum seals onto the quartz centre-piece. The capillary is 10 cm. long and of 4 mm. bore.

Sharma did not give the partial pressures of the constituent gases, but to judge from his other work 10-20 torr would seem to be an "excess" of helium. The pressures of nitrogen and hydrogen had to be well below 1 torr to prevent the ultraviolet spectrum being dominated by the hydrogen molecular continuum, the Second Positive bands of N_2 or even (at higher nitrogen pressures) the γ system of NO. The λ 3064 and λ 2811 bands of OH also appeared and it proved impossible to remove these

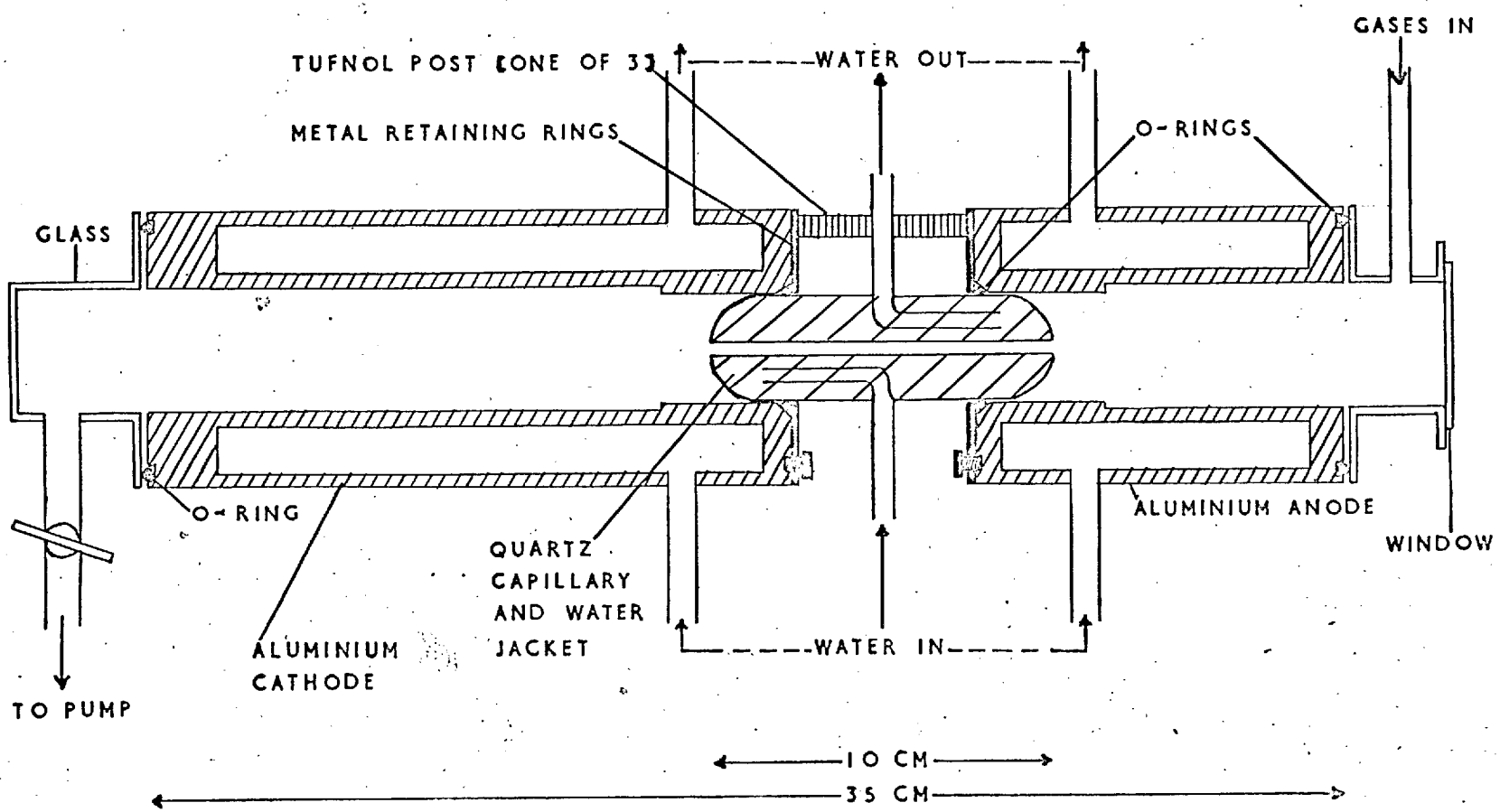

Figure 2.2: Positive Column discharge tube of Clarke and Garton

completely - a common experience when quartz capillaries are used. As the λ2811 band overlapped the (2,1) band of NH^+, attention was concentrated on the (2,0) band.

After a systematic adjustment of the partial pressures, pictures of the (0,0) and (1,0) bands of NH^+ were obtained from the Clarke-Garton tube at a helium pressure of 20 torr and currents approaching 1A. The NH d-c (λ2530) system appeared strongly, but the (2,0) band of NH^+ could not be distinguished from the continuum.

Having thus reproduced Sharma's results (without improvement) a check was made on the effectiveness of a helium-nitrogen-hydrogen mixture in a hollow cathode discharge.

2.4 Hollow cathode discharge

A suitable hollow cathode has been described by Sharma (1959) and is shown in Figure 2.3. The cathode is an aluminium tube 20 cm. long with internal diameter 1 cm. Two anodes are provided to increase the brightness and all the electrodes are cooled with water.

At the operating pressure of 5 torr the ultraviolet NH^+ system was observed, but the exposure time had to be increased by a factor of ten as compared with the positive column tube in order to obtain bands of comparable density. If the current was increased beyond 0.8A, the hydrogen background became too intense. The general usefulness of the hollow cathode in the

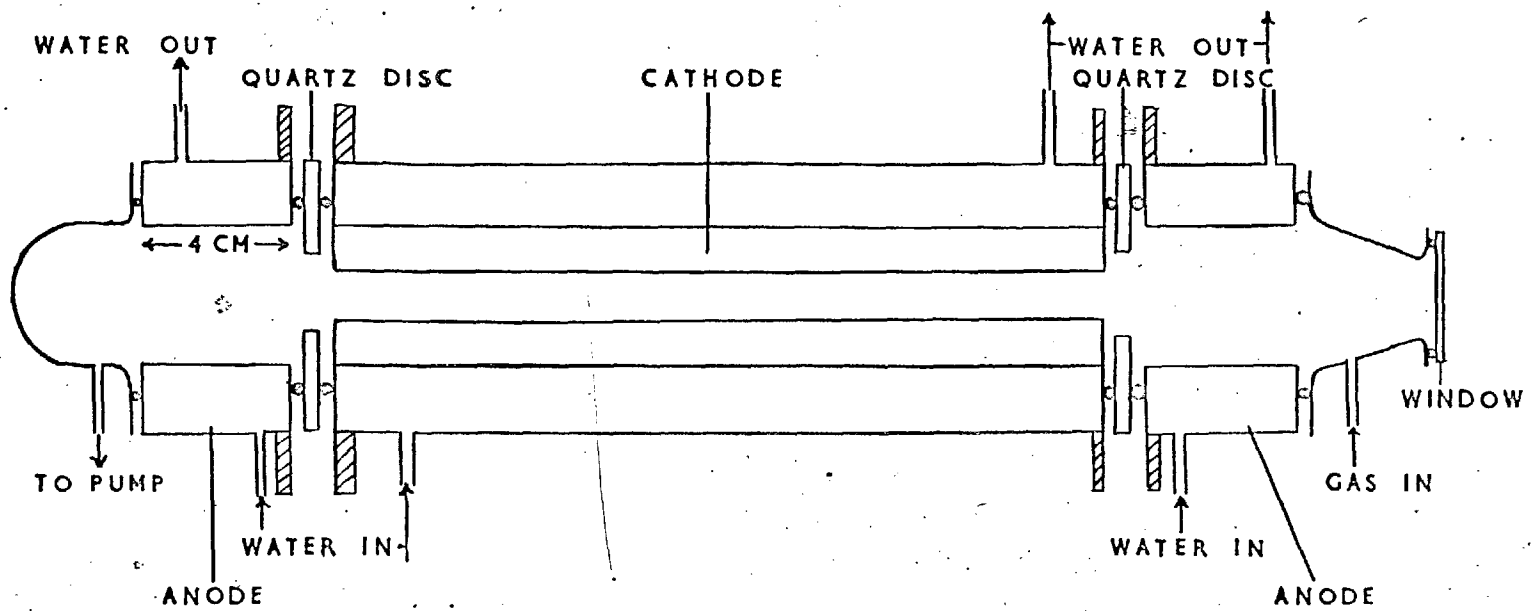

Figure 2.3: Hollow Cathode

observation of positive molecular ions was indicated by the relatively intense bands of the N_2^+ First Negative system; but for NH^+ the limited working pressure range was a great disadvantage.

When argon was substituted for helium, no NH^+ bands were observed under any conditions. (Since the absorption of argon by charcoal is appreciable, the argon was cleaned by passing it at high pressure through molecular sieve type 13X (B.D.H.) cooled in liquid oxygen. This follows the recommendations of Chamberlain (1962)).

2.5 Optimum conditions in the ultraviolet

It was clear that the positive column discharge offered the best chance of observing weaker bands (or systems) in NH^+, but the best operating conditions had still to be found. When argon was substituted for helium, no NH^+bands were observed. When ammonia was substituted for nitrogen and hydrogen - being pumped directly through the discharge tube in order to avoid liquefaction in the liquid nitrogen traps - the NH^+ bands were observed with an intensity comparable to that with nitrogen and hydrogen at the same helium pressure. In the absence of helium, no NH^+ was observed with ammonia. As ammonia offered no distinct advantage, and since the partial pressures of nitrogen and hydrogen could not then be independently controlled, further experiments were done with the three gases.

The main problem was that of suppressing the

hydrogen molecular continuum in a discharge tube designed specially to produce it! Fortunately, tests showed that the discharge would run at quite high pressures of helium - greater than 170 torr if necessary. When the pressure of helium was increased from about 20 torr, the intensity of all the emitted systems decreased; but the decrease was most marked for the hydrogen continuum and for the nitrogen bands. At pressures higher than 80 - 90 torr the improvement was negligible; but at these pressures small increases in the partial pressures of the minority gases improved the contrast of the NH^+ system considerably. The bands were also favoured by high current densities, but the total current was limited to 2A by the heat dissipation in the resistor bank. The optimum conditions were:

partial pressure of helium 90 torr
" " " hydrogen (or deuterium) 1 torr
" " " nitrogen 0.6 torr
Current 2A

In these conditions, exposures of only a few seconds were required with Ilford Zenith plates in a medium quartz spectrograph. With deuterium, the (2,0) ND^+ band was sufficiently intense for analysis and several bands of the hitherto unknown d-c ND system appeared. With hydrogen, the (2,0) NH^+ band was fairly clear, but a marginal improvement was needed. Accordingly, plates were taken with a large quartz spectrograph so that the line-to-continuum intensity ratio would be improved by the higher

dispersion. Satisfactory plates of the (2,0) NH^+ band were then obtained with exposures of 15 min. to the fine-grained Ilford N.30 Ordinary plate. It is instructive to compare the exposures to Zenith plates with those of Feast, who used a similar spectrograph:

Band	Feast	Present work
(0,0)	12 hours	10 seconds
(1,0)	30 hours	30 seconds

In view of the considerable intensity of the strongest bands, and the fact that the weak bands were clearer at high dispersion, all the final plates in the region 2450-3020Å (covering the d-c system of NH and ND and the $^2\Sigma^+ - {}^2\Pi$ system of NH^+ and ND^+) were taken with a 21ft. concave grating in an Eagle mounting. Particulars of the grating are as follows:

Aluminium-coated replica by Bausch and Lomb

30,000 lines per inch

Blazed for 7500Å (blaze angle 26° 45')

Ruled area originally 7" x 4"; present working area $5\frac{1}{2}$" x 3" - consequently f/47.

In order to be 'above' the blaze, it was convenient to use the third order for the ultraviolet, and this gave a mean reciprocal dispersion of 0.36 Å/mm, or 160Å on an 18" plate. A prismatic pre-disperser was used to select an appropriate range of wavelengths for admission to the spectrograph, so that spectra in other orders would not appear on the plates. Ilford Zenith and Zenith Astronomical plates were used and exposures

varied between 1 hour and 7½ hours. An iron arc running in air was used to give a reference spectrum.

Two experiments in the ultraviolet which failed are nevertheless worthy of mention:

1) Using a large quartz (Hilger E.478) spectrograph with a very narrow slit (5 microns) and Q2 plates, a search was made for the (1,0) band of the d-c system of NH and ND; but it could not be distinguished from the background continuum.

2) Using a 3 metre normal incidence vacuum spectrograph, a search was made for any other bands of these molecules in the 'Lithium Fluoride' region (1200-2000Å). No hydride bands were found, although of course the hydrogen line spectrum was troublesome at wavelengths below 1600Å.

2.6 New bands in the visible region.

When the intense source for NH^+ bands had been developed, it was appropriate to search for new systems at longer wavelengths. A survey of the low dispersion plates showed that there was a strong, unidentified hydride head at λ 4348 which appeared only on those plates which showed the ultraviolet NH^+ system. The corresponding deuteride head was at λ 4334, which suggested - by virtue of the small shift - that this was the (0,0) band of a system. In this region nitrogen bands were very intense, so it was clear that the nitrogen partial pressure would have

to be less than that used in the ultraviolet; otherwise (for example) the λ4502 band of NH would not be seen.

Further plates were taken with a large glass prism spectrograph (reciprocal dispersion of 6.1Å/mm at 4400Å), and the optimum gas pressures were found to be:

helium	90 torr
hydrogen (or deuterium)	1 torr
nitrogen	0.2 torr

In these conditions the λ4502 band of NH was very clear and the new λ4348 band well-developed. If the hydrogen pressure was increased, the hydride bands were suppressed and H_2 lines became intense. If the nitrogen pressure was as low as 0.1 torr the hydride bands were very weak.

It was established from plates taken with different gas mixtures that the λ4348 band was emitted by a nitrogen hydride; but none of the NH_2 bands given by Herzberg and Ramsay (1953) were found. A preliminary analysis showed that the lower state of the transition was in fact Feast's $^2\Pi$ (v=o) of NH^+. Six main branches were found, the R branches being more intense than the P branches. This corresponds to a $^2\Delta - ^2\Pi$ band in which six of the main branches are not resolved. (The final analysis is given in section 3.2).

In the wavelength region 4650-4800Å a very open branch of doublets, belonging to a nitrogen hydride molecule and degraded to the red, was observed. Other branches of this band were much weaker and the head was buried in

nitrogen bands. We shall call this the λ4650 band and discuss it in chapter 3.

As the λ4502 band of NH and the corresponding λ4484 band of ND were obtained with considerable intensity, a search was made for the (1,0) and (0,1) bands of this c-b system. Feast (1951) mentioned a weak band near 4120Å which may be the (1,0) band of NH, but this could not be distinguished from the nitrogen bands in the present experiments. Calculations showed that the (0,1) band of NH should be at about 5367Å and the spectrograms from the large glass prism instrument indeed showed a band of simple structure at λ5348. The predicted region for ND was 5081Å and a band was found at λ5096.

Final plates of all the visible bands were taken using the 21 ft. grating. The region 4300-4700Å was photographed in the second order, with a reciprocal dispersion of 0.53Å/mm, and exposures of 5 to 15 minutes were needed with Ilford Zenith or Zenith Astronomical plates. The third and higher order radiations were absorbed by a glass condensing lens, and the plates were not sensitive to the first order wavelengths.

In order to save time by reducing the number of ranges for re-focusing, the region 4700-5590Å was photographed in the first order, where the reciprocal dispersion was 1.2Å/mm. Zenith Astronomical plates were used up to 5100Å (exposure 15 minutes) and Astra 3 plates above 5000Å (exposures 3 to 7½ hours). The λ5348 band mentioned above was found to have <u>doublet</u> branches at high dispersion, so

that it cannot belong to the NH c-b system. However, it was overlapped by a weak singlet band at λ 5254, and the exposure time was lengthened in order to obtain a good spectrogram of this weak band. The deuteride band at λ 5096 was also found to have doublet branches.

2.7 Reduction of the spectrograms

Some of the plates were very 'clean' - that is, they contained only wanted lines - while others contained several hundred unwanted lines belonging to bands of N_2, N_2^+ or H_2. This was particularly true in the visible region where, although the strong branches of the hydride bands were clearly seen, the weak branches were necessarily confused with the background. In order to save the labour of measuring unwanted lines and to help in the analysis, plates were taken with one of the minority gases absent from the discharge. The plate with nitrogen and helium showed the unwanted lines of N_2, N_2^+, HeI etc. at the same intensity as the chosen spectrogram, while the plate with hydrogen (or deuterium) and helium served the same purpose for H_2, HI, HeI, CH etc (or deuterides). The two plates for comparison were placed in a Jarrell-Ash microphotometer, which contained the optics for juxtaposing magnified images of the spectrograms on a screen. In this way unwanted lines could be picked out and marked off on a suitably enlarged print. In the ultraviolet the only troublesome bands were the (2,0) and (3,0) sequences of the N_2 Second Positive system, and wanted lines in these regions were

found by comparison of the final hydride and deuteride plates.

Suitable evenly-spaced iron arc wavelength standards were chosen from Crosswhite (1958) and each plate was measured at least twice with a Zeiss Abbe comparator. The measurements were divided into small ranges (say 50Å wide) and the standard wavelengths for each range were fitted by the method of least squares to low order polynomials in the comparator readings, using an Elliott 803A computer. The computer also gave the residual for each line and the sum of the squares of the residuals, so that any mistakes in identification could be picked out and the polynomial giving the best fit could be chosen. (A quadratic expression was usually satisfactory).

Another programme evaluated the unknown wavelengths and calculated the vacuum wave numbers to the nearest 0.001 cm^{-1} using Edlén's expression for the refractive index of air. (This is the method used in the National Bureau of Standards 'Table of Wavenumbers' (1960)). Comparison of the values obtained from the different sets of measurements gave an estimate of the overall accuracy in the wavelength region considered. Most of the wavelengths were consistent to $\pm$ 0.002Å, and the accuracy of the wave numbers will be indicated when the band data are presented.

CHAPTER 3: ANALYSIS OF BANDS OF NH^+ AND ND^+

The analysis of band spectra usually involves two distinct activities. Starting from the wave numbers and relative intensities of the lines the spectroscopist picks out branches, identifies the electronic states, assigns vibrational and rotational quantum numbers to bands and lines, and confirms the whole system by equating the differences between energy levels.

Afterwards he fits mathematical models to the observed energy levels in order to derive information about the physical characteristics of the molecule.

In this chapter we shall be concerned with the first of these activities.

3.1 The v" = 0 progression in the $^2\Sigma^+ - {}^2\Pi$ system

We begin with the (0,0), (1,0) and (2,0) bands of the system investigated by Feast. Details of the plates are given in table 3.1.

Table 3.1 : $^2\Sigma^+ - {}^2\Pi$; v" = 0 progression

Band	$\lambda(NH^+)$	$\lambda(ND^+)$	Wavenumber accuracy	Exposure	Plate
(0,0)	2886	2878	$\pm 0.02 cm^{-1}$	1 hour	Zenith
(1,0)	2730	2760	$\pm 0.03 cm^{-1}$	3 hours	Zenith
(2,0)	2599	2657	$\pm 0.03 cm^{-1}$	7½ hours	Zenith Astronomical

The $\lambda\lambda$ 2886 and 2878 bands are the most intense and must be the (0,0) bands because of the small isotope shift. The heads of these bands are shown in Plate 2,

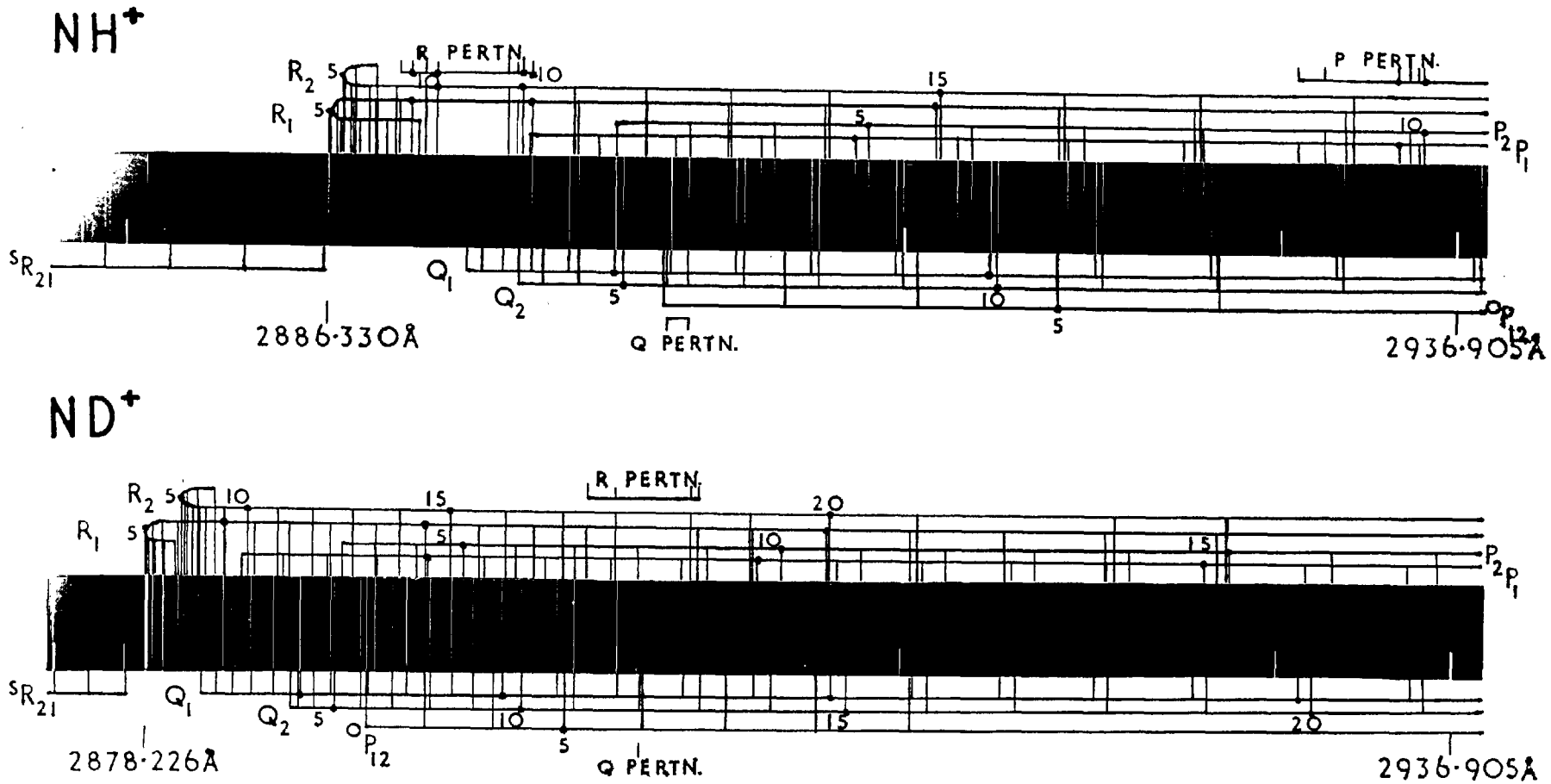

PLATE 2 : (0,0) BANDS OF $C^2\Sigma^+ - X^2\Pi$

from which the following points may be made:-

1) The branches consist of doublets. Therefore the carrier cannot be NH(ND) which has states of odd multiplicity.

2) There are strong Q branches. Therefore $\Delta\Lambda = \pm 1$ (Herzberg, p207).

3) There are six main branches. Therefore the transition is either $^2\Sigma - ^2\Pi$ or $^2\Pi - ^2\Sigma$ (compare $^2\Delta - ^2\Pi$ in section 3.2).

4) The separation of the R_1 and R_2 heads is only some 7 cm^{-1}(NH^+), 20 cm^{-1}(ND^+). Therefore A is small and the $^2\Pi$ state is near to Hund's case (b). We shall therefore use N, rather than J, for numbering the branches, and shall give the label F_1 to those rotational levels for which $J=N+\frac{1}{2}$ and F_2 to the levels where $J=N-\frac{1}{2}$.

The combination differences used in band analysis are defined as follows,

$$\Delta_2 F(J) = F(J+1) - F(J-1) \qquad (3.1)$$

$$\Delta_1 F(J) = F(J+1) - F(J) \qquad (3.2)$$

In any band values of $\Delta_2 F(J)$ are given by

$$\Delta_2 F'(J) = R(J) - P(J) \qquad (3.3)$$

$$\Delta_2 F''(J) = R(J-1) - P(J+1) \qquad (3.4)$$

If two or more bands have a common vibrational (and electronic) state, then the values of $\Delta_2 F(J)$ for that state must be the same in each band.

Tables 3.2 and 3.3 show some combination differences for the first few members of the bands we are

considering.

Table 3.2 : Some differences for v"=o in NH^+ $^2\Sigma^+ - ^2\Pi$, in cm^{-1}

N	$\Delta_2F_{1c}"(N)$			$\Delta_2F_{2c}"(N)$		
	(0,0)	(1,0)	(2,0)	(0,0)	(1,0)	(2,0)
1	96.14	96.17	96.21	-	-	-
2	154.76	154.73	154.79	-	-	-
3	214.65	214.63	214.76	212.09	212.24	211.97/
4	274.58	274.62	274.55	273.68	273.68	273.77/
5	334.06	334.14	334.11	334.22	334.28	334.37/
6	392.63	392.70	392.70	393.83	393.93	393.95
7	449.09	449.17	449.13/	451.88	451.98	452.03
8	500.37	500.47	500.41/	505.54	505.54	505.53/
	563.75	563.77	563.79	550.19	550.30	550.07/
9	605.95	605.99	606.00/	590.27	590.28	590.30
	540.90	540.91	541.01	544.46	544.45	544.57
10	664.19	664.19	664.17/	648.29	648.17	648.23
	600.87	600.84	600.78	603.66	603.53	

Table 3.3 : Some differences for v"=o in ND^+ $^2\Sigma^+ - ^2\Pi$, in cm^{-1}

N	$\Delta_2F_{1c}"(N)$			$\Delta_2F_{2c}"(N)$		
	(0,0)	(1,0)	(2,0)	(0,0)	(1,0)	(2,0)
1.	57.88	57.86	57.65/	-	-	-
2.	88.20	88.21	88.44/	-	-	-
3.	119.44/	119.33	119.43	109.24	109.19	108.98/
4.	151.01	150.94	150.98/	143.86	143.82	
5.	182.96	182.88	183.04	177.76	177.67/	177.77
6.	214.98	214.91	214.98	211.15	211.07	211.24
7.	246.98	246.89	214.96	244.13	244.07	244.11
8.	278.91	278.89	278.89	276.77	276.71	276.78
9.	310.67	310.62	310.66	309.08	309.02	309.06
10.	342.21	342.21	342.19	341.04/	341.18/	341.06

Differences involving one or more blended lines are marked with an asterisk (/). This symbol will be used throughout this thesis for lines which have been used more than once and for quantities derived from them. Quantities with an asterisk are therefore likely to be

less trustworthy than others.

It is clear from these tables that, even if we ignore the names of the differences and the absolute numbering, the bands do at least have a state in common and the relative numbering of the branches is correct. With this amount of information we can substitute an approximation for F(N) from (1.8) into $\Delta_2 F(N)$ and deduce the absolute numbering (Herzberg, p190).

Since the band at the longest wavelength is (0,0)it follows that the lower state is the common one and the other bands are (1,0) and (2,0). There are perturbations which occur at the same values of N in the different bands. Therefore the perturbations are in the lower state. Furthermore, for NH^+ (for example) both $F_1''(9)$ and $F_2''(9)$ are perturbed - as shown by the R and P branches - yet neither $Q_1(9)$ nor $Q_2(9)$ is perturbed. It follows that the perturbations are in the $^1\Pi$ state, which possesses Λ-doubling as well as spin doubling; so that $^2\Pi$ is the lower state.

We shall assume for the present that the upper state is $^2\Sigma^+$, by analogy with the λ3143 system of CH. This will be confirmed later by the relative positions of other electronic states. The first lines of the branches are shown in the energy level diagram (not to scale) of Figure 3.1. The main branches, shown by full lines in the diagram, represent the following energy differences:

$$\begin{aligned} P_1(N) &= \nu_0 + F_1'(N-1) - F_{1c}''(N) & P_2(N) &= \nu_0 + F_2'(N-1) - F_{2c}''(N) \\ Q_1(N) &= \nu_0 + F_1'(N) - F_{1d}''(N) & Q_2(N) &= \nu_0 + F_2'(N) - F_{2d}''(N) \\ R_1(N) &= \nu_0 + F_1'(N+1) - F_{1c}''(N) & R_2(N) &= \nu_0 + F_2'(N+1) - F_{2c}''(N). \end{aligned} \qquad (3.5)$$

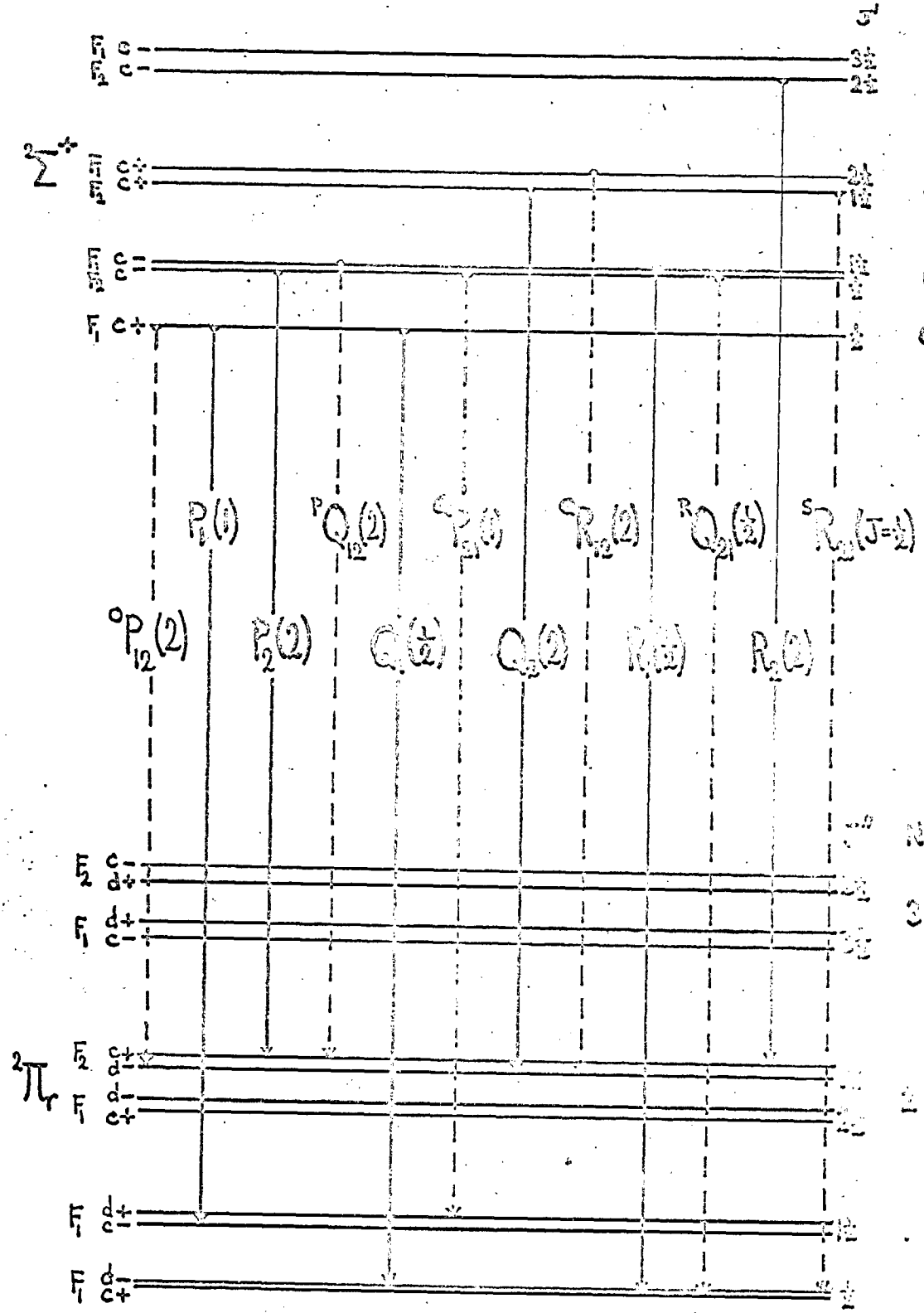

Figure 3.1: First lines for $^2\Sigma^+ - ^2\Pi_r$

The following combination differences for the lower state are constant in the progression of bands:

$$\Delta_1 F''_{idc}(N) = R_i(N) - Q_i(N+1) \qquad (3.6)$$

$$\Delta_1 F''_{icd}(N) = Q_i(N) - P_i(N+1) \qquad (3.7)$$

where i = 1 or 2. At small N, $P_1 Q_1$ and R_1 are more intense than P_2 Q_2 and R_2 (Jevons (1932), p.177) so in this case P_1 Q_1 R_1 lie to the violet of P_2 Q_2 R_2. This means that F''_2 (N) has more energy than F''_1 (N).

The wave numbers of all the bands of this system are presented in tables 3.6(NH^+) and 3.7(ND^+). The assignments for the (0,0) and (1,0) bands of NH^+ agree in the main with those of Feast, but two important corrections must be explained.

1) The rotational energy of $^2\Sigma$ states is given to a good approximation by

$$F_1(N) = BN(N+1) - DN^2(N+1)^2 + HN^3(N+1)^3 + \tfrac{1}{2}\gamma N \qquad (3.8)$$

$$F_2(N) = BN(N+1) - DN^2(N+1)^2 + HN^3(N+1)^3 - \tfrac{1}{2}\gamma(N+1) \qquad (3.9)$$

where the splitting $F_1(N) - F_2(N)$ is caused by a small magnetic coupling between N and S. Substitution in (3.1) yields

$$\Delta_2 F_1(N) - \Delta_2 F_2(N) = 2\gamma \text{ (constant)} \qquad (3.10)$$

The values of 2γ as calculated from the present measurements but using Feast's assignments are shown in table 3.4. There is an abrupt change of sign, showing that for N=10ff Feast's assignments are wrong and R_1,P_1 and R_2,P_2 should be interchanged.

Table 3.4: Values of 2γ for NH^+ $^2\Sigma^+$ state, using Feast's numbering.

N	(0,0)	(1,0)	N	(0,0)	(1,0)
2	0.29/	0.11	10	- 0.16	- 0.20
3	0.20	0.23		- 0.19	- 0.15/
4	0.22	0.22	11	- 0.07	- 0.17
5	0.26	0.24	12	0/	0/
6	0.23	0.21	13	- 0.20	- 0.18
7	0.20	0.22	14	- 0.13/	- 0.10
8	0.23	0.20	15	- 0.15	- 0.16
9	0.16	0.23	16	- 0.04/	- 0.19
	0.20	0.16	17	- 0.15/	- 0.11

Why did this mistake occur? There is a large perturbation in the F_c'' levels which culminates at N"=9,10. It is not therefore possible to connect the R and P branches at high N with those at low N in a regular fashion. Since Feast could not resolve the spin splitting in the upper state, he could only decide which pair of branches belonged to the F_1 levels by using equations (3.6) and (3.7). In this case the differences would agree within experimental error for either choice of sub-band! (The corrected assignments have been verified from the other band systems of NH^+).

2) For $^2\Pi$ states the rotational term values for any magnitude of the coupling between S and Λ are given by the equation of Hill and Van Vleck (1928):

$$F_{1,2}(J) = B_v((J+\tfrac{1}{2})^2 - 1 \mp \tfrac{1}{2}(4(J+\tfrac{1}{2})^2 + Y(Y-4))^{\frac{1}{2}}) \quad (3.11).$$

Here $Y = A/B_v$, where A is the spin-orbit coupling constant. The solution of (3.11) for observed values of $F_1(J)-F_2(J)$ gives two values of Y which are symmetrical about Y=2. There is only one level for which $J=\frac{1}{2}$ and if $Y>2$ this belongs to the F_1 series whereas if $Y<2$ it belongs to the F_2 series (Mulliken (1930),p.111). Since this is the lowest possible value of J, the first lines of the branches should have different patterns for the different values of Y. Thus the ambiguity in the solution to (3.11) may be removed with favourable data.

Now Feast (p.352) gives Y=0.56, so that $J''=\frac{1}{2}$ belongs to F_2, and he assigns lines $R_2(1)$ and $Q_2(1)$ accordingly. These lines were blended with others (according to Feast) and they have not been found in the present work. Instead, additional members of the Q_1 and R_1 branches have been found, corresponding to a level with $J'' = \frac{1}{2}$. Furthermore an open branch has been found at shorter wavelengths than the R_1 band head and this corresponds to the $^{S}R_{21}$ branch which would be forbidden if the $^{1}\Pi$ state were strictly case (b). This branch has $\Delta K = 2$ and $\Delta J = 1$; it may be predicted from the relation

$$^{S}R_{21}(N) = Q_1(N) + \Delta_2 F_1'(N+1) - (F_1'(N+2)-F_2'(N+2)) \quad (3.12).$$

The first member of the $^{S}R_{21}$ branch corresponds to the prediction from the Q_1 line with $J'' = \frac{1}{2}$. It follows that, contrary to Feast, the level with $J''=\frac{1}{2}$ belongs to the F_1 series and Y is <u>greater</u> than 2. Examination of equation (3.11) shows that if Y is between 0 and 4 (the

two values corresponding to pure case (b)) then for a given N the F_2 levels lie below the F_1 levels. This is not so here, so that again Feast's value for Y must be mistaken.

The ^SR branch of the (0,0) band appears weakly on the plate in Sharma's thesis. He did not comment on this, however, and since he reproduced two typographical errors from Feast's published wave numbers, we may assume that he did not check the analysis. In the $^2\Pi$ states of the CH group of hydrides - with the same electron configuration as NH^+ - Douglas (1957) pointed out that $J'' = \frac{1}{2}$ belonged to F_2 for CH (Y just less than 2) but to F_1 for SiH (much nearer to case (a)).

Since Y is greater than 2, A is positive and the $^2\Pi$ state is <u>regular</u>. This eliminates NH^- as a possible carrier since, like OH, its only $^2\Pi$ state of low energy is inverted. Thus, provided that we ignore triply-charged ions, the present system must be carried by NH^+. The lines $^SR_{21}(\frac{1}{2})$, $Q_1(\frac{1}{2})$ and $R_1(\frac{1}{2})$ were also found for ND^+, confirming the above argument.

The rotational lines have been found for N'' as high as 29(ND^+) &21 (NH^+). The development for NH^+ is comparable to that of Feast and better than that of Sharma (N'' ≃15) who said that the presence of helium lowers the rotational temperature of the molecule. As the present experiment was directed chiefly towards the (2,0) bands, the nitrogen pressure was higher than that used in the visible region and so the N_2 Second Positive bands obscured more of the

(0,0) bands than in Feast's discharge. There was also a very weak violet-degraded nitrogen band at λ2609 which overlapped the head of the (2,0) NH^+ band. This nitrogen band is being investigated as it does not seem to correspond with any published band head.

Extra lines have been found at the perturbations as follows:

NH^+: $P_1(9)$, $P_1(10)$, $P_2(9)$, $P_2(10)$, $Q_2(6)$, $R_1(9)$, $R_1(10)$, $R_2(9)$, $R_2(10)$

ND^+: $P_1(18)$, $P_2(18)$, $R_1(18)$, $R_2(18)$.

For ND^+, $Q_2(12)$ was also perturbed, but no extra lines were found.

The first lines of the satellite branches are indicated in Figure 3.1 by dashed lines. Their frequencies were predicted from the following equations. Since γ for the $^2\Sigma^+$ state is known (table 3.4), the spin splitting at any rotational level of the upper state can be calculated.

$$^{O}P_{12}(N) = Q_2(N) - \Delta_2F_2'(N-1) + F_1'(N-2) - F_2'(N-2) \quad (3.13)$$

$$^{R}Q_{21}(N) = R_1(N) - (F_1'(N+1) - F_2'(N+1)) \quad (3.14)$$

$$^{P}Q_{12}(N) = P_2(N) + F_1'(N-1) - F_2'(N-1) \quad (3.15)$$

$$^{Q}P_{21}(N) = Q_1(N) - (F_1'(N) - F_2'(N)) \quad (3.16)$$

$$^{Q}R_{12}(N) = Q_2(N) + F_1'(N) - F_2'(N) \quad (3.17)$$

From the formulae of Earls (1935) one would expect the $^{O}P_{12}$ branch ($\Delta N = -2$) to be the most intense satellite, followed by $^{R}Q_{21}$ and $^{S}R_{21}$. In practice most lines have been found for $^{S}R_{21}$, as it was photographed at longer exposure along with weaker bands. The spin splitting in

the $^2\Sigma$ state is so small that early members of the satellite branches with $|\Delta N| < 2$ cannot be resolved from lines of the main branches. Table 3.5 shows the number of satellite lines included in the tables of wave numbers.

Table 3.5: Number of satellite lines found in $^2\Sigma^+ - ^2\Pi$

		$^SR_{21}$	$^OP_{12}$	$^RQ_{21}$	$^PQ_{12}$	$^QP_{21}$
NH^+	(0,0)	10	5			
	(1,0)	9	8			
	(2,0)		3			
ND^+	(0,0)	12	8	3	1	1
	(1,0)	12	8			
	(2,0)	5	6			

Table 3.6 : Wave numbers of the $^2\Sigma^+ - {}^2\Pi$ system of NH^+, in cm^{-1}

(0,0) band

N	P_1	Q_1	R_1	P_2	Q_2	R_2
($J=\frac{1}{2}$)	-	34561.06	34587.17	-	-	-
1	34527.74	552.85	604.97	-	-	-
2	491.03	541.72	619.60	34481.76*	34533.37	34610.04
3	450.21	526.41	629.83	442.56	520.18	621.98
4	404.95	506.48	635.27	397.95	501.47	628.05
5	355.25	481.76*	635.92	348.30	477.68	628.71
6	301.21	452.18	631.63	293.83	443.10	624.02
	-	-	-	-	454.37	-
7	243.29	417.63	622.84	234.88	413.31	614.23
8	182.54	378.06	610.58	172.14	374.15	599.95
9	122.47	333.36	598.16	108.69	329.67	584.22
	059.09	-	534.84	064.04	-	539.59
10	004.63	283.49	527.14	009.68	279.91	532.03
	069.68	-	592.19	055.49	-	577.81
11	33933.97*	228.33	502.37*	33935.93*	224.85	504.26*
12	853.37*	167.80	466.43*	853.37*	164.38	466.43*
13	N_2	101.85	422.51	N_2	098.45	421.20
14	672.11	030.31	371.35	670.11*	026.90	369.22
15	572.82	33953.10	313.27	570.27	33949.80	310.57
16	468.08	N_2	248.24*	465.03*	N_2	245.15
17	357.85	782.13	176.41	354.48*	N_2	172.79
18	241.96	N_2	097.71	238.23	685.13	093.34
19	120.45	N_2		116.39	N_2	
20		487.57			484.95	
21		386.13			383.93	

N	$^oP_{12}$	$^sR_{21}$
($J=\frac{1}{2}$)	-	34638.06
1	-	681.06
2	34,456.33	720.90
3	391.94	756.17
4	322.36*	786.43
5	248.24*	811.38
6	163.28	830.89
7		844.72
8		852.70
9		854.69

Table 3.6 (NH^+) continued

(1,0) band

N	P_1	Q_1	R_1	P_2	Q_2	R_2
($J=\frac{1}{2}$)	-	36566.03	36590.61	-	-	-
1	36532.68	556.27	605.25	-	-	-
2	494.44	542.04	615.26	36485.16	36533.67	36605.87
3	450.52	522.07	619.32	442.91	515.87	611.48
4	400.63	495.99/	617.09	393.63	490.98	609.87
5	344.70	463.55	608.42	337.80	459.52	601.28
6(	282.95	424.74	593.41	275.59	415.68	585.84
(	-	-	-	-	426.96	-
7	215.72	379.43	572.37	207.35	375.14	563.78
8.	144.24	327.56	546.35	133.86	323.65	535.77
9(	071.90	269.07	518.69	058.24	265.41	504.80
(	008.60	-	455.34	013.58	-	460.16
10(	35940.36	203.91	430.97	35945.49	200.40	435.90
(	36005.44	-	495.99/	991.32	-	481.72
11	35854.50	132.06	388.03	856.63	128.62	389.99
12	757.16/	053.41	332.53/	757.16/	050.02	332.53/
13	651.31	35967.87/	267.54	650.23	35964.52	266.28
14	538.13	875.39	193.96	536.21	872.07	191.94
15	417.90	775.86	112.19	415.44	772.61	109.57
16	290.79	669.34	022.16	287.88	666.13	019.06
17	156.75	555.90	35923.78	153.41	552.80/	35920.33
18	015.79	435.66	817.03	012.18	432.69	813.10
19	34867.83	309.28	701.72	34863.89	306.43	
20	712.86	176.76		708.65		

N	$^oP_{12}$	$^sR_{21}$
($J=\frac{1}{2}$)	-	36638.41
1	-	676.75
2	36461.36	710.43
3	395.34	737.98
4	322.67	759.03
5	243.57	773.45/
6	152.71	780.49/
7	065.48	780.49/
8	35967.87/	773.45/
9	864.35	

Table 3.6 (NH^+) continued

(2,0) band

N	P_1	Q_1	R_1	P_2	Q_2	R_2
($J=\frac{1}{2}$)	-	38423.40	38446.59	-	-	-
1	38390.14	412.13	458.30	-	-	-
2	350.38	395.05	463.97	38341.22	38386.64	38454.31/
3	303.51	370.67	462.00	296.03/	364.46	454.31/
4	249.21	338.69	452.48	242.34/	333.72	445.38/
5	187.45	298.98	435.08	180.54	294.95	427.97
6	118.37	251.39/	409.85	111.01	242.34/	402.41
(	-	-	-	-	253.60	-
7	042.38	195.85	377.20	034.02	191.63	368.63/
8	37960.72/	132.38/	338.14	37950.38	128.59	327.65
9	876.79/	060.88	296.03/	863.10	057.28	282.23
(	813.41	-	232.64	818.56		
10	732.14/	37981.32	192.50	737.35	37977.84	197.44
(	797.13	-	257.58	783.08	-	243.29
11	631.86	893.67	132.38/	634.00	890.24	134.43
12	518.77/	797.82	058.38/	518.77/	794.48	058.38/
13	395.63	693.70	37973.50	394.61	690.44	37972.34
14.	264.03/	581.37	878.83	262.22/	578.14	876.79/
15	123.88/	460.74	774.62	121.50/	457.51	772.06
16	36975.62	331.78	660.91	36972.85	328.65	657.95
17	819.18	194.61	537.74	815.89	191.50	534.21
18	654.30		404.88/	650.88	046.47	400.88
19	481.75/	36896.82			36894.21	258.16

N	$^oP_{12}$
2	
3	38251.39/
4	
5	092.33
6	37995.26

Table 3.6 (NH^+) continued

(1,1) band

N	P_1	Q_1	R_1	P_2	Q_2	R_2
1	N_2			-	-	-
2	N_2			33574.64/	N_2	
3	33543.94	N_2		541.51	N_2	
4	499.86	N_2		498.90	33574.64/	
5	450.25	33560.80		449.70	550.90	
6	395.16	530.32		394.72	521.74	N_2
7	334.77	494.64		334.10	487.05	N_2
8	269.02	453.58		268.26	446.80	33670.11/
9	198.12	406.93	N_2	196.97	400.78	N_2
10	121.87	354.48/	N_2	120.45/	348.92	N_2
11		296.67	33573.79		291.23	
12		232.85			227.50	
13		162.99			158.01	

(2,1) band

N ($J=\frac{1}{2}$)	P_1	Q_1	R_1	P_2	Q_2	R_2
	-	N_2	N_2	-	-	-
1		N_2	N_2	-	-	-
2	35438.68	35479.55	N_2	35430.82	N_2	N_2
3	397.05	N_2	35555.46	394.44	35441.64	35552.80/
4	348.43/	429.24	N_2	347.55	417.38	N_2
5	292.94	396.24	N_2	292.46	386.35	N_2
6	230.59	356.98	N_2	230.13	348.43/	N_2
7	161.42	311.09	496.21	160.80	303.56	495.47
8	085.53	258.39	N_2	084.73	251.67	N_2
9	002.98	198.74	422.24	001.98	192.58	421.12
10	34913.68	132.06	374.11	34912.48	126.34	372.71
11	817.71	058.21	318.30	816.29	052.84	316.63
12	715.10	34977.22	254.79	713.45	34972.04	253.09
13		888.87	183.58		883.96	181.54
14		793.24	104.90		788.38	102.24
15		690.19			685.51	

N	$^oP_{12}$
2	35391.37

Table 3.6 (NH^+) continued

(3,1) band

N	P_1	Q_1	R_1	P_2	Q_2	R_2
($J=\frac{1}{2}$)	-	37243.76	37252.73	-	-	-
1	37196.85	223.96		-	-	-
2	157.60	195.74	264.03/	37149.76	37175.60	
3	113.26	168.60	262.22/	110.69	153.65	37259.66/
4	060.62	135.77	251.18	059.56	123.88/	250.06
5	36999.38	095.81	231.74	36998.93	085.93	231.07
6	929.83/	048.15	203.59	929.83/	039.65	
7	852.60	36992.54	166.70	851.98	36985.12	165.96
8	767.03	928.86	121.50/	766.29	922.23	120.13
9	673.43	856.84	066.89	672.40	850.70	065.54
10	571.67	776.44	003.30	570.75	770.83	002.18
11		687.63			682.33	
12				342.86		

Table 3.7 : Wave numbers of the $^2\Sigma^+ - ^2\Pi$ system of ND^+, in cm^{-1}

(0,0) band

N	P_1	Q_1	R_1	P_2	Q_2	R_2
($J=\frac{1}{2}$)	-	34702.93	34716.97	-	-	-
1	34681.62	695.18	723.22	-	-	-
2	659.09	686.38	728.35	34626.98	34654.67	34696.13
3	635.02	676.03	731.86	608.91/	650.36	705.52
4	608.91/	663.80	733.43	586.89	642.39	711.14
5	580.85	649.38	732.71	561.66	631.08	713.33
6	550.47	632.68	729.56	533.38	616.69	712.33
7	517.73	613.47	723.88	502.18	599.33	708.23
8	482.58	591.84	715.59	468.20	579.10	701.12
9	444.97	567.60	704.63	431.46	556.04	691.00/
10	404.92	540.73	691.00/	392.04	530.22	677.98
11	362.42	511.20	674.55	349.96	501.85	661.99
12	317.48	479.00	655.40	305.23	466.87	643.04
13	270.14	444.01	633.55	257.92	434.52	621.19
14	220.57/	406.30	608.91/	208.11	397.50	596.46
15	168.98	365.76	582.20	155.91	357.44	569.01
16	115.94	322.36	553.47	101.82	314.46	539.26
17	062.71	276.09	524.13	047.14	268.51	508.50
18	N_2	226.86	496.62	N_2	219.59	480.40
(		-	437.01	33955.56	-	440.34
19	33899.21	174.68	407.06	900.70	167.63	408.41
20	N_2	119.44	368.62	837.35	112.64	367.61
21	N_2	061.16	323.79/	N_2	054.60	321.22
22	N_2	33999.54/	274.31	697.07		
23	N_2	N_2	220.57/	N_2	N_2	216.14
24	547.77	N_2	162.52	543.19	N_2	157.84
25	466.33	N_2		461.48	N_2	
26	381.69	723.15		376.57	N_2	
27	293.80	N_2		288.41	N_2	
28	202.44	566.55		196.99	33561.94	
29		484.88				

Table 3.7 (ND^+) (0,0) band continued

N	$^{O}P_{12}$	$^{S}R_{21}$	$^{R}Q_{21}$	$^{P}Q_{12}$	$^{Q}P_{21}$
($J=\frac{1}{2}$)	-	34744.41			
1	-	764.45			
2	34613.47/	783.15/			
3	581.21	800.24			
4	545.71	815.33			
5	506.98	828.08			
6	465.22	838.37	/		
7	420.63	846.04	/		/
8	373.43	850.94	34715.01	/	/
9	323.79/	853.07	703.97	/	34567.03
10		852.18	690.34	34392.69	
11		848.41			

Table 3.7 (ND^+) continued

(1,0) band

N	P_1	Q_1	R_1	P_2	Q_2	R_2
($J=\frac{1}{2}$)	-	36198.80	36212.26	-	-	-
1	36177.53	190.48	217.28	-	-	-
2	154.40	180.44	220.60	36122.28	26148.74	36188.35
3	129.07	168.28	221.65	102.87	142.62	195.33
4	101.27	153.54/	220.16	079.16	132.19	197.85/
5	070.71	136.14	215.77	051.51	117.86	196.44
6	037.28	115.73	208.35	020.18	099.81	191.15
7	000.86	092.34	197.85	35985.37	078.18	182.17
8	35961.46	065.78/	184.03	947.08	053.16/	169.56
9	918.96	036.09	167.03	905.46	024.55	153.54/
10	873.41	003.16	146.67	860.54	35992.68	133.70
11	824.82	35966.99	123.02	812.36	957.68	110.45
12	773.17	927.52	096.02	760.94	915.42	083.69
13	718.56	884.66	065.78/	706.33	875.18	053.16/
14	661.09	838.46	032.23	648.62	829.71	019.60
15	601.07	788.89	35995.76	588.00	780.61	35982.61
16	538.96	735.88	956.86	524.86	727.98	942.68
17	476.19	679.39	916.78	460.66	671.82	901.18
18(	415.12	619.41	877.94	399.03	612.16	861.78
(	355.48	-	818.29	359.04/	-	821.81
19	291.88	555.92	776.60	293.33	548.93	777.96
20	219.60	488.86	725.67	218.64	482.09	724.72
21	141.05	418.23	667.94	138.60	411.68	665.35
22	057.68	343.95/	N_2	054.19	337.62	
23	34970.04	265.98	N_2	34966.01	259.84	N_2
24	878.45	184.35	N_2	873.90	178.47	N_2
25	783.15/	099.07	387.88	778.26	093.43	382.91
26		010.26	306.62		004.82	301.43
27		34917.81	220.93		34912.80	215.62
28					817.65	

Table 3.7 (ND^+) (1,0) band continued

N	$^{o}P_{12}$	$^{s}R_{21}$
$(J+\frac{1}{2})$	-	36238.55/
1	-	256.50/
2	36109.12	272.86
3	076.60	286.88
4	039.83	298.36
5	35999.21	306.78
6	955.13	312.18
7	907.49	314.30
8	856.57	313.20
9	802.35	308.62
10		300.40
11		288.98

Table 3.7 (ND^+) continued

(2,0) band

N	P_1	Q_1	R_1	P_2	Q_2	R_2
($J=\frac{1}{2}$)	-	37613.57	37626.14/	-	-	-
1	37592.23	604.51	630.42/	-	-	-
2	568.49	593.40	631.78	37536.41	37561.74	37599.44
3	541.98/	579.47	630.42/	515.74	553.78	
4	512.35	562.41	626.14/	490.46/	540.97	603.79
5	479.44/	541.98/	618.12	460.23	523.75/	598.87
6	443.10	518.03	606.56	426.02	502.11	589.38
7	403.14	490.46/	591.32	387.63	476.39	575.73
8	359.60	459.26	572.32	345.27	446.58	557.88
9	312.43	424.31	549.41	298.95	412.80	535.84
10	261.66	385.50	522.65	248.82	375.05	509.69
11	207.22	342.90	491.95	194.78	333.62	479.44/
12	149.15	296.49	457.49	136.95	284.37	445.13
13	087.59	246.07	419.05	075.39	236.60	406.72
14	022.59	191.78	376.88	010.12	183.05/	364.33
15	36954.37	133.55	331.18	36941.37	125.30	318.00
16	883.66	071.30/	282.50	869.66	063.48	268.38
17	811.55	005.06	232.16	796.18/	36997.60	216.57
18(	740.72	36934.86	183.05/	724.92/	927.61	166.40
(	681.18	-	122.84	684.68	-	126.21
19	607.27	860.48	069.76	608.60/	853.54	071.30/
20	524.16	782.05	006.95	523.33	775.31/	006.01
21	434.16	699.52		431.75	693.04	36934.34
22	339.00	612.67/		335.59	606.57	857.41
23	238.60/	522.05		234.83	515.92	775.31/
24		427.47/			421.10	688.71
25					321.93	

Table 3.7 (ND^+) (2,0) band continued

N	$^oP_{12}$	$^sR_{21}$
(J=½)	-	37651.54
1	-	667.90
2	37523.75≠	681.69
3	490.46≠	
4	452.70	
5	410.38	705.01
6		
7	313.37	
8		695.74
9	200.52	

(2,1) band

N	P_1	Q_1	R_1	P_2	Q_2	R_2
(J=½)	-	35465.52≠	N_2	-	-	-
1	35445.57	N_2	N_2	-	-	-
2	423.59	447.22	35486.71≠	35395.61≠	35420.79	N_2
3	399.49	435.00	N_2	376.49	414.58	N_2
4	373.12	420.08	486.71≠	353.37≠	404.85	N_2
5	344.56	402.37	483.12	327.04	395.61≠	35465.52≠
6	314.05	381.63≠	N_2	297.96	364.42	N_2
7	282.57	357.63	N_2	267.39	343.95≠	N_2
8	195.40	330.56	408.15	190.55	318.88	463.19
(	251.57	-	N_2	237.17	-	449.65
9	161.37	300.21≠	398.34	156.33	290.00	393.17
10	120.63	266.71	381.63≠	115.11	257.57	376.08
11	074.33	229.92	359.04	068.58	221.78	353.37≠
12	023.53	189.91	331.78	017.67	182.63	325.76
13	34968.67	146.71	300.21≠	34962.70	140.26	294.04
14	910.00	100.49	264.31	904.09	094.84	258.29
15	847.74	051.32	224.42	841.88	046.59	218.64≠
16	781.91	34999.62	180.71	776.17	34995.78	174.82
17		945.77	132.97		942.91	127.20
18		890.45	081.39		888.44	075.59
19			025.75			020.18

Table 3.7 (ND^+) continued

(3,1) band

N	P_1	Q_1	R_1	P_2	Q_2	R_2
$(J=\frac{1}{2})$-		36803.17		-	-	-
1	36783.33/	794.42	36819.64	-	-	-
2	760.64	783.33/	821.14	36732.50	36756.90	
3	735.57	769.43	820.08	712.58	748.99	36796.96
4	707.51/	752.26	816.01	687.87	736.99	796.18/
5	676.69/	731.64	809.04	659.22	724.92/	791.43
6	643.39	707.51/	799.41	627.36	690.41	783.33/
7	608.60/	679.59	788.19	593.39	665.97	772.89
8	517.26	648.00	720.52	512.51	636.36	715.51
	573.52/	-	776.49	559.13	-	762.01
9	478.85	612.67/	705.25	473.70	602.38	
10	432.96	573.52/	682.30	427.47/	564.38	676.69/
11	381.07	530.52	653.07	375.30	522.42	647.11
12	324.03	483.79	618.45	318.15	476.52	612.67/
13		433.31	578.93	256.55/	426.89	572.88
14		379.30		190.53/	373.69	
15	126.46			120.74		

3.2 The λ4348 and λ4334 bands

The λ4348 band of NH^+ and the λ4334 band of ND^+ were photographed on Zenith Astronomical plates with an exposure time of 15 minutes. This was sufficient to record the satellite branches as well as the more intense structure, and the wave numbers of strong lines are accurate to $\pm$ 0.01cm^{-1}. The λ4300 system of CH(CD) was present but did not interfere with the analysis. A more striking "impurity" was the third member of the Balmer series, Hγ(4340Å); and in fact Dγ(4339Å) obscured quite a portion of the ND^+ band, but fortunately this was near the gap where the branches begin.

As the isotope shift is small, these must be the (0,0) bands of a system. Preliminary analysis at lower dispersion showed that the lower state was $^2\Pi$ (v = 0). Accordingly we expect the system to be the analogue of one of the CH systems - $^2\Sigma - ^2\Pi$ at λ3900 or $^2\Delta - ^2\Pi$ at λ4300. It is clear from Plate 3, which shows part of the bands, that there are so many branches that the transition must be $^2\Delta - ^2\Pi$. The first line of each of the 24 possible branches in such a band is shown in Figure 3.2.

As the $^2\Pi$ state is near to case (b), twelve of the branches - indicated by full lines in the figure - will be much more intense than the others for moderate values of N. These branches may be written

$$\begin{aligned} P_{ic}(N) &= \nu_o + F_{ic}'(N-1) - F_{ic}''(N) \\ Q_{icd}(N) &= \nu_o + F_{ic}'(N) - F_{id}''(N) \\ R_{ic}(N) &= \nu_o + F_{ic}'(N+1) - F_{ic}''(N) \end{aligned} \qquad (3.18)$$

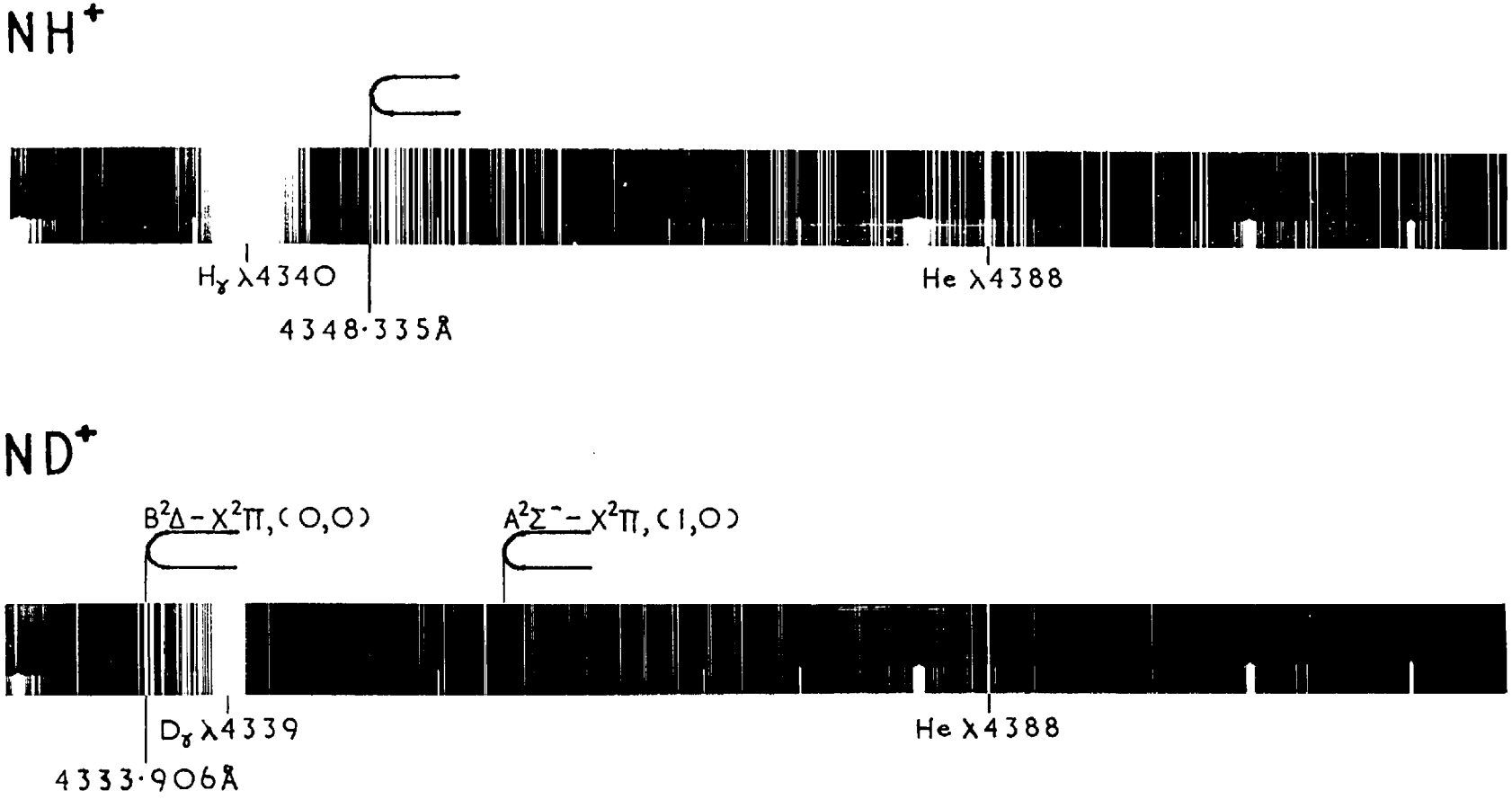

PLATE 3 : (0,0) BANDS OF $B^2\Delta - X^2\Pi$

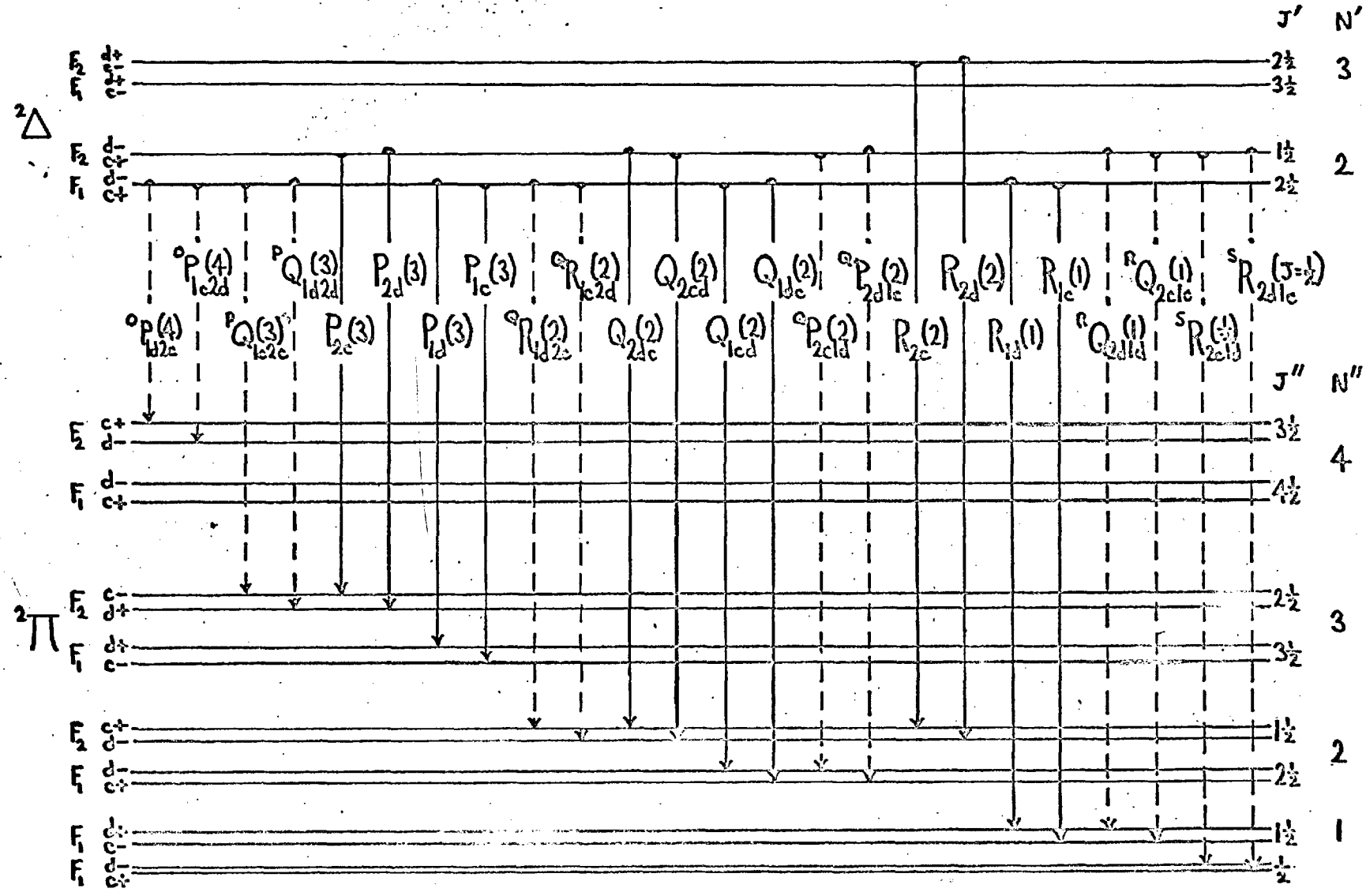

Figure 3.2: First lines for $^2\Delta - {}^2\Pi$(b)

$$P_{id}(N) = \nu_0 + F_{id}'(N-1) - F_{id}''(N)$$
$$Q_{idc}(N) = \nu_0 + F_{id}'(N) - F_{ic}''(N) \qquad (3.19)$$
$$R_{id}(N) = \nu_0 + F_{id}'(N+1) - F_{id}''(N)$$

where i = 1 or 2. Consider the lower state combination differences for the trio (3.18):

$$Q_{icd}(N) - P_{ic}(N+1) = \Delta_1 F_{icd}''(N) \qquad (3.20)$$
$$R_{ic}(N) - Q_{icd}(N+1) = \Delta_1 F_{idc}''(N) \qquad (3.21)$$

These equations are essentially the same as equations (3.6) and (3.7). In other words, P_{1c}, Q_{1cd} and R_{1c} are related by the same lower state differences as P_1 Q_1 R_1 for the ultraviolet $^2\Sigma^+ - {}^2\Pi$ system. Similarly P_{2c} Q_{2cd} and R_{2c} are related in the same way as P_2 Q_2 R_2 in the ultraviolet system.

Now consider the lower state combination differences for the trio (3.19):

$$Q_{idc}(N) - P_{id}(N+1) = \Delta_1 F_{idc}''(N) \qquad (3.22)$$
$$R_{id}(N) - Q_{idc}(N+1) = \Delta_1 F_{icd}''(N) \qquad (3.23)$$

Here we have the same differences, but this time $\Delta_1 F_{dc}(N)$ is obtained as the difference between a Q line and a P line rather than as the difference between a Q line and an R line. $\Delta_1 F_{cd}(N)$ is obtained from a Q line and an R line instead of from a Q line and a P line. This means that the four lower state differences known accurately from $^2\Sigma^+ - {}^2\Pi$, namely $\Delta_1 F_{1cd}(N)$, $\Delta_1 F_{1dc}(N)$, $\Delta_1 F_{2cd}(N)$ and $\Delta_1 F_{2dc}(N)$, can be used to relate the four Q branches of $^2\Delta - {}^2\Pi$ with the four P branches (or the four R branches) in a unique manner.

For example, if we take one line Q(N) and

predict members of possible P branches by combining it with $\Delta_1 F_{1dc}''(N)$, $\Delta_1 F_{2dc}''(N)$, $\Delta_1 F_{1cd}''(N)$ and $\Delta_1 F_{2cd}''(N)$, then only one of these predictions will in fact coincide with a P line. Having found the successful difference, we know immediately which of the Q and P branches are involved.

Fragments of the Q branches can be picked out by eye, and these were used to predict the P branches (as described above) and to establish the absolute numbering. In this way the congested R heads were avoided during the early stages of the analysis. The final assignments were checked by comparison of the combination differences. As an example, table 3.8 shows some of the differences for NH^+ together with similar differences from the λ2886 band to show that the lower state is common. All the extra lines found at perturbations were consistent with the analysis of the ultraviolet system and confirmed the identification of the branches.

Table 3.8 : NH^+-Some differences from $^2\Delta-^2\pi$ (0)and $^2\Sigma^+-^2\pi$(0)

N	$\Delta_1F''_{1dc}(N)$			$\Delta_1F''_{1cd}(N)$		
	$^2\Sigma^+-^2\pi$	$^2\Delta-^2\pi$		$^2\Sigma^+-^2\pi$	$^2\Delta-^2\pi$	
	λ 2886	$R_{1c}(N)$ $-Q_{1cd}(N+1)$	$Q_{1dc}(N)$ $-P_{1d}(N+1)$	λ 2886	$Q_{1cd}(N)$ $-P_{1c}(N+1)$	R_{1d} $-Q_{1dc}(N+1)$
1	63.25	63.34/		61.82	-	61.85/
2	93.19	93.19	93.28/	91.51	91.39/	91.50/
3	123.35	123.37	123.37	121.46	121.47	121.44
4	153.51/	153.53	153.55	151.23	151.24	151.23
5	183.74	183.69	183.71	180.55/	180.57	180.56
6	214.00	214.01	214.01	208.89	208.96	208.93
7	244.78	244.84/	244.80	235.09	235.15	235.15
8	277.22	277.43/	277 22	255.59	255.63	255.69/
				318.97	318.95	319.01
9	314.67	314.70	314.69/	328.73	328.77	328.76
	251.35	251.37	251.37	263.68	263.69	263.71
10	298.81	298.88	298.89	349.52	349.51	349.42/
	363.86	363.93	363.94			

N	$\Delta_1F''_{2dc}(N)$			$\Delta_1F''_{2cd}(N)$		
	$^2\Sigma^+-^2\pi$	$^2\Delta-^2\pi$		$^2\Sigma^+-^2\pi$	$^2\Delta-^2\pi$	
	λ 2886	$R_{2c}(N)$ $-Q_{2cd}(N+1)$	$Q_{2dc}(N)$ $-P_{2d}(N+1)$	λ 2886	$Q_{2cd}(N)$ $-P_{2c}(N+1)$	$R_{2d}(N)$ $-Q_{2dc}(N+1)$
2	89.86	89.99/	89.99/	90.81	90.32/	90.60/
3	120.51	120.50/	120 51	122.23	122.26	122.21
4	150.37	150.38	150.39	153.17	153.21/	153.17
5	185.61	185.59	185.72/	183.85	183.88	183.88
	174.34	174.31	174.38			
6	210.71	210.71	210.71	208.22	208.28	208.28/
				219.49	219.56	219.39/
7	240.08	240.14/	240.13/	241.17	241.14/	241.14/
8	270.28	270.42/	270.38/	265.46	265.40/	265.38/
				310.11	310.10/	310.05/
9	304.31	304.36	304.35	319.99	319.98	319.98
	259.68	259.71	259.68	274.18	274.14	274.15
10	307.18	307.22/	307.25	343.98	343.85	343.82
	352.96		353.08			

In order to predict the lines of satellite branches, values of $F_1'(N)-F_2'(N)$, which we shall call $\Delta\nu_{12}(N)$, were found as follows:

for $^2\Sigma^+-^2\Pi$, $Q_1(N)-Q_2(N) = F_1'(N)-F_2'(N) + F_{2d}''(N)-F_{1d}''(N)$ (3.24)

for $^2\Delta-^2\Pi$, $Q_{1cd}(N)-Q_{2cd}(N) = F_{1c}'(N)-F_{2c}'(N) + F_{2d}''(N)-F_{1d}''(N)$ (3.25)

Equation (3.24) may be used to find $F_{2d}''(N)-F_{1d}''(N)$ from the ultraviolet system. Substitution in (3.25) yields $F_{1c}'(N) - F_{2c}'(N)$ and, since the Λ-doubling in the $^2\Delta$ state is negligible (see chapter 4), this is $\Delta\nu_{12}(N)$. Four of the satellite branches can be found as follows:

$$^{R}Q_{2c1c}(N)=\nu_o+F_{2c}'(N+1)-F_{1c}''(N) = R_{1c}(N) -\Delta\nu_{12}(N+1) \quad (3.26)$$

$$^{P}Q_{1c2c}(N) =\nu_o+F_{1c}'(N-1)-F_{2c}''(N) = P_{2c}(N) +\Delta\nu_{12}(N-1) \quad (3.27)$$

$$^{Q}P_{2d1c}(N)= \nu_o+F_{2d}'(N)-F_{1c}''(N) = Q_{1dc}(N) -\Delta\nu_{12}(N) \quad (3.28)$$

$$^{Q}R_{1d2c}(N)= \nu_o+F_{1d}'(N)-F_{2c}''(N) = Q_{2dc}(N) +\Delta\nu_{12}(N) \quad (3.29)$$

Four more branches are obtained by interchanging c and d in (3.26-29). The remaining satellites are those with $\Delta N= \pm 2$, and these were predicted by comparison with the λ2886 and λ2878 bands, using methods like that of (3.24-25). The transitions concerned are

$$^{s}R_{2c1d}(N)=\nu_o+F_{2c}'(N+2) -F_{1d}''(N) \quad (3.30)$$

$$^{s}R_{2d1c}(N)=\nu_o+F_{2d}'(N+2) -F_{1c}''(N)$$

$$^{o}P_{1c2d}(N)=\nu_o+F_{1c}'(N-2) -F_{2d}''(N) \quad (3.31)$$

$$^{o}P_{1d2c}(N)=\nu_o+F_{1d}'(N-2) -F_{2c}''(N)$$

All 24 possible branches were found for ND^+, although the ^oP branches were very weak. For NH^+ 22 branches were found (not ^oP); the wave numbers are given in tables 3.9(NH^+) and 3.10(ND^+).

As with the $^2\Pi$ state considered in section 3.1, the term values of the $^2\Delta$ state may be represented by a Hill-Van Vleck expression having two roots for Y. The lowest value of J' is $\Lambda'-\frac{1}{2}=1\frac{1}{2}$, and if this belongs to the F_1 series, Y' is greater than 2; if $J'=1\frac{1}{2}$ belongs to the F_2 series, Y' is less than 2. During the analysis, the lines $^sR_{2c1d}(\frac{1}{2})$, $^sR_{2d1c}(\frac{1}{2})$, $^QP_{2d1c}(2)$, $^QP_{2c1d}(2)$, $Q_{2dc}(2)$, $Q_{2cd}(2)$, $^RQ_{2c1c}(1)$ and $^RQ_{2d1d}(1)$ have been found for both isotopes. Furthermore the lines $R_{1c}(\frac{1}{2})$, $R_{1d}(\frac{1}{2})$, $Q_{1dc}(1\frac{1}{2})$, $Q_{1cd}(1\frac{1}{2})$, $P_{1c}(2)$ and $P_{1d}(2)$ were not found. This means that $J' = 1\frac{1}{2}$ belongs to F_2 and that therefore Y' is less than 2. The values of $\Delta\nu_{12}(N)$ found during the prediction of the satellite branches are negative for the low members of each isotope. Thus the F_2 levels are higher than the F_1 levels at the same value of N, so that Y lies outside the range 0 to 4. Since Y is also less than 2, this means that the $^2\Delta$ state is inverted ($A<0$). In this respect it resembles the $^2\Delta$ state of CH.

In the case of ND^+, two weaker bands were found at λ4050 and λ4775 which seem to be the (1,0) and (0,1) bands of this $^2\Delta-^2\Pi$ system. Both bands were badly confused with background features and have not been analysed. Moreover, after all the lines of the (0,0) band had been assigned a number of fairly intense lines in the same region remained unassigned. Some of them were found to form two branches (Q?), but these could not

be assigned to the λ4334 system as part of, say, the (1,1) band. We shall discuss these branches again in the following section.

Table 3.9: Wave numbers of the $^2\Delta - {}^2\Pi(0,0)$ band of NH^+, in cm^{-1}

N	P_{1c}	P_{1d}	Q_{1cd}	Q_{1dc}	R_{1c}	R_{1d}
1	-	-	-	-	22926.76/	22926.07/
2	-	-	22863.42	22864.22	945.86	945.05/
3	22772.03/	22770.94/	852.67	853.55	961.75	960.85
4	731.20	730.18	838.38	839.41	974.08	973.06
5	687.14	685.86	820.55	821.83	982.81	981.53
6	639.98	638.12	799.12	800.97	988.02	986.13
7	590.16	586.96	774.01	777.20	990.00/	986.77
8	538.86	532.40	745.16	751.62	990.00/	983.47
9(	489.53	474.40	712.57	727.78/	990.84/	975.76
(	426.21	-	-	664.45	927.51	-
10(	383.80	413.09	676.14	647.00	934.68	963.79/
(	448.88	-	-	712.05	999.73	-
11	326.63	348.11	635.80	614.37	926.07/	947.59
12	260.82	279.77	591.51	572.58	907.89	926.76/
13	189.40/	207.93	543.17	524.73	882.94	901.44
14	113.46	132.52	490.73	471.70/	852.28	871.33
15	033.24	053.51	434.12	413.86	816.16	836.71/
16	21949.04	21971.05	373.33	351.33	774.63	796.66
17	860.69	885.10	308.39	284.03	727.78/	751.99
18	768.27		239.55	211.97	675.01/	702.62
19	671.72	704.22	167.37	NH		
20			091.49			

Table 3.9 (NH^+) continued

N	P_{2c}	P_{2d}	Q_{2cd}	Q_{2dc}	R_{2c}	R_{2d}
2	-	-	22860.93/	22860.93/	22940.72/	22940.72/
3	22770.61/	22770.94/	850.73	850.12	957.21	957.83
4	728.47	729.61	836.71/	835.62	969.56	970.65
5	683.50	685.23	819.18	817.48	977.89	979.62
6	635.30	631.76/	792.30	795.74	982.33	978.89
	-	643.10	803.58	-	-	990.00/
7	584.02	585.03	771.62	770.61/	983.03/	984.03/
8	530.48/	530.48/	742.89/	742.89/	980.78/	980.78/
9	477.49	472.51	710.36	715.40	978.23	973.25
	432.79	-	-	670.73	933.58	-
10	390.38	411.05	673.87	653.27	940.72/	961.34
	436.22	-	-	699.10		-
11	330.02	346.02	633.50	617.52	929.07	945.05/
12	262.08	277.57	589.12	573.63	908.71	924.22
13	189.40/	205.72/	540.71	524.43	882.49	898.79
14	112.48	130.20	488.21	470.54	850.89	868.64
15	031.58	051.12	431.55	412.03	814.16	833.80/
16	21946.85	21968.57	370.72	348.93	772.03/	793.89
17	858.02	882.64	305.79	281.17	724.61/	749.26
18		793.48	236.98	208.68	671.61	699.99
19	668.26	701.90	164.94	131.27	613.03	
20	567.05					

Table 3.9 (NH^+) continued

N	$P_{Q_{1c2c}}$	$P_{Q_{1d2d}}$	$Q_{R_{1c2d}}$	$Q_{R_{1d2c}}$	$Q_{P_{2c1d}}$	$Q_{P_{2d1c}}$
2	-	-	22855.35	22855.09	22869.14	22869.90
3	22764.57	22765.18	846.82	846.22	856.56	857.45
4	724.61/	725.66	833.80/	832.79	841.20	842.22
5	680.69	682.39	817.03	815.38	822.62	823.90
6		629.83	790.77	794.20		802.50
7	582.51	583.39	770.61/	769.49	775.06	778.31
8	529.41/	529.41/				
9		471.70/				

N	$R_{Q_{2c1c}}$	$R_{Q_{2d1d}}$	$S_{R_{2c1d}}$	$S_{R_{2d1c}}$
($J=\frac{1}{2}$)	-	-	22965.76	22966.21
1	22932.42	22931.76	23011.58	23012.24
2	949.75	948.96	056.07	056.87
3	964.55	963.79/	097.60	098.50
4	976.14/	975.15	135.59	136.60
5	984.30	983.03/	169.63	
6	989.11	987.21		
7	990.84/	987.62/		
8		984.03/		
9		976.14/		

Table 3.10: Wave numbers of the $^2\Sigma - {}^2\Pi(0,0)$ band of ND^+, in cm^{-1}

N	P_{1c}	P_{1d}	Q_{1cd}	Q_{1dc}	R_{1c}	R_{1d}
1	-	-	-	-		23042.04
2	-	-	23005.50	23005.94	23050.16	049.73
3	22954.11	22953.54/	22997.79	22998.34	056.81	056.27
4	930.74	930.18	988.67	989.22	062.03	061.44/
5	905.77	905.13	977.94	978.51	065.59	065.00
6	879.02	878.44	965.48/	966.09	067.39/	066.84/
7	850.60	850.03	951.31/	951.91/	067.39/	066.84/
8	820.40/	819.83	935.26	935.83	065.35	064.78
9	788.43	787.82	917.32	917.92	061.44/	060.81
10	754.66	754.00	897.45	898.13/	055.41	054.78
11	719.13	718.35	875.62	876.41/	047.38	046.58
12	681.85/	680.83/	851.79	852.82	D	036.31
13	642.86/	641.42	825.92	827.40	025.23/	023.76
14	602.42	600.15	797.97	800.24	011.28	008.9
15	560.62	556.92	767.94/	771.61	22995.61	22991.93/
16	518.09/	511.79	735.77	742.07	978.82	972.52
17	476.10	464.66	701.44	712.87	962.06/	950.79
18(	437.08	415.56	664.90	686.44/	948.17	926.62
(	377.51	-	-	626.86	888.41/	-
19	337.36	364.43	626.17	599.07	872.89	900.01
20		311.35	585.20	563.70	849.38	870.87
21	237.36	ND	541.89	523.07	820.40/	839.18
22		199.04	496.31	478.61	787.27	804.87
23	122.31	139.72	448.34	430.97	750.68	767.94/
24		078.27	398.04	380.55/	710.96	728.74/
25	21996.66	014.92	345.38	327.14	668.10	686.44/
26	930.05	21949.61	290.41	271.02		

Table 3.10 (ND^+) continued

N	P_{2c}	P_{2d}	Q_{2cd}	Q_{2dc}	R_{2c}	R_{2d}
2	-	-	22979.74/	22979.74/	23022.34/	23022.34/
3			976.47/	976.47/	033.97/	033.97/
4			970.69	970.45	042.52	042.81
5	22889.85/	22890.36	962.47	962.06/	048.62	049.13/
6	864.63/	865.59/	951.91/	951.31/	052.23	052.87
7	837.46	838.32	939.22	938.36	053.55/	054.39/
8	808.10	809.22	924.35	923.23	052.48	053.55/
9	776.77/	778.15	907.39	905.98	049.13/	050.64
10	743.40/	745.17	883.41/	886.66/	043.72	045.49
11	708.11	710.52	867.61	865.21	035.97	D
12	670.97/	670.09	840.89	841.70	026.04	025.23/
13	631.85	633.17	817.50	816.18	013.87	015.19
14	591.03	592.50	790.18/	788.70	22999.59	001.07
15	548.54	549.69	760.55	759.41	983.31	22984.43
16	504.87/	504.87/	728.74/	728.74/	965.48/	965.48/
17	461.38	458.00	694.65	698.07	947.33	943.90
18	421.76	409.15	658.36	670.97/	932.67	919.97
(		-	-	630.99/	892.58/	-
19	339.49		619.83	601.14	874.86	893.57
20	ND	305.27	579.05	563.34	848.93	864.63/
21		250.30	535.91	521.09	818.28	833.14
22	178.42	193.28	490.48	475.63	784.16	799.05
23	118.81	134.17	442.71	427.35	746.93	762.32
24	056.71	072.90	392.61	376.35	706.70	722.99
25		009.72	340.21		663.50	680.83/
26	21925.48	21944.64				

Table 3.10 (ND^+) continued

N	$^PQ_{1c2c}$	$^PQ_{1d2d}$	$^QR_{1c2d}$	$^QR_{1d2c}$	$^QP_{2c1d}$	$^QP_{2d1c}$
2	-	-	22973.91/	22973.91/	23011.28/	23011.86
3	22928.02/	22928.02/	972.23/	972.23/	002.03	002.52
4	908.77	909.02	967.52/	967.26	22991.93/	22992.38
5	886.66/	887.18	959.96	959.54	980.42	981.01
6	862.26	862.86	949.94	949.31	967.52/	968.05
7	835.47	836.31	937.57	936.69	952.92	953.54/
8	806.49	807.60	923.05	921.88	936.53/	937.15
9	775.42	776.77/	906.36	904.89/	918.35	918.97
10	742.36	744.12	887.56	885.97/	898.13/	898.97
11	707.28	709.68	866.98	864.63/	876.41/	876.98
12		669.47	840.42			
13	631.38	632.71				

N	$^RQ_{2c1c}$	$^RQ_{2d1d}$	$^sR_{2c1d}$	$^sR_{2d1c}$	$^oP_{1c2d}$	$^oP_{1d2c}$
($J=\frac{1}{2}$)	-	-	23069.69/	23069.69/	-	-
1	23048.30	23047.94	090.51	090.82	-	-
2	054.39/	053.92	111.38	111.85	-	-
3	059.99	059.48	131.55	132.11	-	-
4	064.53	063.96	150.51	151.06	22864.63/	22864.63/
5			167.89	168.47	828.75	
6	069.01	068.46	183.54	184.14	790.18/	789.51
7	068.63	068.06	197.32	197.87	749.27	748.54/
8					706.25	705.15
9						
10					614.75	

3.3 A new $^2\Sigma - {}^2\Pi$ system

In section 2.6 reference was made to an open branch of doublets at λ4650 belonging to a nitrogen hydride molecule. At high dispersion other branches were found, and a deuteride band was seen in the same region. It was possible to show that the deuteride band was part of a $^2\Sigma - {}^2\Pi$ system and to establish the absolute numbering of its branches without reference to any other work. When a comparison was made with the ultraviolet $^2\Sigma^+ - {}^2\Pi$ system of ND^+, it was found that the differences Q(N)-P(N+1) for the new system were in excellent agreement with the differences R(N)-Q(N+1) for $^2\Sigma^+ - {}^2\Pi$. Similarly R(N)-Q(N+1) for the new system agreed with Q(N)-P(N+1) for $^2\Sigma^+ - {}^2\Pi$.

This is reminiscent of the difference between equations (3.20-21) and equations (3.22-23). We remarked that the combination differences (3.20-21) for the trio of branches (3.18) were similar to the differences for $^2\Sigma^+ - {}^2\Pi$. Therefore the new $^2\Sigma - {}^2\Pi$ system, which has differences of the form (3.22-23), must have branches of the form (3.19), where the levels of the upper state are d levels. This means that the upper state of this system is $^2\Sigma^-$ (paragraph 1.1.2). An energy level diagram for $^2\Sigma^- - {}^2\Pi$ showing the first lines of the possible branches is given in Figure 3.3, which may be compared with Figure 3.1 ($^2\Sigma^+ - {}^2\Pi$). In each of these figures the levels of the $^2\Pi$ state have been labelled according to the experimental results for this particular case. Table 3.11 shows some of the differences for ND^+ $^2\Pi$(v=0) from

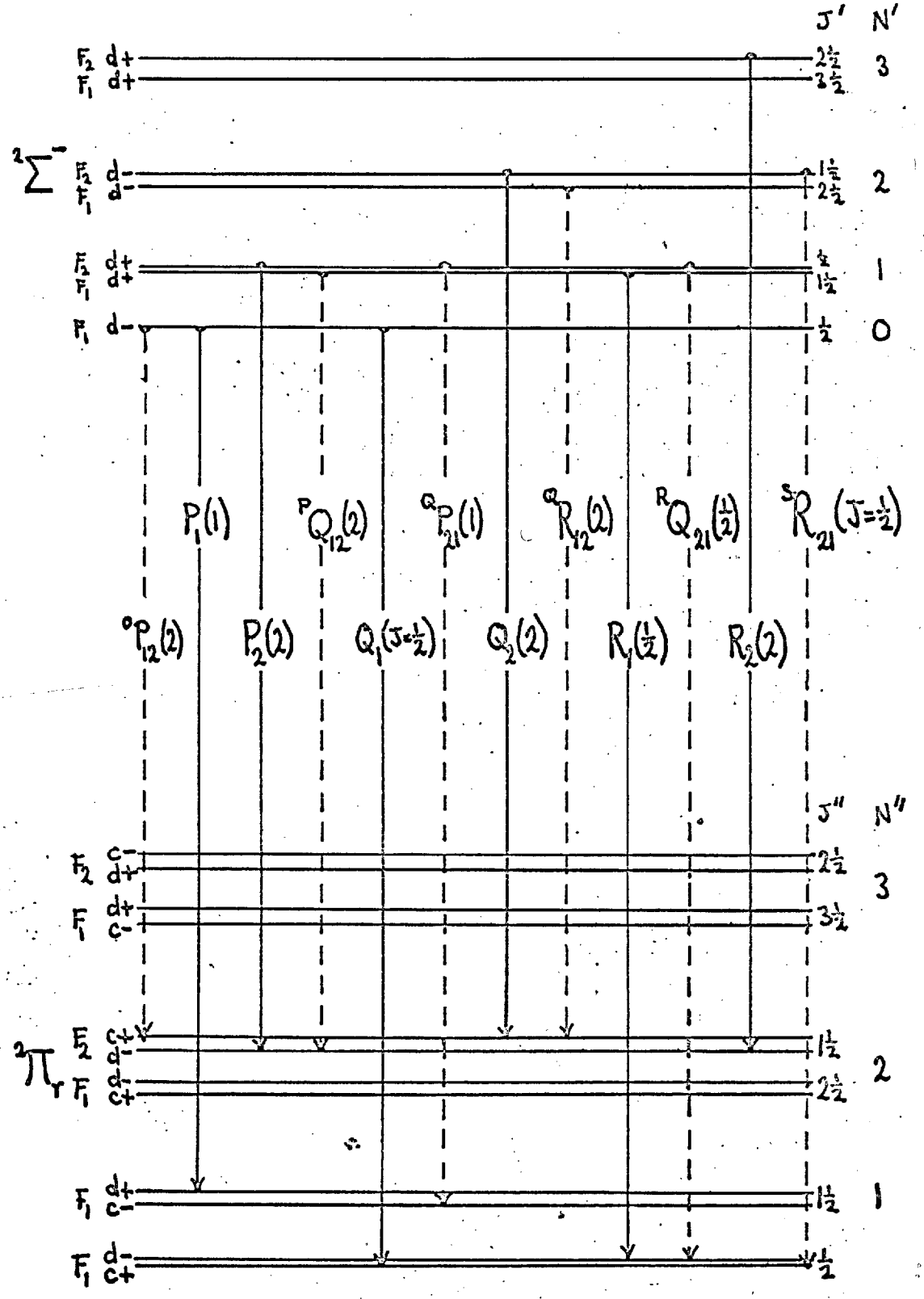

Figure 3.3: First lines for $^2\Sigma^- - ^2\Pi_r$

Table 3.11: Some differences for $^2\Pi^-(0)$ from the λ2878 and λ4593 bands of ND^+.

N	$\Delta_1 F''_{1dc}(N)$		$\Delta_1 F''_{1cd}(N)$	
	λ2878	λ4593	λ2878	λ4593
1	36.84		36.09	36.11/
2	52.32	52.32/	51.36	51.49
3	68.06	68.10	67.12/	67.06
4	84.05	84.08	82.95	82.90
5	100.03	100.04	98.91	
6	116.09	116.09	114.95	114.95
7	132.04	132.06	130.89	130.91
8	147.99	148.02	146.87	146.79/
9	163.90	163.91/	162.68	162.66
10	179.80/	179.75/	178.31	178.30

N	$\Delta_1 F''_{2dc}(N)$		$\Delta_1 F''_{2cd}(N)$	
	λ2878	λ4593	λ2878	λ4593
1	-	-	-	-
2	45.77	45.83	45.76/	45.87
3	63.13	62.57/	63.47	
4	80.06	80.05	80.73	80.74
5	96.64	96.64	97.70	97.71
6	113.00	113.01/	114.51	114.48
7	129.13	129.16	131.13	
8	145.08	145.06	147.64	147.63
9	160.78/	160.76/	164.00	163.98
10	176.13	176.14/	180.26	180.27

the bands at λ2878 ($^2\Sigma^+ - ^2\Pi$) and λ4593 ($^2\Sigma^- - ^2\Pi$).

The hydride band at about 4650Å proved to be part of the corresponding NH^+ $^2\Sigma^- - ^2\Pi$ system. The head of the band is in fact at λ4628 as shown in Plate 4(a). The region near the head is somewhat overexposed in Plate 4(a), which shows a spectrogram photographed in the first order to obtain the higher members of the branches. For each isotope, lines with frequencies greater than 21,240 cm^{-1} were measured in the second order (accuracy $\pm$0.01 cm^{-1}). Photographs in each order were obtained with Ilford Zenith Astronomical plates after exposures of 15 minutes. The first order measurements were accurate to $\pm$0.03 cm^{-1}.

Since the isotopic shift is small the above must be (0,0) bands. The rotational analysis suggested that ω_0' was relatively small: about 1669 cm^{-1} for NH^+ and 1229 cm^{-1} for ND^+. It follows that for ND^+ the (1,0) band of $^2\Sigma^- - ^2\Pi$ may be expected to overlap the (0,0) band of $^2\Delta - ^2\Pi$ in the region of the two hitherto unidentified branches mentioned at the end of Section 3.2. It was possible to show that these were indeed the Q branches of the (1,0) band by successfully predicting the positions of the other main branches. As shown in Plate 3, the band head is at λ4357, only 23Å to the red of the (0,0) $^2\Delta - ^2\Pi$ band head. The corresponding NH^+ band will be masked by the λ4300 system of CH.

The (0,1) band of $^2\Sigma^- - ^2\Pi$ has been found for

(a) NH^+ (0,0) BAND

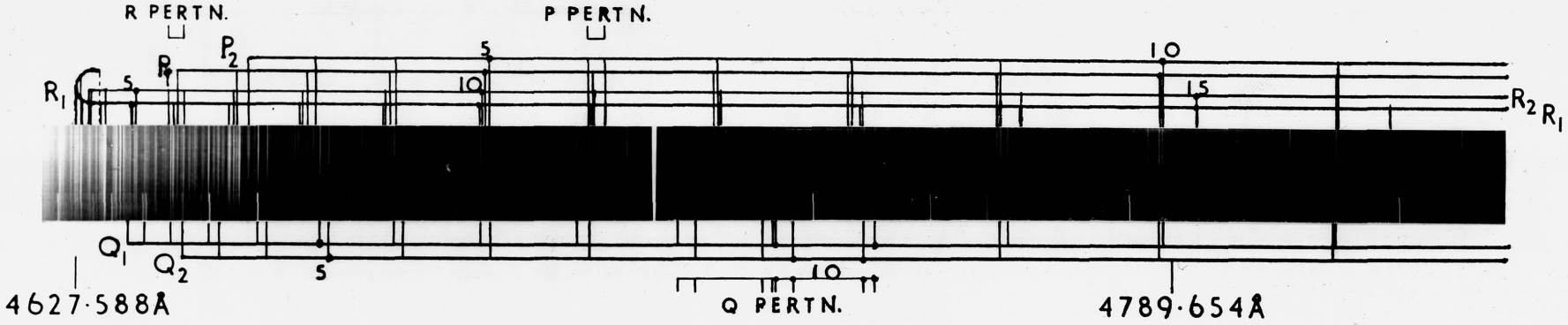

(b) ND^+ (0,1) BAND

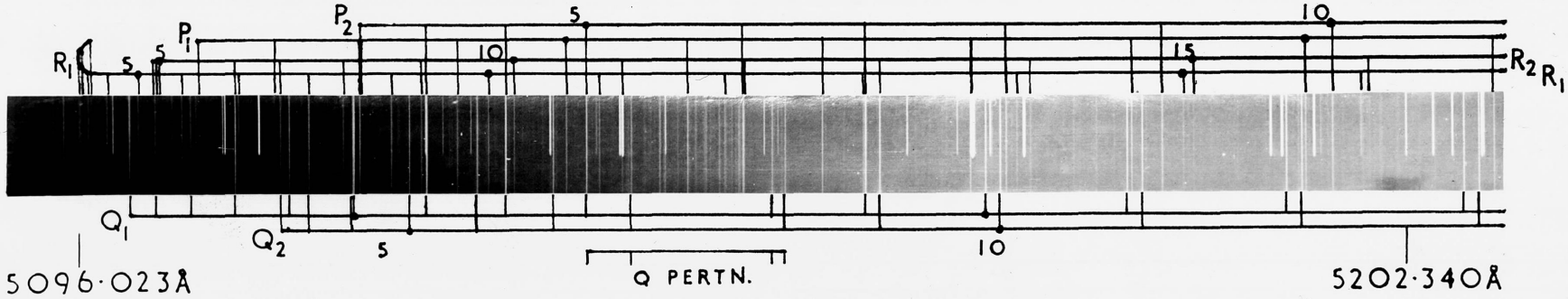

PLATE 4: $A^2\Sigma^- - X^2\Pi$ SYSTEM

each isotope and will be discussed in Section 3.4. The wave numbers of all the bands in this system are presented in tables 3.12 (NH^+) and 3.13 (ND^+).

Satellite branches were predicted in the same way as for the $^2\Sigma^+ - ^2\Pi$ bands, but none were found except for the first members of $^oP_{12}$.

Table 3.12: Wave numbers of the $^2\Sigma^- - ^2\Pi$ system of NH^+, in cm^{-1}

(0,0) band

N	P_1	Q_1	R_1	P_2	Q_2	R_2
($J=\frac{1}{2}$)	-	21567.65		-	-	-
1	21533.21	556.07		-	-	-
2	492.78	537.92	21603.48	21484.80	21529.03	21595.73
3	444.69	511.97	599.40/	439.09	504.99	594.09
4	388.61	477.94	586.99	384.46	471.80	583.04
5	324.41	435.75	566.00	321.40	429.84	563.19
6	252.04	385.45	536.30	244.25	379.32	528.74
	-	-	-	255.51	-	539.99
7	171.42	327.39	497.78	168.62	320.45	495.15
8	082.60	262.65	450.31	080.36	253.93	448.30
9	20985.41	194.68	393.74	20983.61	182.81	392.12
	-	131.41	-	-	138.19	-
10	879.95	064.93	327.91	878.45	072.10	326.68
	-	130.09	-	-	117.96	-
11	766.06/	20978.44	252.80	764.88	20982.78	
12	643.82	877.75	168.22	642.92	880.35	167.29
13	513.07/	766.06/	073.98	512.42/	767.63	073.38
14	373.78	644.22	20969.84	373.28	645.15	
15	225.95/	512.42/	856.16/	225.95/	513.07/	20856.16/
16		371.17	732.63			
17		219.93				

N	$^oP_{12}$
2	21462.26

Table 3.12 (NH^+) continued

(0,1) band

N	P_1	Q_1	R_1	P_2	Q_2	R_2
($J=\frac{1}{2}$)-		18654.65/	18688.71	-	-	-
1	18626.27/	641.99/	692.60	-	-	-
2	577.22/	626.27/	688.14	18557.56	18618.79	
3	530.78	605.57	685.44	516.37	603.57	18671.20
4	479.28	577.22/	677.66	468.17	577.22/	666.73
5	421.79	541.29		412.86	541.82	654.65/
6	357.72	497.67	641.99/	350.39	498.44	634.87
7	286.71	446.42	613.11	280.58	447.25	607.17
8	208.61	387.54	576.34	203.46	388.37	571.40
9	123.31	320.93	531.64	118.93	321.72	527.45
10	030.66	246.56	478.70	026.93	247.32	475.18
11	17930.71	164.36	417.41	17927.52	165.10	414.39
12		074.20	347.61		074.92	345.04
13		17976.00	269.11		17976.73	266.97
14			181.91			180.00
15			085.65			084.08

N	$^oP_{12}$
2	18552.06

Table 3.13: Wave numbers of the $^2\Sigma^- - ^2\Pi$ system of ND^+, in cm^{-1}

(0,0) band

N	P_1	Q_1	R_1	P_2	Q_2	R_2
($J=\frac{1}{2}$)	-		21762.38	-	-	-
1	21728.49/	N_2	764.60	-	-	-
2	704.14	21728.49/	763.89	21672.61	21696.53	21732.36
3	676.17/	712.40	759.61	650.70	686.49	
4	644.30	692.55	751.47	623.92/	670.81	730.63
5	608.47	668.57	N_2	590.76	649.89	721.63
6	568.52	640.36	722.74	553.25	623.92/	707.53
7	524.27	607.78	701.73	510.91	593.04	
8	475.73	570.82	676.17/	463.88	557.35	664.51
9	422.81	529.38	646.11	412.29	516.88/	635.69
10	365.47/	483.45	611.31	356.12	471.71	602.04
11	303.71	433.01	571.83	295.57/	421.77/	
12	237.39	378.09	527.52	226.78/	367.16	516.88/
13	166.69	318.66	478.39	158.60	307.84	470.37
14	091.39	254.87	424.39	084.15	243.93	417.24
15	011.59	186.89/	365.47/	004.91	175.59	358.90
16	20927.13	115.54		20921.02	103.18	295.57/
17	838.25	041.75		832.41	028.11	226.78/
18	744.36	20968.11		739.16	20953.99	153.07
	-	908.47	-	-	913.95	-
19	646.03	830.69				

N	$^oP_{12}$
2	21660.58
3	626.59
4	587.13

Table 3.13 (ND^+) continued

(1,0) band

N	P_1	Q_1	R_1	P_2	Q_2	R_2
($J=\frac{1}{2}$)	-		22944.24	-	-	-
1			945.41	-	-	-
2	22885.97/	22909.29	943.03	22854.48	22877.37	
3	856.92	891.56	936.53/	831.53	865.59/	22911.26
4	823.42	869.49	925.66	802.45	847.77	904.89/
5	785.41	842.78	910.15	767.73	824.10	892.58/
6	742.72	811.26	889.85/	727.42	794.83	874.62
7	695.17	774.87	864.63/	681.85/	760.14	851.19
8	642.86/	733.53	834.07	630.99/	720.09	822.36
9	585.54	687.20	798.53	575.03	674.72	788.14
10	523.33	635.87	757.79	513.96	624.12	748.54/
11	456.11	579.52	711.86	448.03	568.29	703.88
12	383.92	518.09/	660.60	373.12	507.25	649.95
13	306.74	451.78	604.10	298.65	441.00	596.15
14	224.49	380.55/	542.18	217.29	369.62	535.05
15	N_2	304.73	474.76	130.61	293.29	468.24
16	044.86	224.88	N_2	038.73		
17	21947.48	142.26		21941.77	128.72	
18	844.92		239.81	839.61		
	-	21999.63	-	-		
19		ND	150.29/			
20	624.43	813.95				
21	506.49					

Table 3.13 (ND^+) continued

(0,1) band

N	P_1	Q_1	R_1	P_2	Q_2	R_2
($J=\frac{1}{2}$)	-	19602.23	19614.16	-	-	-
1	19581.21	594.33/	617.16	-	-	-
2	557.92	583.44	617.68	19531.64/	19555.59	
3	531.64/	569.86/	615.10	511.31/	547.19	19595.02
4	501.99	553.20	609.19	487.16/	533.94	594.33/
5	468.79	533.57/	599.59	462.67/	516.64	593.63
6	431.95	511.31/	586.16	415.41	495.84	569.86/
7	391.35	487.16/	568.81	378.37/	472.78	556.03
8	346.94	406.55	547.42	336.16	402.55	536.76
(	-	462.67/	-	-	449.16	-
9	298.70	378.37/	522.01	289.46	374.13/	512.86
10	246.60	342.43	492.48	238.57	337.98	484.57
11	190.66	300.13	458.77	183.72	295.53	451.96
12	130.90	252.38	420.94	124.93	247.89	415.12
13	067.34	199.69	379.00	062.30	195.16	374.13/
14	000.08	142.26	333.01	18995.99	137.85	329.05
15	18929.35	080.27	283.17	926.19	076.03	280.17
16	855.38	013.71	229.69	853.29	009.62	227.72
17	778.76	18942.60	173.05		18938.67	172.17
18	699.94/	866.93	114.01/	699.94/	863.21	114.01/
19		786.71			783.11	
20		701.87			698.42	

3.4 Bands with v"=1

All the bands so far discussed have had $^2\Pi(v=0)$ as their final state. It may be recalled, however, that Feast gave the numbering (2,1) to a band of NH^+ at 2825Å, and that new bands with doublet branches have been found (section 2.6) at λ5348 (hydride) and λ5096 (deuteride).

The (2,1) band of the ultraviolet NH^+ system was overlapped by the λ2811 band of OH; but the OH band was weak on the final plates, and the dispersion was sufficiently great for the NH^+ branches to be picked out. A more serious impurity was the (3,0) band of the N_2 Second Positive system at λ2820 which overlapped the heads of both the NH^+ band - found to be at λ2812 - and the corresponding ND^+ band at λ2817. Furthermore, the lower states of both these bands are strongly perturbed. Consequently it was necessary to find other bands with v"=1 and to analyse them all simultaneously. In order to confirm the numbering of the above bands as (2,1) we present in table 3.14 some of the differences for v'=2 taken from the final analyses of the (2,0) and (2,1) bands of ND^+.

On the deuteride plates there was a very weak band with a head at λ2715 which proved to be the (3,1) band of the ultraviolet ND^+ system. No band head was apparent for the (3,1) NH^+ band, but its position was successfully predicted from the wave numbers of the strong bands. The head is at λ2683, just overlapped by the (0,1) band of the NH d-c system, and the band is very weak. On the

Table 3.14: Some differences for v'=2 in the $^2\Sigma^+$ state of ND^+

N	$\Delta_2F_1(N)$		$\Delta_2F_2(N)$	
	(2,0)	(2,1)	(2,0)	(2,1)
5	138.68≠	138.56	138.64	138.48≠
6	163.46		163.36	
7	188.18		188.10	
8	212.72	212.75	212.61	212.64
	-		-	212.48
9	236.98	236.97	236.89	236.84
10	260.99	261.00≠	260.87	260.97
11	284.73	284.71	284.66≠	284.79≠
12	308.34	308.25	308.18	308.09
13	331.46	331.54≠	331.33	331.34
14	354.29	354.31	354.21	354.20
15	376.81	376.68	376.63	376.76≠

hydride plates several lines to the red of the N_2 Second Positive head at λ2977 remained unidentified when the (0,0) $^2\Sigma^+ - ^2\Pi$ band had been analysed. Two pairs of doublet branches were found and identified with the main Q and P branches of the (1,1) NH^+ band. The R branches were badly overlapped by the nitrogen bands, so the (1,1) band was of little value in the analysis; but it is worthy of mention since it must be the 'band at λ2980' mentioned by Lunt, Pearse and Smith but not found by Feast. In fact the R_1 head is at λ2965, according to predictions from the known combination differences in both states. The (1,1) band of ND^+ was completely obscured by the nitrogen bands in the present experiments.

All the bands of $^2\Sigma^+ - ^2\Pi$ having v"=1 are either overlapped or very weak. The (0,1) band of $^2\Delta - ^2\Pi$ found for ND^+ at λ4775 is too weak for rotational analysis. Fortunately, the well-defined bands at λ5348 and λ5096 are the (0,1) bands of the $^2\Sigma^- - ^2\Pi$ system of NH^+ and ND^+ respectively. The λ 5096 band is shown in Plate 4(b), a print of a spectrogram taken in the first order of the 21 ft. grating using an exposure of 3 hours to Ilford Astra 3 plate. An exposure of $7\frac{1}{2}$ hours was used for the λ5348 band in order to record also the weak singlet band at λ5254 (see section 2.6 and chaper 5). The wave numbers are accurate to $\pm$ 0.02 cm^{-1} for intense lines. Table 3.15 shows some of the combination differences for the upper state of the NH^+ bands at λ4628 and λ5348 to

demonstrate that this state is common.

Table 3.15: Some differences for v'=0 in the $^2\Sigma^-$ state of NH^+

N	$\Delta_2F_1(N)$		$\Delta_2F_2(N)$	
	λ 4628,(0,0)	λ 5348,(0,1)	λ 4628,(0,0)	λ 5348,(0,1)
2	110.70		110.93	
3	154.71/	154.66	155.00	154.83
4	198.38	198.38	198.58	198.56
5	241.59		241.79	241.79/
6	284.26	284.27/	284.49	284.48
7	326.36	326.40	326.53	326.59
8	367.71	367.73	367.94	367.94
9	408.33	408.33	408.51	408.52
10	447.96	448.04	448.23	448.25

For each isotope the (2,1) and (3,1) bands of $^2\Sigma^+-^2\Pi$ and the (0,1) band of $^2\Sigma^--^2\Pi$ were analysed simultaneously. The wave numbers have been included in tables 3.6, 3.7 ($^2\Sigma^+-^2\Pi$) and 3.12, 3.13 ($^2\Sigma^--^2\Pi$). For ND^+, perturbations in the F_{1c}'' and F_{2c}'' levels culminated at N"=8 and extra lines were found for $P_1(8)$, $P_2(8)$, $R_1(8)$ and $R_2(8)$ of $^2\Sigma^+-^2\Pi$ and for $Q_1(8)$ and $Q_2(8)$ of $^2\Sigma^--^2\Pi$. The F_{2d}'' levels were perturbed for N"=5,6 without extra lines being seen. Some of the combination differences for the lower state of these three bands are presented in table 3.16.

The NH^+ bands were more difficult to analyse, especially at low values of N, where the F_{1c}'', F_{2c}'' and F_{1d}'' levels seem to be strongly perturbed, and where the

Table 3.16: Some differences for ND^+ bands with v"=1

N	$\Delta_1 F''_{1dc}(N)$			$\Delta_1 F''_{1cd}(N)$		
	$^2\Sigma^+ - ^2\Pi$		$^2\Sigma^- - ^2\Pi$	$^2\Sigma^+ - ^2\Pi$		$^2\Sigma^- - ^2\Pi$
	(2,1)	(3,1)	(0,1)	(2,1)	(3,1)	(0,1)
($J=\frac{1}{2}$)			21.02	19.95≠	19.84≠	19.83≠
1		36.31≠	36.41≠		33.78	33.72
2	51.71≠	51.71	51.80≠	47.73	47.76≠	47.82
3		67.82	67.87≠	61.88	61.92≠	61.90
4	84.34≠	84.37	84.41	75.52	75.57≠	75.62
5	101.49≠	101.53≠	101.62	88.32	88.25	88.28
6		119.82	119.96	99.06≠	98.91≠	99.00≠
7		140.19	140.22	162.23	162.33	162.26
	-	-	-	106.06	106.07≠	106.14≠
8	107.94≠	107.85≠	107.85	169.19	169.15	169.05≠
		163.82≠	163.97≠	-	-	-
9	131.63	131.73	131.77	179.58≠	179.71≠	179.58
10	151.71≠	151.78	151.77	192.38	192.45	192.35

N	$\Delta_1 F''_{2dc}(N)$			$\Delta_1 F''_{2cd}(N)$		
	$^2\Sigma^+ - ^2\Pi$		$^2\Sigma^- - ^2\Pi$	$^2\Sigma^+ - ^2\Pi$		$^2\Sigma^- - ^2\Pi$
	(2,1)	(3,1)	(0,1)	(2,1)	(3,1)	(0,1)
2			44.28≠	44.30	44.32	
3		59.97	60.03≠	61.21≠	61.12	61.08
4		71.26≠	71.27≠	77.81	77.77	77.69≠
5	101.10≠	101.02	101.23	97.65	97.56≠	97.79
6		117.36≠	117.47≠	97.03	97.02	97.08≠
7		136.53	136.62	153.40≠	153.46	153.48
	-	-	-	106.78≠	106.84	106.87
8	113.19	113.13	113.09	162.55	162.66	162.63≠
	159.65	159.63	159.70	-	-	-
9	135.60		135.56≠	174.89	174.91≠	174.88
10	154.30	154.27≠	154.26	188.99	189.08	189.04

$^2\Sigma^+$-$^2\Pi$ bands are overlapped or very weak. No extra lines were identified at the perturbations. Some of the combination differences for the four bands of NH^+ having v"=1 are presented in table 3.17 to show that the identifications are correct. After the (2,1) band had been analysed, unassigned lines in the same region were compared with the λ 2811 band of OH as measured by Dieke and Crosswhite (1962). A total of 66 lines - including all but the weakest ones - were identified, and the agreement of the wave numbers with those of Dieke and Crosswhite was particularly good.

All the bands with v"=1 were too weak for satellite branches to be observed, and the only satellite lines found were the $^oP_{12}(2)$ lines of two NH^+ bands.

The band heads of all the observed bands of NH^+ and ND^+ are presented in table 3.18. All the heads are in the R_1 branches, and the two given in brackets have been predicted from neighbouring lines by using combination differences.

Table 3.17: Some differences for NH^+ bands with v" = 1

N	$\Delta_1 F''_{1dc}(N)$			$\Delta_1 F''_{1cd}(N)$			
	$^2\Sigma^+ - ^2\Pi$		$^2\Sigma^- - ^2\Pi$	$^2\Sigma^+ - ^2\Pi$			$^2\Sigma^- - ^2\Pi$
	(2,1)	(3,1)	(0,1)	(1,1)	(2,1)	(3,1)	(0,1)
($J=\frac{1}{2}$)		28.77	28.38≠			46.91	46.72≠
1			64.77≠			66.36	66.33≠
2		95.43≠	95.49		82.50	82.48	82.57
3	126.22	126.45≠	126.29			107.98	108.22≠
4		155.37	155.43≠		136.30	136.39	136.37
5		183.59	183.57	165.64	165.65	165.98≠	
6		211.05	210.96	195.55	195.56	195.55	195.57
7	237.82	237.84	237.81	225.62	225.56	225.51	225.57
8		264.66≠	264.23	255.46	255.41	255.43	255.41
9	290.18	290.45	290.27	285.06	285.06	285.17	285.08
10	315.90	315.67	315.85		314.35		314.34

N	$\Delta_1 F''_{2dc}(N)$			$\Delta_1 F''_{2cd}(N)$			
	$^2\Sigma^+ - ^2\Pi$		$^2\Sigma^- - ^2\Pi$	$^2\Sigma^+ - ^2\Pi$			$^2\Sigma^- - ^2\Pi$
	(2,1)	(3,1)	(0,1)	(1,1)	(2,1)	(3,1)	(0,1)
2			102.42			64.91	
3	135.42≠	135.78≠	135.40		94.09	94.09	93.98≠
4		164.13	164.36≠	124.94≠	124.92	124.95≠	124.91
5		191.42	191.43	156.18	156.22	156.10≠	156.21≠
6			217.86	187.64	187.63≠	187.67	187.62
7	243.80	243.73	243.79	218.79	218.83	218.83	218.80
8		269.43	269.44	249.83	249.69	249.83	249.68
9	294.78	294.71	294.79	280.33≠	280.10	279.95	280.13
10	319.87	319.85	319.80		310.05		310.08

Table 3.18: Wavelengths in Å of the band heads of NH^+ and ND^+

	NH^+	ND^+
$^2\Sigma^+ - ^2\Pi$		
(0,0)	2886.330	2878.226
(1,0)	2729.991	2759.965
(2,0)	2599.059	2656.538
(1,1)	(2965.06)	
(2,1)	2811.68	(2817.03)
(3,1)	2682.76	2715.027
$^2\Delta - ^2\Pi$		
(0,0)	4348.335	4333.906
(0,1)		4775.0
$^2\Sigma^- - ^2\Pi$		
(0,0)	4627.588	4593.329
(0,1)	5348.224	5096.023
(1,0)		4356.945

CHAPTER 4 : THE ELECTRONIC STATES OF NH^+ AND ND^+.

Having presented the analysis of bands of NH^+ and ND^+, we now derive the rotational and vibrational constants for each electronic state, compare the values obtained for each isotope, and examine the perturbations in $^2\Pi_r$. Unless otherwise stated, the observations have been fitted to the various mathematical expressions for the energy by the method of least squares, using an Elliott 803A computer. The computer was programmed to give the standard deviation of each coefficient in the resulting polynomials, and the error in each molecular constant is given as the standard deviation of the last significant figure. The error is given in brackets following the constant so that, for example, 7.62(3) means 7.62 ± 0.03.

Figure 4.1 - showing the bands which have been analysed - indicates the levels which can be investigated and the number of bands which can be used.

4.1 The $^2\Sigma$ states

$^2\Sigma^+$ is the upper state of the ultraviolet system and $^2\Sigma^-$ is the upper state of one of the visible systems. Neither state is perturbed, and their rotational energy levels are given by equations (3.8-9), which are now repeated:

$$F_1(N)=BN(N+1)-DN^2(N+1)^2+HN^3(N+1)^3+\tfrac{1}{2}\gamma N \qquad (4.1)$$

$$F_2(N)=BN(N+1)-DN^2(N+1)^2+HN^3(N+1)^3-\tfrac{1}{2}\gamma(N+1) \qquad (4.2)$$

The constant γ is best determined by observation of those

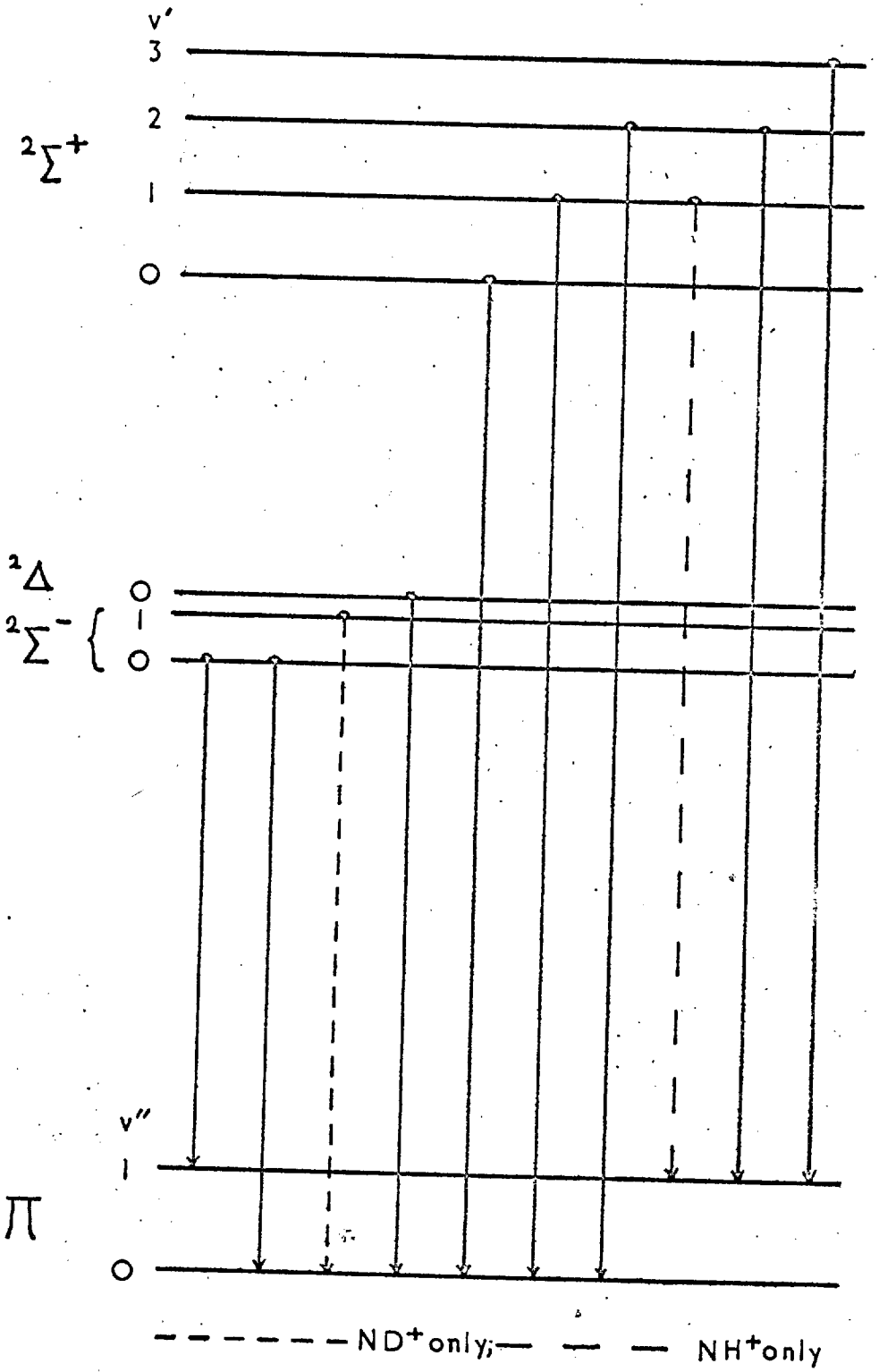

Figure 4.1: NH^+ and ND^+ bands of which the rotational structure has been analysed

satellite branches whose lines are separated from those of the main branches by $\gamma(N+\frac{1}{2})$ - for example, the branches given in equations (3.14-17). In the present case, however, the values of γ are so small that these lines cannot be resolved, and γ has been determined from the combination differences:

$$\Delta_2F_1(N) - \Delta_2F_2(N) = 2\gamma \qquad (4.3)$$

The consistency of the values of 2γ may be gauged from those already presented in table 3.4. According to Mulliken and Christy (1931), γ is expected to be proportional to B_v and to need correction for rotational distortion at high values of N. Such variations are within the experimental error in the present work, so the mean value of $\Delta_2F_1(N)-\Delta_2F_2(N)$ has been found for each vibrational level, data from blended and weak lines being omitted. The resulting values of γ are presented in table 4.1, together with the standard deviations (in brackets) and the number of measurements used. As in the case of CH (Gero (1941)), γ is positive for $^2\Sigma^+$ but negative for $^2\Sigma^-$.

Table 4.1: Values of γ for the $^2\Sigma$ states, in cm^{-1}

		NH^+		ND^+	
	v	γ	No. of values	γ	No. of values
$^2\Sigma^+$	0	0.097(18)	13	0.059(16)	15
	1	0.091(23)	16	0.055(16)	18
	2	0.095(25)	11	0.058(11)	14
	3	0.093(17)	7	0.064(25)	10
$^2\Sigma^-$	0	-0.100(13)	10	-0.054(13)	13
	1			-0.059(15)	11

The mean of $\Delta_2F_1(N)$ and $\Delta_2F_2(N)$ represents the following expression:

$$\Delta_2F(N)=(4B_v-6D_v+6.75H_v)(N+\tfrac{1}{2})-(8D_v-34H_v)(N+\tfrac{1}{2})^3+12H_v(N+\tfrac{1}{2})^5 \quad (4.4)$$

The rotational constants for v=o were found from (4.4) by expressing $\Delta_2F(N)/(N+\frac{1}{2})$ as a polynomial in $(N+\frac{1}{2})^2$ by a least squares fitting. For the other vibrational levels it was convenient to use the method introduced by Jenkins and McKellar (Herzberg, p 188) which depends on the differences between corresponding lines in two bands having the same lower state.

If two bands (a,v), (b,v) of a system have a common lower state, we may define a quantity M'(N) such that

$$M'(N)=R_{a,v}(N-1)-R_{b,v}(N-1)=Q_{a,v}(N)-Q_{b,v}(N)=P_{a,v}(N+1)-P_{b,v}(N+1) \quad (4.5)$$

$$M'(N)=G'(a)-G'(b)+F'_a(N)-F'_b(N) \quad (4.6)$$

On substituting an energy expression of the form (4.1) we have

$$M'(N)=G'(a)-G'(b)+(B_a-B_b)N(N+1)-(D_a-D_b)N^2(N+1)^2 +(H_a-H_b)N^3(N+1)^3+\tfrac{1}{2}N(\gamma_a-\gamma_b) \quad (4.7)$$

On taking the average value of M'(N) from the two sub-bands of $^2\Sigma-^2\Pi$, the final term of (4.7) vanishes -- it is in any case almost always negligible - and we have a polynomial in N(N+1), whose coefficients give a vibrational interval and the increments in the rotational constants. The results of the curve-fitting procedures are presented in table 4.2.

The "equilibrium" values of the rotational

Table 4.2 : Rotational constants and Vibrational quanta, in cm^{-1}

		NH^+	ND^+
$^2\Sigma^+$state:	B_o	12.8720(9)	6.9297(6)
	B_1	12.0975(9)	6.6234(6)
	B_2	11.3626(9)	6.3282(6)
	B_3	10.6652(13)	6.0443(8)
	10^4D_o	19.67(8)	5.485(11)
	10^4D_1	19.04(8)	5.360(11)
	10^4D_2	18.37(8)	5.220(11)
	10^4D_3	17.73(11)	5.08(3)
	$H_o=H_1=H_2$	$(1.00\pm0.19)10^{-7}$	-
	$\triangle G(\frac{1}{2})$	2004.96(1)	1495.94(1)
	$\triangle G(3/2)$	1857.40(1)	1414.70(1)
	$\triangle G(5/2)$	1720.38(2)	1337.83(2)
	B_1-B_o	-0.77457(14)	-0.30630(12)
	B_2-B_o	-1.5094(2)	-0.60147(10)
	B_3-B_2	-0.6974(9)	-0.2839(5)
	$10^4(D_1-D_o)$	-0.633(4)	-0.125(2)
	$10^4(D_2-D_o)$	-1.302(6)	-0.265(2)
	$10^4(D_3-D_2)$	-0.64(7)	-0.144(24)
$^2\Sigma^-$state:	B_o	11.1069(7)	5.9812(4)
	B_1		5.7055(4)
	10^4D_o	19.67(3)	5.670(11)
	10^4D_1		5.413(12)
	$\triangle G(\frac{1}{2})$		1182.44(1)
	B_1-B_o		-0.27569(13)
	$10^4(D_1-D_o)$		-0.257(4)

constants - corresponding to the bottom of the potential curve - have been derived from the values of (B_1-B_o), (D_1-D_o) etc. For $^2\Sigma^+$, B_v and D_v are well represented by equations of the form (1.9-10) and the appropriate constants are presented in table 4.3. The data for $^2\Sigma^-$ are rather limited for this purpose.

Table 4.3: Equilibrium rotational constants for $^2\Sigma$ states, in cm^{-1}

		NH^+	ND^+
$^2\Sigma^+$ state:	B_e	13.2735 (12)	7.0871 (6)
	α_e	0.8126 (15)	0.31752(7)
	γ_e	0.0193 (5)	0.00560(2)
	$10^4 D_e$	19.99 (8)	5.552 (11)
	$10^4 \beta_e$	-0.639 (4)	-0.133 (5)
$^2\Sigma^-$ state:	B_e		6.1190 (4)
	α_e		0.27569(13)
	$10^4 D_e$		5.798 (11)
	$10^4 \beta_e$		-0.257 (4)

Table 4.4: Ratios of the rotational constants for $^2\Sigma^+$

Ratio	Experimental value	Theoretical value
B_e^D/B_e	0.53393 (7)	0.53392
D_e^D/D_e	0.2777 (12)	0.2851
α_e^D/α_e	0.3907 (7)	0.3901
γ_e^D/γ_e	0.290 (8)	0.285
β_e^D/β_e	0.208 (8)	0.208

The ratios of the rotational constants of ND^+ $^2\Sigma^+$ to those of NH^+ $^2\Sigma^+$ are presented in table 4.4

and (except for D_e) are in excellent agreement with the values predicted by the simple isotope theory (table 1.1). This is conclusive evidence that the carrier of the bands is a diatomic compound of nitrogen and hydrogen.

The vibrational constants of $^2\Sigma^+$ have been derived from the vibrational quanta by means of equation (4.8) and the results are presented in table 4.5.

$$\Delta G(v+\tfrac{1}{2}) = \omega_e - 2\omega_e x_e + 3.25\omega_e y_e - (2\omega_e x_e - 6\omega_e y_e)v + 3\omega_e y_e v^2 \quad (4.8)$$

Table 4.5: Vibrational constants for $^2\Sigma^+$, in cm^{-1}

	NH^+	ND^+
ω_e	2162.66 (5)	1581.37 (5)
$\omega_e x_e$	81.70 (3)	43.90 (3)
$\omega_e y_e$	1.76 (1)	0.73 (1)

When several vibrational quanta have been measured for an electronic state it is usually possible to extrapolate them to a dissociation limit, and hence estimate the dissociation energy (Birge-Sponer extrapolation). For this particular state, however, the graph of ΔG against v has a small positive curvature, so that it cannot be extrapolated to $\Delta G=0$. Such behaviour may indicate a vibrational perturbation, but the extrapolation is too great for a definite interpretation to be given. If the constant $\omega_e y_e$ is neglected and the data are fitted to the formula

$$G(v) = \omega_e(v+\tfrac{1}{2}) - \omega_e x_e (v+\tfrac{1}{2})^2 \quad (4.9),$$

then ω_e=2145.5 cm^{-1}(NH^+), 1574.3 cm^{-1}(ND^+) and $\omega_e x_e$=71cm^{-1}(NH^+), 39.5 cm^{-1}(ND^+). The dissociation energy from a linear extrapolation is given by

$$D_e = \frac{\omega_e^2}{4\omega_e x_e} \qquad (4.10)$$

and on substituting the above values we obtain $D_e \sim 15{,}900\ cm^{-1}$. This value must be treated with caution, however, as table 4.6 shows that the constants of table 4.5 are the more consistent with the isotope effect.

Table 4.6: Ratios of the vibrational constants for $^2\Sigma^+$

Ratio	Model with 3 constants	Model with 2 constants	Theoretical value
ω_e^D/ω_e	0.7312	0.7338	0.7307
$\omega_e x_e^D/\omega_e x_e$	0.5373	0.5556	0.5339
$\omega_e y_e^D/\omega_e y_e$	0.4136	-	0.3901

For $^2\Sigma^-$ we have $\Delta G(\frac{1}{2})$ of ND^+ only, and vibrational constants can be determined only by means of approximate relationships such as that of Kratzer:

$$\omega_e^2 = \frac{4B_e^3}{D_e} \qquad (4.11)$$

Using (4.11) for ND^+ $^2\Sigma^-$ we obtain $\omega_e^D = 1257 cm^{-1}$, $\omega_e x_e^D = 37 cm^{-1}$ and $D_o \sim 10000\ cm^{-1}$. The highest rotational level observed for $^2\Sigma^-$ lies 3483 cm^{-1} above v=0, so that the state is certainly more stable than the corresponding one in CH, which predissociates through rotation ($D_o = 2300 cm^{-1}$).

4.2 The $^2\Delta$ state

$^2\Delta$ is the upper state of the intense bands at $\lambda\lambda$4348 and 4334 : only the v=0 level has been analysed.

The rotational term values may be represented by a modified Hill-Van Vleck expression (compare 3.11):

$$F_{1,2}(J)=B_v((J+\tfrac{1}{2})^2-4)\mp B_v((J+\tfrac{1}{2})^2+Y(Y-4))^{\frac{1}{2}}-D_vJ^2(J+1)^2 \quad (4.12)$$
$$+\tfrac{1}{2}\gamma(J(J+1)-N(N+1)-\tfrac{3}{4}).$$

The final term represents the NS coupling energy and contributes $+\frac{1}{2}\gamma N$ to the F_1 levels and $-\frac{1}{2}\gamma(N+1)$ to the F_2 levels in the same way as for $^2\Sigma$ states. Λ-type doubling is usually negligible in Δ states, but would show itself by differences in the values of $Q_{dc}(N)-Q_{cd}(N)$, $R_c(N)-R_d(N)$, $P_c(N)-P_d(N)$ etc. No such differences could be detected, so that the widths of the Λ-doublets are less than the experimental error.

If the mean of $F_1(J)$ and $F_2(J)$ is found, the second (square root) term in (4.12) vanishes. It follows that the mean value of $\Delta_2F(J)$ is given by an expression of the form (4.4), N being replaced by J. The rotational constants were found by expressing $(\Delta_2F_{1c}(J)+\Delta_2F_{2c}(J)+\Delta_2F_{1d}(J)+\Delta_2F_{2d}(J))\ /\ (4J+2)$ as a polynomial in $(J+\frac{1}{2})^2$ by a least squares fitting. There are no perturbations, and the combination differences were found from the main R and P branches of the $^2\Delta - ^2\Pi$ bands. The constants are given in table 4.7; their isotopic ratios ($B_o^D/B_o=0.538$, $D_o^D/D_o=0.287$, $H_o^D/H_o=0.168$) differ slightly from those of table 1.1 which refer to the vibrationless state.

We showed in section 3.2 that $^2\Delta$ is <u>inverted</u> (negative A). We now require the exact value of $Y(=A/B_v)$, and hence of A. Substitution of $F_2(2\frac{1}{2})-F_1(2\frac{1}{2})$ in the expression

$$F_2(J)-F_1(J) = 2B((J+\tfrac{1}{2})^2+Y(Y-4))^{\frac{1}{2}} \quad (4.13)$$

yields the preliminary values $Y= -0.24(NH^+), -0.49(ND^+)$.

Thus $^2\Delta$ is very near to Hund's case (b) - Y=0 or 4 - and the term values may be written in terms of N:

$$F_1(N)=B((N+1)^2-4)-B((N+1)^2+Y(Y-4))^{\frac{1}{2}}-DN^2(N+1)^2+\tfrac{1}{2}\gamma N \quad (4.14)$$

$$F_2(N)=B(N^2-4)+B(N^2+Y(Y-4))^{\frac{1}{2}}-DN^2(N+1)^2-\tfrac{1}{2}\gamma (N+1) \quad (4.15).$$

Further, Y(Y-4) is much less than N^2 or $(N+1)^2$, so that the square root terms of (4.14-15) may be expanded by the Binomial Theorem to give

$$\Delta\nu_{12}(N)=F_1(N)-F_2(N)=-\frac{Bz}{2}\left\{\frac{1}{(N+1}+\frac{1}{N}\right\}+\frac{Bz^2}{8}\left\{\frac{1}{(N+1)^3}+\frac{1}{N^3}\right\}$$

$$-\frac{Bz^3}{16}\left\{\frac{1}{(N+1)^5}+\frac{1}{N^5}\right\}+\text{---}+\gamma(N+\tfrac{1}{2}) \quad -(4.16)$$

where z=Y(Y-4). At low values of N, $\Delta\nu_{12}(N)$ was found from the relations

$$\begin{aligned}\Delta\nu_{12}(N)&={}^{P}Q_{1c2c}(N+1)-P_{2c}(N+1) \quad (4.17)\\ &=Q_{1dc}(N)-{}^{Q}P_{2d1c}(N)\\ &={}^{Q}R_{1d2c}(N)-Q_{2dc}(N)\\ &=R_{1c}(N-1)-{}^{R}Q_{2c1c}(N-1)\end{aligned}$$

together with four similar expressions with c and d interchanged. At higher values of N, $F_1(N)-F_2(N)$ was found with the aid of term values for the $^2\Pi$ state, as given later in the chapter. As shown in Figure 4.2, F_1 is initially below F_2, but the order changes when the γ term predominates. The curves are similar to that for CH given by Gero (1941).

If the terms in z^2 and higher orders are neglected, (4.16) may be rearranged to give

$$\frac{\Delta\nu_{12}(N)}{N+\frac{1}{2}} = -\frac{Bz}{N(N+1)}+\gamma \quad (4.18).$$

Graphs of $\Delta\nu_{12}(N)/(N+\frac{1}{2})$ against $1/N(N+1)$ were linear

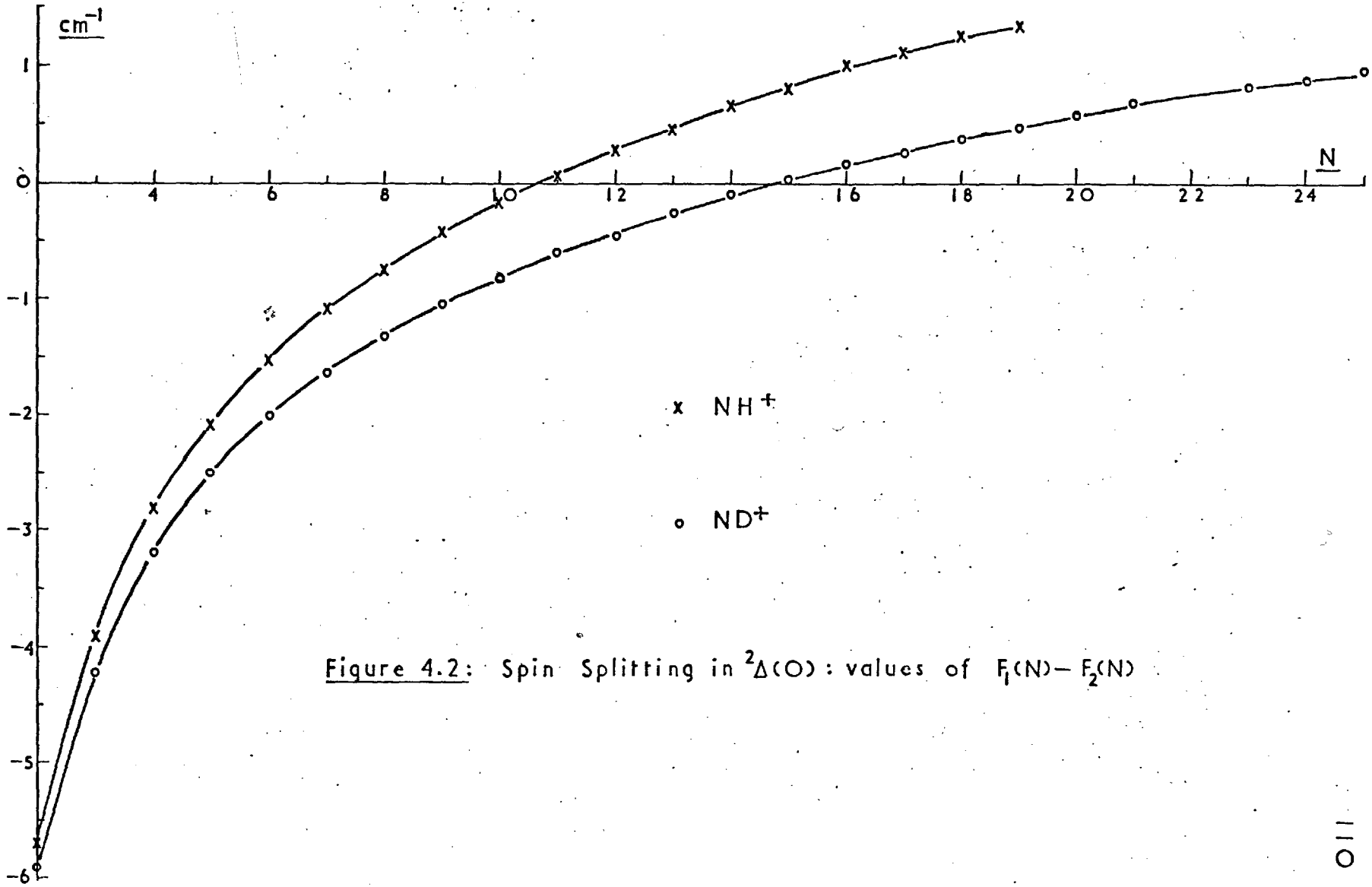

Figure 4.2: Spin Splitting in $^2\Delta(O)$: values of $F_1(N) - F_2(N)$

for N greater than 5, and the slopes of the lines gave $z = 1.082$ (NH^+), 2.176(ND^+). These preliminary values were used to calculate all the higher order terms of (4.16) which could contribute significantly to $\Delta\nu_{12}(N)$ at low values of N. The revised expression

$$\frac{1}{(N+\frac{1}{2})}\left\{\Delta\nu_{12}(N)-\frac{Bz^2}{8}\left\{\frac{1}{(N+1)^3}+\frac{1}{N^3}\right\}+\text{---}\right\},$$

which represents the right-hand side of equation (4.18) exactly, was plotted against $1/N(N+1)$. All points now lay on a straight line except for those having the three highest values of N, which deviated slightly - probably because of higher-order terms in the NS coupling energy. The final values of Y, A and γ were deduced from the coefficients of the straight line and are presented in table 4.7.

Table 4.7 : Rotational constants for $^2\Delta$ (v=0), in cm^{-1}

	NH^+	ND^+
B_o	13.5295(4)	7.2765(5)
$10^4 D_o$	19.24 (3)	5.52 (2)
$10^8 H_o$	10.7 (6)	1.8 (2)
Y	- 0.2615(4)	-0.4882(2)
A	- 3.538 (5)	-3.552 (2)
γ	0.118 (1)	0.0667(3)

The spin-orbit coupling constant, A, is almost independent of the mass, in agreement with theory. By contrast, Klynning et al (1965, 1966a) have found large (unexplained) differences in A for the $^2\Delta$ states of GeH(10.28) and GeD(14.39), and of SnH(20.41) and SnD(8.52).

The approximate vibrational constants provided by relation (4.11) are ω_o=2269 cm^{-1}, ω_o^D=1671 cm^{-1}.

4.3 NH^+ $^2\Pi$(v=0) and the state perturbing it

The Hill-Van Vleck treatment of $^2\Pi$ states was extended by Almy and Horsfall (1937) to take better account of the rotational D term, with the result that the term values are expressed as

$$F_{1,2}(J)=B(J(J+1)-\tfrac{3}{4})-D(J^2(J+1)^2-J(J+1)/2+13/16)\mp B\underline{a}^{\frac{1}{2}} \quad (4.19)$$

where the minus sign refers to F_1, and $\underline{a}$ is given by

$$\underline{a}=\tfrac{1}{4}(Y-2)^2+(J(J+1)-\tfrac{5}{4})\left[1-u(4J(J+1)+1-2Y)+u^2(2J(J+1)-\tfrac{1}{2})^2-u^2\right] \quad (4.20)$$

In (4.20), Y=A/B, u=D/B and the sign of terms in D has been changed from that of Almy and Horsfall to accord with the modern convention.

From (4.19) one finds

$$\tfrac{1}{2}(\Delta_2F_1(J)+\Delta_2F_2(J))=4(B-D)(J+\tfrac{1}{2})-8D(J+\tfrac{1}{2})^3 \quad (4.21)$$

so that the mean of the combination differences for each value of J(notN) may be used to find B and D in a manner similar to that used for $^2\Delta$. When the Λ-doubling is taken into account, the equation of Mulliken and Christy (1931) shows that the mean of all four combination differences (for 1c, 1d, 2c and 2d levels) gives an expression of the form (4.21), except that B is replaced by $B+\frac{1}{2}q$, where q is a small constant. The value of q may sometimes be derived from the Λ-doubling, but the theory given by Mulliken and Christy does not apply to the electron configurations of CH-type molecules, so that we shall follow the usual practice and leave the B values uncorrected.

The best values of the combination differences for $NH^{+2}\Pi(0)$ were found from the five available bands, and separate graphs of $\Delta_2F(N)/(N+\frac{1}{2})$ against $(N+\frac{1}{2})^2$ for F_{1c}, F_{1d}, F_{2c} and F_{2d}, and of $(\Delta_2F_1(J)+\Delta_2F_2(J))/(J+\frac{1}{2})$ against $(J+\frac{1}{2})^2$ for F_d and F_c were drawn. In an unperturbed state such graphs give straight lines; but in this case there were large departures from linearity in the perturbed regions, and all points in these regions were ignored. There remained sufficient points for a linear plot of the mean $\Delta_2F(J)/(J+\frac{1}{2})$ against $(J+\frac{1}{2})^2$ to be made, yielding the constants

$$B_o = 15.301 \pm 0.003$$

$$D_o = (15.78 \pm 0.06)\ x10^{-4}.$$

From the wave numbers of $^2\Delta - ^2\Pi$ and the average combination differences, a scheme of term values was constructed for $^2\Pi(0)$ and this is presented as table 4.8. The lowest level - $F_{1c}(J=\frac{1}{2})$ - was chosen as zero, and the differences between these observed terms and the expression $B_oN(N+1) - D_oN^2(N+1)^2$ were plotted in Figure 4.3 as functions of N. This figure shows the combined effects of spin-doubling, Λ-doubling and the perturbations. It is similar to a figure given by Feast, except that the behaviour at low and high N is more regular because of the corrected assignments, and the positions of some "extra" levels at the perturbations are different.

The expected variations in the Λ-doubling are disrupted by the perturbations, but table 4.8 shows that at the lowest values of N, the splitting for $F_1(^2\Pi_{\frac{1}{2}})$ is

Table 4.8 : Term values for NH^+ $^2\Pi$ (v=o), in cm^{-1}

N	F_{1c}	F_{1d}	F_{2c}	F_{2d}
($J=\frac{1}{2}$)	0	0.45	-	-
1	33.77	34.44	-	-
2	96.16	97.02	105.29	105.03
3	188.53	189.46	195.86	195.25
4	310.81	311.83	317.42	316.33
5	463.14	464.42	469.57	467.84
6	644.91	646.78	651.68	655.12
	-	-	-	643.86
7	855.80	859.00	863.51	862.50
8	1094.07	1100.53	1103.60	1103.50
9	1356.22	1371.37	1369.05	1374.03
	1419.57	-	1413.71	-
10	1700.04	1670.90	1693.88	1673.26
	1634.98	-	1648.06	-
11	2020.44	1998.99	2017.27	2001.28
12	2373.86	2354.92	2372.54	2357.04
13	2757.16	2738.68	2757.01	2740.72
14	3168.26	3149.21	3168.77	3151.05
15	3606.85	3586.59	3607.89	3588.35
16	4071.50	4049.49	4072.91	4051.12
17	4562.29	4537.93	4564.04	4539.42
18	5077.86	5050.28	5079.87	5051.53
19	5618.25	5585.71	5620.45	5586.80
20	6182.03	6143.07	6184.38	

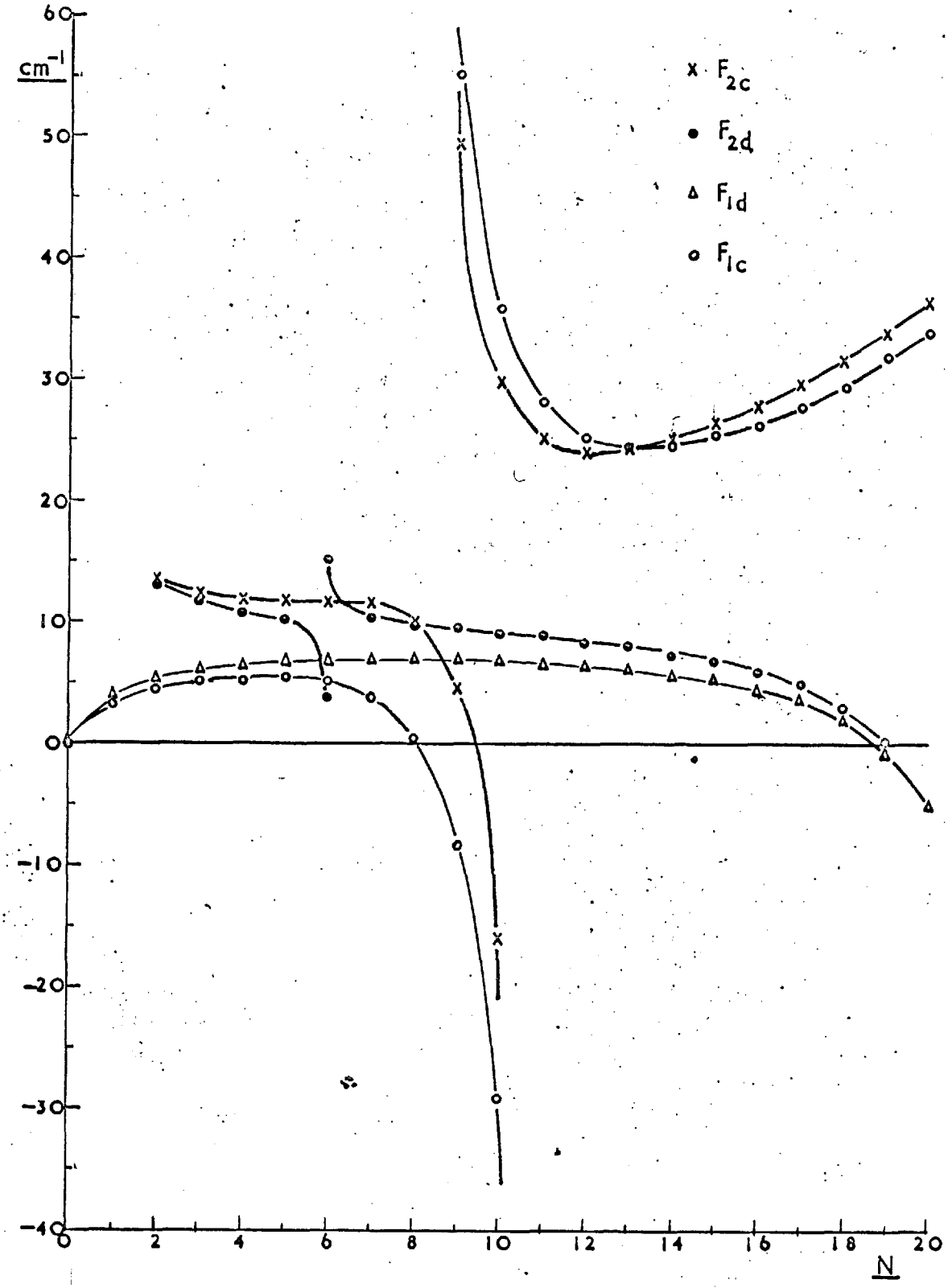

Figure 4.3: $F(N) - (15{\cdot}301N(N+1) - 15{\cdot}78N^2(N+1)^2 \times 10^{-4})$ for $NH^+\ ^2\Pi\ (v=0)$

greater than that for $F_2(^2\Pi_{3/2})$, in agreement with theory (Mulliken and Christy).

Since the $^2\Pi$ state is near to case (b), it is best to determine Y and A from N-doublets. From (4.19) one finds

$$(Y-2)^2=\frac{((g(N)-\Delta\nu_{12}(N)/B)^2-f(N)-f(N+1))^2-4f(N)f(N+1)}{(g(N)-\Delta\nu_{12}(N)/B)^2} \quad (4.22)$$

where $g(N) = 2N+1 - 4u(N+\frac{1}{2})^3$ (4.23)

$$f(N) = (N^2-1)\ (1+2Yu-4(u+u^2)N^2 + 4u^2N^4) \quad (4.24)$$

The value of Y used in f(N) is given to sufficient accuracy from J-doublets:

$$F_2(J)-F_1(J)=B(4(J+\tfrac{1}{2})^2+Y(Y-4))^{\frac{1}{2}} \quad (4.25)$$

The average values of $\Delta\nu_{12}(N)$ for the F_c and F_d components were found from the $^2\Delta - ^2\Pi$ band and substituted in (4.22). The value of Y was not constant, but increased with increasing N. However, since the perturbation of the F_{2d} levels culminates at N=6, we must restrict ourselves to the lowest values of N, which give

$$Y_o=5.11\pm0.02,\ A_o=78.2\pm0.3\text{cm}^{-1}$$

Figure 4.3 enables us to examine the perturbations using arguments similar to those of Feast.

1) After the large perturbation at N=9,10, the F_c levels show a residual shift. Therefore the perturbations are "heterogeneous" and $\Delta\Lambda=\pm1$ (Dieke (1935)).

(The existence of the shift is less obvious now that the assignments have been revised; but even if it could be shown to be zero - so that the term values resemble those in CaH (Mulliken and Christy, Fig. 4) - perturbation by a Π state would be eliminated by argument 2) below).

2) Any level of a Δ state has two sub-levels of opposite parity for each value of J (Λ-doubling). In perturbing a $^2\Pi$ state it would necessarily repel both the c and d components having that value of J. In the present case only F_c or F_d levels are perturbed for any one J. Therefore the perturber is a Σ state.

3) The perturbed state is a doublet. Therefore the perturber must have even multiplicity.

4) If the perturber is $^2\Sigma$, then $\Delta S=0$ and the rule $\Delta N=0$ holds. Let us use the subscripts p and s to refer to the N values of the Π state and the Σ state respectively. $N_p=6$ can in this case be perturbed only by $N_s=6$; but $N_s=6$ would perturb both $F_{2d}(6)$ and $F_{1d}(6)$. Since $F_{1d}(6)$ is not perturbed, the perturbing state cannot be $^2\Sigma$.

5) We have established that the $^2\Pi$ state belongs to NH^+. The only stable Σ state of NH^+ of low energy and with a multiplicity greater than two is the $^4\Sigma^-$ state arising from the lowest state of the united atom, $O^+(^4S_u)$, and the lowest pair of dissociation products, $N(^4S_u)$ + $H^+(^1S_g)$. This state must be responsible for the perturbations in $^2\Pi$ (v=o).

6) The sub-levels of a $^4\Sigma^-$ state are given by $J=N_s+3/2$, $N_s+\frac{1}{2}$, $N_s-\frac{1}{2}$, $N_s-3/2$. Since $F_{2d}(6)$ is perturbed but $F_{1d}(6)$ is not perturbed, N_s must contain $J=5\frac{1}{2}$ but not $J=6\frac{1}{2}$. Therefore $N_s=4$; and for convenience we refer to this as the "6/4" perturbation.

As shown in chapter 1, levels with even N in

Σ^- states have negative parity. Because of the selection rule (1.27) for perturbations, $F_{2d}(6)$ of $^2\Pi$ must also have negative parity. Since this agrees with the labelling of Figures 3.1 and 3.3, the parities given to the $^2\Sigma$ states of NH^+ are now confirmed.

7) At $N_p=9,10$, the F_{1c} and F_{2c} levels are strongly perturbed. The c levels of $N_p=10$ have positive parity and must therefore be perturbed by a level of <u>odd</u> N_s containing both $J=10\frac{1}{2}$ and $J=9\frac{1}{2}$. The two possibilities are $N_s=9$ and $N_s=11$. Similarly, $N_p=9$ is perturbed by $N_s=8$ or by $N_s=10$.

8) Since Figure 4.3 shows that the $F_c(8)$ and $F_c(7)$ levels are perturbed downwards, the relative positions of the rotational levels must be those indicated schematically in Figure 4.4(a). It follows that $N_s=6$ perturbs F_{1c} and F_{2c} of $N_p=7$ and that $N_s=8,9$ perturb $N_p=9,10$.

If a level $F_p(J)$ of a $^2\Pi$ state is perturbed by a level $F_s(J)$ of a $^2\Sigma$ state whose vibrational level is an energy C above that of the $^2\Pi$ state, then the <u>mean</u> energy, $\bar{T}$, of the perturbed levels is given by

$$\bar{T} = \tfrac{1}{2}\,(C+F_p(J)+F_s(J)) \qquad (4.26)$$

This is because the shifts of the levels are equal and opposite. In the present case we have three perturbations- 6/4, 9/8 and 10/9 - for which $\bar{T}$ can be found; and the unperturbed energies $F_p(J)$ may be found from Figure 4.3 by estimating the widths of the Λ-doublets. The following are the energies in cm^{-1} above the level $F_{1c}(J=\frac{1}{2})$:-

6/4 perturbation: $\bar{T} = 649.49$, $F_p = 650.0$

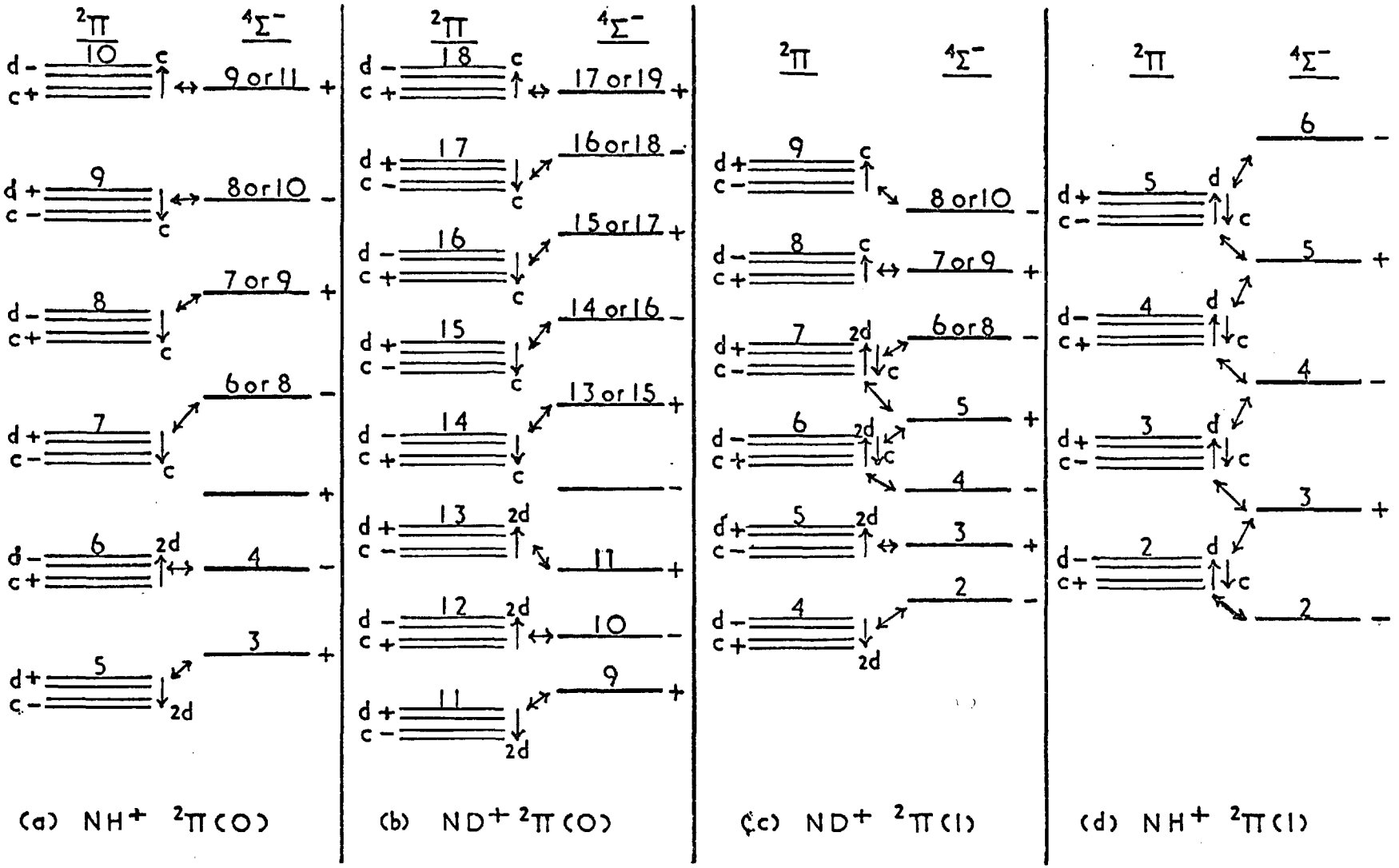

Figure 4.4 : Positions of the perturbed and perturbing levels in $^2\Pi$ and $^4\Sigma^-$

9/8 perturbation: $\bar{T} = 1389.64$, $F_p = 1373.9$

10/9 " : $\bar{T} = 1669.24$, $F_p = 1673.7$

Let the $^4\Sigma$ state have the vibrational number vh.

Then $F_s(N) = B_{vh}N(N+1) - D_{vh}N^2(N+1)^2$ (4.27)

Feast assumed a value of $15 \times 10^{-4} cm^{-1}$ for D_{vh} and used the perturbations 6/4 and 10/9 to obtain $B_{vh} = 14.94$ and $C=331.4\ cm^{-1}$. If the same value of D_{vh} is assumed here, the values of B_{vh} and C obtained by substitution in (4.26) are almost the same for the three possible "pairs" of perturbations (6/4 and 9/8, 6/4 and 10/9, 9/8 and 10/9). It was therefore decided to use all three equations without assuming a value for D_{vh}. The results are:

$B_{vh} = 14.72$

$D_{vh} = 18.9 \times 10^{-4}$

$C = 355.36\ cm^{-1}$ above $F_{1c}(J=\frac{1}{2})$.

The evaluation of the term values for $^4\Sigma^-$ (vh) shows that $N_s=21$ will perturb $N_p=21$. Inspection of Figure 4.4 indicates that this will affect F_{1d} and F_{2d}, both of which are indeed perturbed slightly at the highest N values of Figure 4.3.

4.4 $ND^+\ ^2\Pi$ (v=0) and the state perturbing it

The combination differences for $ND^+\ ^2\Pi(0)$ were found from the six available bands, and graphs were drawn as before to indicate the perturbations. The F_c levels were strongly perturbed at high values of N and the unperturbed positions were difficult to estimate. On the other hand, the only noticeable perturbation in the F_d

levels was a relatively small one at $F_{2d}(12)$. Constants were determined from a linear fit of $(\Delta_2F_{1d}(J)+\Delta_2F_{2d}(J))/(J+\frac{1}{2})$ to the variable $(J+\frac{1}{2})^2$ and are

$$B_o^d = 8.2338 \pm 0.0006$$
$$D_o^d = (4.60\pm0.01) \times 10^{-4}.$$

It is estimated that $B_o = B_o^d \pm 0.003$, so that the constants for the d components may be used for B_o, D_o whenever necessary.

The spin-splitting was found in the same way as for NH^+, and the values of Y determined from equation (4.22) show a small increase with N, comparable to that found for the similar $^2\Pi$ states of SiH (Klynning and Lindgren (1966b)), GeH (Klynning and Lindgren (1966a)) and SnH (Klynning et al (1965)). Using the lowest values of N, we obtain

$$Y_o=9.56\pm0.01,\ A_o=78.72\pm0.08\text{cm}^{-1}$$

in fair agreement with the hydride values.

A scheme of term values for ND^+ $^2\Pi(0)$ was constructed from the wave numbers and combination differences of the bands. $F_{1c}(J=\frac{1}{2})$ was again chosen as zero, and the results are presented in table 4.9. The deviations from $B_oN(N+1) - D_oN^2(N+1)^2$ are shown in Figure 4.5, which is similar in many respects to Figure 4.3. In particular, $F_{2d}(12)$ is perturbed while $F_{1d}(12)$ is unperturbed (compare $F_d(6)$ in NH^+), and both F_c components are strongly perturbed at N=18 (N=9, 10 for the hydride).

The arguments used to identify the perturbing state in the hydride apply equally here, so that $^4\Sigma^-$ is

Table 4.9 : Term values for ND^+ $^2\Pi$ (v=o), in cm^{-1}

N	F_{1c}	F_{1d}	F_{2c}	F_{2d}
($J=\frac{1}{2}$)	0	0.15	-	-
1	21.46	21.79	-	-
2	57.87	58.30	90.02	89.97
3	109.66	110.20	135.92	135.78
4	177.29	177.84	199.24	198.98
5	260.79	261.37	279.76	279.31
6	360.27	360.83	377.00	376.38
7	475.77	476.35	490.89	490.02
8	607.24	607.83	621.13	620.03
9	754.67	755.25	767.66	766.23
10	917.92	918.58	930.21	928.43
11	1096.88	1097.69	1108.72	1106.35
12	1291.46	1292.47	1302.99	1303.82
13	1501.35	1502.84	1512.86	1511.53
14	1726.35	1728.62	1738.00	1736.52
15	1965.97	1969.66	1978.19	1977.03
16	2219.55	2225.84	2232.69	2232.72
17	2485.51	2496.96	2500.05	2503.47
18	2761.29	2782.82	2776.34	2788.98
	2820.87	-	2816.39	-
19	3110.39	3083.29	3107.85	3089.14
20	3419.60	3398.09	3419.37	3403.66
21	3745.92	3727.05	3747.17	3732.39
22	4087.59	4069.92	4089.89	4074.97
23	4443.82	4426.51	4446.67	4431.35
24	4814.04	4796.52	4817.34	4801.07
25	5197.90	5179.64	5201.33	5183.95
26	5594.91	5575.39	5598.58	5579.39

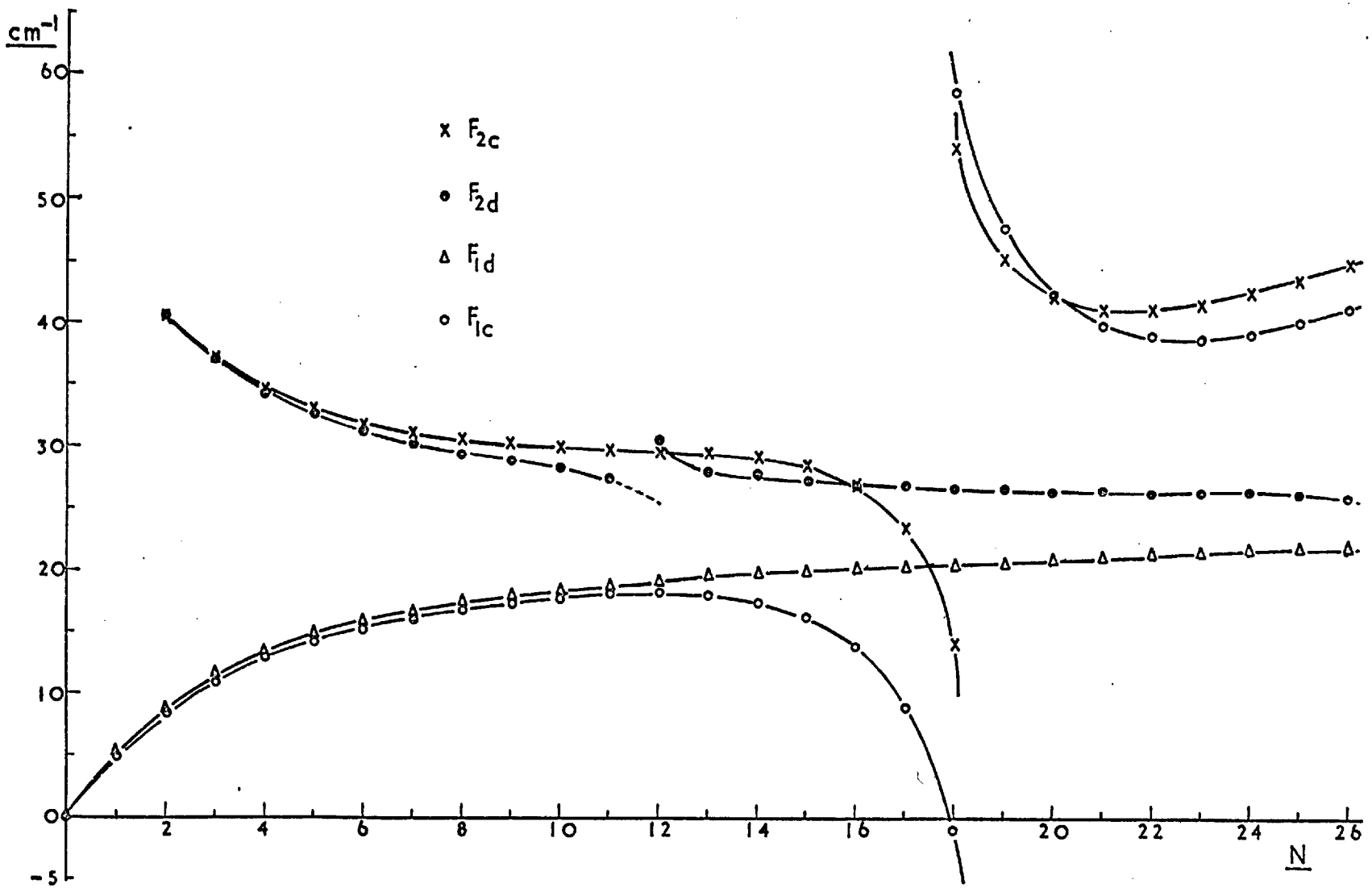

Figure 4.5: $F(N) - (8.2338N(N+1) - 4.6\times10^{-4}N^2(N+1)^2)$ for $ND^{+2}\Pi(v=0)$

the perturber. $F_{2d}(12)$ is perturbed by a level N_s which contains $J=11\frac{1}{2}$ but not $J=12\frac{1}{2}$. Therefore $N_s=10$, and we call this the 12/10 perturbation. (As before, the parity selection rules agree with our assignment of $^2\Sigma^+$ and $^2\Sigma^-$ states).

$F_{1c}(18)$ and $F_{2c}(18)$ must be perturbed by a level of <u>odd</u> N_s containing $J=18\frac{1}{2}$ and $J=19\frac{1}{2}$. The two possibilities are $N_s=17$ and $N_s=19$, the higher of which is eliminated when the relative positions of all the $^4\Sigma^-$ levels are considered (see Figure 4.4(b)). $F_{2d}(13)$ is raised by interaction with $N_s=11$, and $F_{1c}(14)$ and $F_{2c}(14)$ are both depressed by $N_s=13$ or 15. Since only one $^4\Sigma^-$ level can be fitted between the levels responsible for these two perturbations, $N_s=13$ must perturb $N_p=14$, and hence the strongest perturbation is 18/17.

In order to use equation (4.26) for the 12/10 perturbation, the position of the 'extra' level has been estimated from Figure 4.5. The energies in cm^{-1} above $F_{1c}(\frac{1}{2})$ are

12/10 perturbation : $\bar{T} = 1301.3$, $F_p = 1301.3$

18/17 " : $\bar{T} = 2793.72$, $F_p = 2797.0$

If we let "vd" be the vibrational level of $^4\Sigma^-$ perturbing $ND^+\ ^2\Pi(0)$, the value of D_{vd} may be obtained from D_{vh} by the isotope effect, without implying anything about the values of vd or vh.

Hence $D_{vd} = 5.4 \times 10^{-4}$ cm^{-1}.

Substitution in (4.26) yields $B_{vd} = 7.86$

$C = 443.45$ cm^{-1} above $F_{1c}(\frac{1}{2})$

Extrapolation of the term values for $^2\Pi$ and $^4\Sigma^-$ shows that the perturbation in both d components would culminate at N=30.

4.5 ND^+ $^2\Pi$ (v=1) and the state perturbing it.

For ND^+ $^2\Pi(1)$ there are three available bands, all from the $^2\Sigma - ^2\Pi$ systems. The average values of the combination differences were found and graphs of $\Delta_2F(N)/(N+\frac{1}{2})$ against $(N+\frac{1}{2})^2$ were drawn for the various components. There was no range of N values for which none of the components were perturbed, so the rotational constants for the c and d levels were found separately and the averages taken. The graph of $(\Delta_2F_{1d}(J) + \Delta_2F_{2d}(J))/(J+\frac{1}{2})$ against $(J+\frac{1}{2})^2$ was used in the region $J=9\frac{1}{2}$ to $J=13\frac{1}{2}$, and $(\Delta_2F_{1c}(J)+\Delta_2F_{2c}(J))/(J+\frac{1}{2})$ against $(J+\frac{1}{2})^2$ was used in the range $J=14\frac{1}{2}$ to $J=17\frac{1}{2}$. The constants are

$$B_1 = 7.983 \pm 0.006$$

$$D_1 = (5.0 \pm 0.2) \times 10^{-4}.$$

Since no $^2\Delta - ^2\Pi$ bands are available for this level, there is no direct way of relating the energies of the sub-levels to one another. We do however have two pairs of $^2\Sigma - ^2\Pi$ bands with common upper levels, and can therefore use the method of Jenkins and McKellar to obtain several relationships similar to (4.6):

$$M''(N) = \Delta G''(\tfrac{1}{2}) + F''_{v=1}(N) - F''_{v=0}(N) \qquad (4.28)$$

All the available equations of this type were used to obtain term values relative to those for v"=0, and after comparison with the combination differences, table 4.10

Table 4.10: Term values for ND^+ $^2\Pi$ (v=1), in cm^{-1}

N	F_{1c}	F_{1d}	F_{2c}	F_{2d}
($J=\frac{1}{2}$)	0	0.07	-	-
1	19.94	21.02	-	-
2	54.74	56.31	82.78	82.72
3	104.01	106.51	127.01	126.85
4	168.41	171.96	187.95	186.97
5	247.56	252.80	264.79	259.19
6	341.07	349.20	356.89	365.96
7	448.13	460.98	462.96	474.23
8	623.24	588.40	627.68	599.57
	567.09	-	581.11	-
9	757.55	731.10	762.15	740.83
10	910.74	889.22	915.71	897.74
11	1081.63	1062.50	1086.76	1070.00
12	1268.91	1250.86	1274.15	1257.38
13	1472.10	1453.96	1477.34	1459.65
14	1690.70	1671.72	1695.84	1676.53
15	1924.45	1903.64	1929.51	1907.53
16	2173.08	2149.35	2178.03	2152.27
17	2436.45	2408.05	2441.30	2409.90
18	2714.19	2679.05	2718.90	2680.05
19	3006.21		3010.90	

$F_{1c}(J=\frac{1}{2})$ is 2148.18 cm^{-1} above $F_{1c}(J=\frac{1}{2})$ of $^2\Pi$ (0).

was constructed. These term values are relative to $F_{1c}(J=\frac{1}{2})$ of v=1, which is 2148.18 cm^{-1} above the corresponding level of v=0.

The deviations of the term values from $B_1N(N+1)-D_1N^2(N+1)^2$ are plotted in Figure 4.6. The perturbations are similar to those in v=0 but occur at lower values of N. $F_{2d}(5)$ is strongly perturbed, but only one of the levels has been found; both levels have been observed for the perturbations in $F_{1c}(8)$ and $F_{2c}(8)$. The F_{1d} and F_{2d} levels are affected by a perturbation which culminates outside the observed range of N values.

The arguments used for NH^+ $^2\Pi(0)$ may be applied again to show that the perturber is $^4\Sigma^-$. At $N_p=5$, N_s must contain $J=4\frac{1}{2}$ but not $J=5\frac{1}{2}$, and therefore $N_s=3$ ($5\not/3$ perturbation). At $N_p=8$, the c components have positive parity and must be perturbed by an <u>odd</u> N_s containing $J=8\frac{1}{2}$ and $J=7\frac{1}{2}$. At $N_p=6,7$ both the F_c levels <u>and</u> the F_{2d} levels are perturbed somewhat, but in opposite senses. $F_{2d}(7)$ can be raised only by $N_s=5$ (since $F_{1d}(7)$ is not perturbed), so that $F_{1c}(7)$ and $F_{2c}(7)$ must be depressed by $N_s=6$. It follows that the perturbation at $N_p=8$ is caused by $N_s=7$. The relative positions, parities and directions of shift are shown in Figure 4.4(c).

The vibrational level of $^4\Sigma^-$ producing the perturbations is evidently (vd + 1). In order to calculate its position we estimate the position of the 'extra' level for $N_p=5$ and obtain the following energies (in cm^{-1}) above $F_{1c}(\frac{1}{2})$ of $^2\Pi(1)$:-

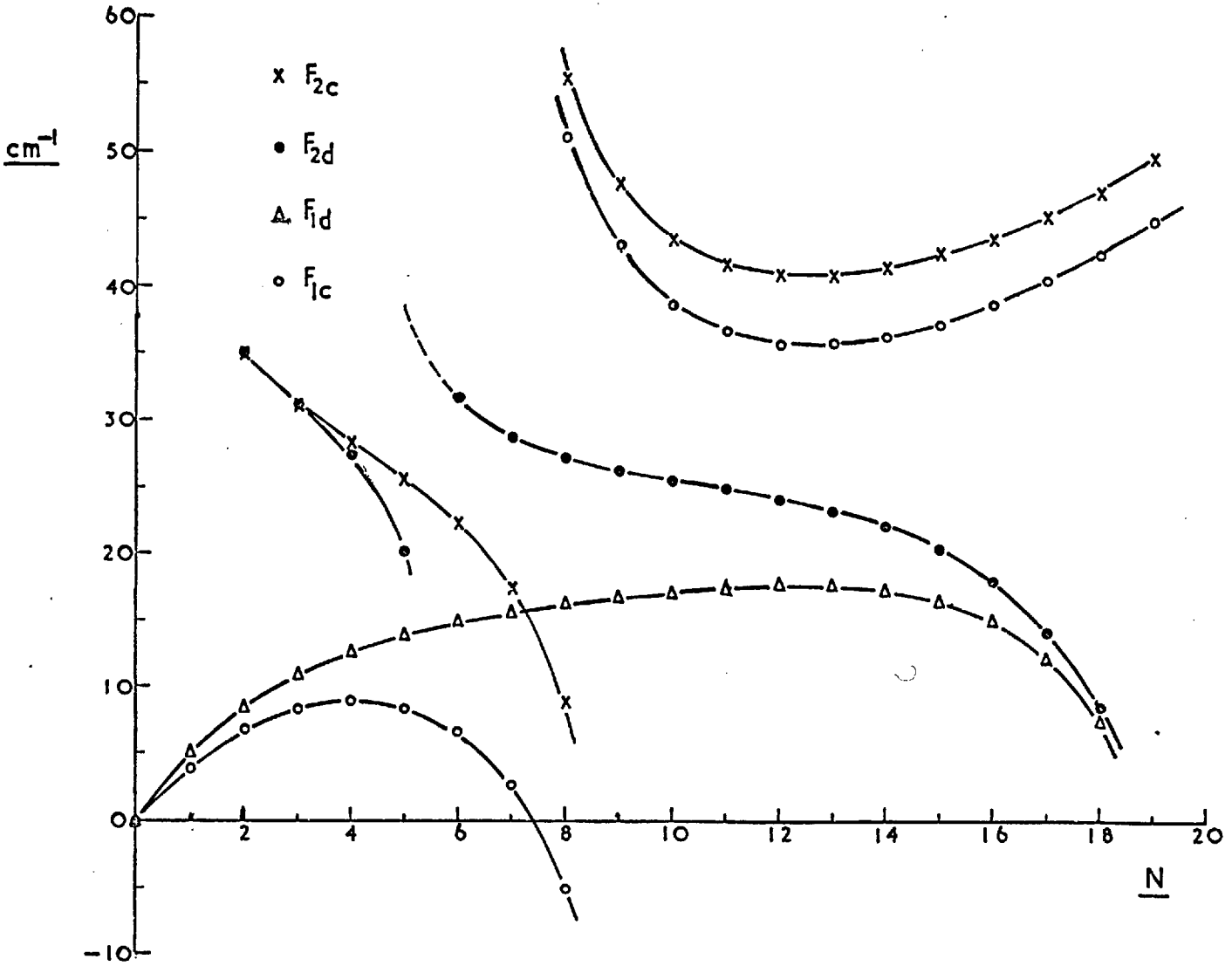

Figure 4.6: $F(N) - (7{\cdot}983N(N+1) - 5{\cdot}01\times10^{-4}N^2(N+1)^2)$ for $ND^+\ ^2\Pi(v=1)$

5/3 perturbation: $\bar{T} = 268.62$, $F_p = 268.44$

8/7 " : $\bar{T} = 599.78$, $F_p = 594.49$

On the assumption that $D_{vd+1} = D_{vd} = 5.4 \times 10^{-4}$, substitution in (4.26) gives $B_{vd+1} = 7.68$

$C = 176.73\ cm^{-1}$ above $F_{1c}(\frac{1}{2})$ of $^2\Pi(1)$

$= 2324.91 cm^{-1}$ above $F_{1c}(\frac{1}{2})$ of $^2\Pi(0)$

By making use of the results of section 4.4, we deduce that

$$\alpha_e^D = 0.18 cm^{-1}$$

$$\Delta G(vd+\tfrac{1}{2}) = 1881.46\ cm^{-1}.$$

Extrapolation shows that the perturbation in both d components culminates at N=21,22.

The spin-splitting for $^2\Pi(1)$ is certainly affected by the 5/3 perturbation, but for N=2 and N=3 equation (4.22) gives

$$Y_1 = 8.99 \pm 0.01,\ A_1 = 71.8 \pm 0.1\ cm^{-1}.$$

4.6 NH^+ $^2\Pi(v=1)$ and the state perturbing it.

NH^+ $^2\Pi(1)$ behaves in a very unusual manner. Graphs of $\Delta_2 F(N)/(N+\frac{1}{2})$ against $(N+\frac{1}{2})^2$ suggested that F_{1c}, F_{2c} and F_{1d} are strongly perturbed at low values of N; and a graph of the mean $\Delta_2 F(J)/(J+\frac{1}{2})$ against $(J+\frac{1}{2})^2$ showed that if values of J less than $9\frac{1}{2}$ are ignored, plausible rotational constants ($B_1 = 14.664 \pm 0.004$, $D_1 = (14.40 \pm 0.13) \times 10^{-4}$) can be obtained. If, however, separate constants are obtained for the c and d components, B_1^c is found to be $0.14\ cm^{-1}$ larger than B_1^d. This enormous difference can only be understood when the perturbations are explained.

Since perturbations occur for very low values

of N, no attempt was made to find the spin-orbit coupling constant, A.

The term values were determined in the same way as for ND^+ $^2\Pi(1)$, and they are presented in table 4.11. The base has been taken 2901.05 cm^{-1} above $F_{1c}(J=\frac{1}{2})$ of NH^+ $^2\Pi(0)$. This is, according to the analysis, the position of $F_{1d}(\frac{1}{2})$ of $^2\Pi(1)$; but the assignments of all the four lowest levels - $F_{1c,d}(\frac{1}{2})$ and $F_{1c,d}(1\frac{1}{2})$ - are doubtful and will be ignored in the analysis of the perturbations.

The deviations of the term values from $B_1N(N+1) - D_1N^2(N+1)^2$ are plotted in Figure 4.7, on the basis of which we now discuss the perturbations.

1) There are no discontinuities in the curves, such as were observed at the strong perturbations of earlier sections. It follows that the energy levels of the perturbing state do not 'cross' the levels of equal J in the Π state.

2) We cannot find the rotational constants of the perturbing state by the method used previously. It is reasonable to suppose, however, that the perturber is the (vh+1) level of $^4\Sigma^-$, in which case we can predict the rotational constant B_{vh+1} by means of the isotope effect; and D_{vh+1} may be assumed to be equal to D_{vh}.

We have $\alpha_e^D=0.18$; therefore $\alpha_e=\alpha_e^D/\rho^3= 0.46$

$$B_{vh+1} = B_{vh} - \alpha_e = \underline{14.26}$$

$$D_{vh+1} = D_{vh} = 18.9\times10^{-4}$$

3) If the values of $\frac{1}{2}(F_{1c}(N)+F_{1d}(N))-(B_1N(N+1)-D_1N^2(N+1)^2)$

Table 4.11 : Term values for NH^+ $^2\Pi$ (v=1) and $^4\Sigma^-$(vh+1), in cm^{-1}

N	F_{1c}	F_{1d}	F_{2c}	F_{2d}	$^4\Sigma^-$
($J=\frac{1}{2}$)	11.65	0	-	-	(-10)
1	46.72	40.45	-	-	18.5
2	106.78	111.31	114.55	131.26	75.5
3	193.88	202.27	196.21	217.02	160.8
4	310.38	320.11	311.16	331.59	274.4
5	456.54	465.99	456.52	475.32	416.1
6	631.64	640.06	631.51	647.93	585.6
7	835.66	842.65	835.59	849.39	782.6
8	1068.19	1073.47	1068.17	1079.35	1006.9
9	1328.90	1332.44	1329.09	1337.64	1258.1
10	1617.48	1619.15	1617.72	1623.82	1535.7
11	1933.49	1933.36	1933.93	1937.59	1839.4
12	2276.50	2274.55	2276.99	2278.46	2168.6
13	2646.05	2642.44	2646.78	2646.11	2522.7
14	3041.16	3036.27	3042.38	3039.81	2901.3
15		3456.0		3459.2	3303.5

$F_{1d}(J=\frac{1}{2})$ is 2901.05cm^{-1} above $F_{1c}(J=\frac{1}{2})$ of $^2\Pi(0)$

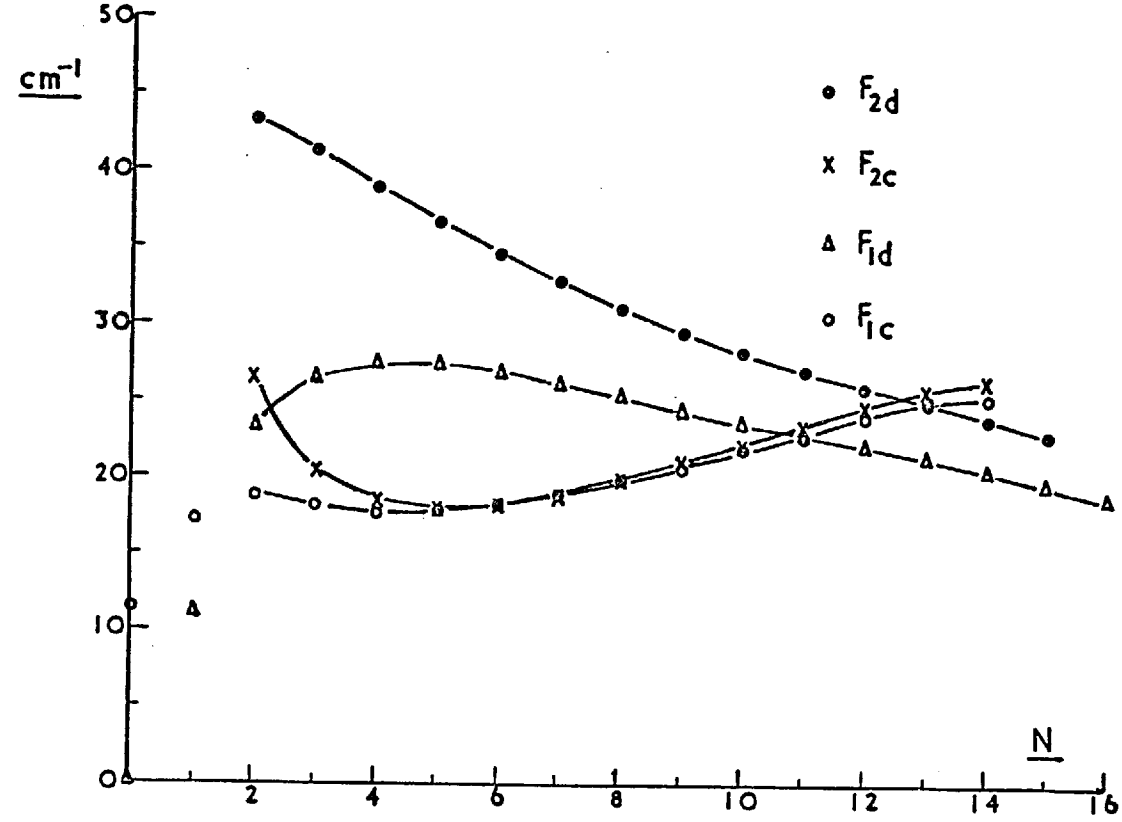

Figure 4.7: $F(N) - (14.664\,N(N+1) - 14.4\times10^{-4}N^2(N+1)^2)$ for $NH\,^2\Pi(1)$

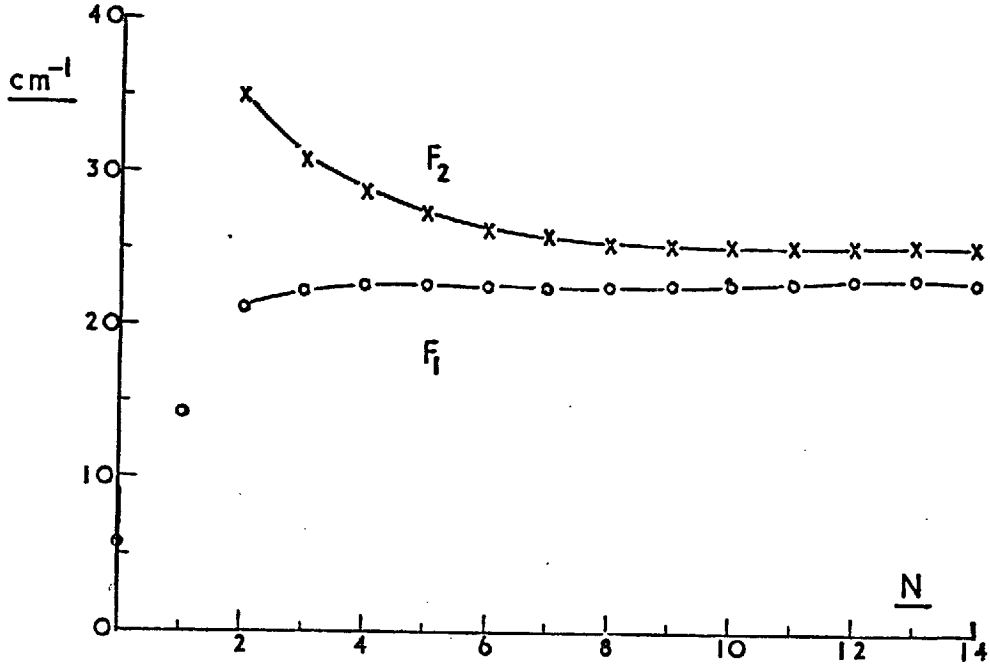

Figure 4.8: $\frac{1}{2}(F_c(N) + F_d(N)) - (14.664\,N(N+1) - 14.4\times10^{-4}N^2(N+1)^2)$ for $NH\,^2\Pi(1)$

and $\frac{1}{2}(F_{2c}(N)+F_{2d}(N))-(B_1N(N+1)-D_1N^2(N+1)^2)$ are plotted against N - see Figure 4.8 - the results are in broad agreement with the normal behaviour of a $^2\Pi$ state (compare Herzberg's Figure 108(a), or the d components of Figure 4.5 for ND^+). This suggests that all four types of sub-level are perturbed, and that the d and c components are shifted in opposite directions and by approximately equal amounts.

4) The above interpretation is supported by an examination of the Λ-doubling. Not only is the splitting $F_c(N)-F_d(N)$ unusually large at the low values of N, but it is <u>negative</u> for both sub-bands. From the theory of Mulliken and Christy and also from the behaviour of NH^+ $^2\overline{\Pi}$ (0), one would expect $F_{2c}(N)-F_{2d}(N)$ to be positive, whereas in fact $F_{2c}(2)-F_{2d}(2)=-16.71cm^{-1}$, $F_{2c}(3)-F_{2d}(3)=-20.81cm^{-1}$ etc. (In the paper by Mulliken and Christy the labels c and d should be interchanged for Π states when Herzberg's convention is used). It therefore appears that the d components are perturbed to higher energies and the c components are depressed.

5) In ND^+ $^2\overline{\Pi}$(1), the level $N_s=5$ is able to perturb $F_{2d}(7)$ and $F_{1c,2c}(6)$ in opposite senses (see Figure 4.4 (c)). In NH^+ $^2\overline{\Pi}$(1) we require a value of N_s which, provided that the energy differences are suitable, would raise (say) $F_{1d}(5)$ and $F_{2d}(5)$ <u>and</u> depress $F_{1c}(4)$ and $F_{2c}(4)$. Such a value of N_s must have positive parity and contain sub-levels with $J=3\frac{1}{2}$,

$J=4\frac{1}{2}$ and $J=5\frac{1}{2}$. These conditions are satisfied only by $N_s=5$, and similar arguments for other levels lead to the scheme of Figure 4.4(d).

6) In order to examine whether the relative positions of Figure 4.4(d) are energetically possible, term values for $^4\Sigma^-(vh+1)$ were obtained from the expression

$$F_s(N)=14.26N(N+1)-18.9\times10^{-4}N^2(N+1)^2.$$

The results show that if $F_s(0)$ were coincident with the lowest level of $^2\Pi(1)$, then $F_s(N)$ would lie <u>below</u> $F_p(N)$ and <u>above</u> $F_p(N-1)$ until $F_s(30)$ crossed $F_p(29)$. Therefore the numbering of Figure 4.4(d) is possible without a cross-over perturbation being observed in the region investigated.

This and other conclusions may be checked by reference to table 4.11, where the <u>final</u> term values of $^4\Sigma^-$ are listed alongside those of $^2\Pi(1)$.

7) Examination of the range of forces between $^2\Pi$ and $^4\Sigma^-$ in the other perturbed states (NH^+ v=0, ND^+ v=0,1) shows that shifts of 10 cm^{-1} can occur in levels which before interaction are 40 cm^{-1} apart. Shifts of 2 cm^{-1} can occur if the levels are 70 cm^{-1} apart, shifts of 1 cm^{-1} occur at distances of 100 cm^{-1}, and weak disturbances are made at ranges of up to 130 cm^{-1}. For rotational perturbations in a diatomic molecule these shifts are exceptionally large, and the shift in a particular case depends somewhat on the J-value of the levels; but the figures show that the range of the repulsive forces is consistent with the above

interpretation of the perturbations in NH^+ $^2\Pi(1)$.

8) It is necessary to find the position of the (vh+1) level of $^4\Sigma^-$ as closely as possible in order to establish the value of vh. The possible range of positions may be reduced by - for example - the observation that if $F_s(10)$ were mid-way between $F_p(9)$ and $F_p(10)$, then $F_s(3)$ would be <u>below</u> $F_p(2)$ and a cross-over perturbation would be observed. Moreover, examination of Figure 4.8 shows that there is a considerable asymmetry at the lower values of N, in that both curves are higher than expected. This suggests that at low N the d components are perturbed more than the c components, and that therefore $F_s(N)$ is somewhat closer to $F_p(N)$ than to $F_p(N-1)$. This conclusion is supported by examination of the term values; for it can be shown that, when N increases, the difference between $F_s(N)$ and $F_p(N)$ - governing the perturbations of the d components- increases at a much slower rate than the difference between $F_s(N)$ and $F_p(N-1)$. In view of these considerations the level $^4\Sigma^-(vh+1)$ is given as (10 ± 10) cm^{-1} <u>below</u> the "zero" of table 4.11, and the term values of $^4\Sigma^-$ included in table 4.11 have been adjusted accordingly. If the energy is referred to the base of table 4.8, then $^4\Sigma^-(vh+1)$ is 2891 ± 10 cm^{-1} above $F_{1c}(\frac{1}{2})$ of $^2\Pi(0)$, and so <u>$\Delta G(vh+\frac{1}{2}) = 2536\pm10$ cm^{-1}</u>.

The values of the rotational constants for $^2\Pi$ are summarised in table 4.12. Because of the perturbations, these have been more than usually

difficult to determine, and the ratios for the two isotopes (table 4.13) show small discrepancies from theory.

Table 4.12: Rotational constants for $^2\Pi$, in cm^{-1}

	NH^+	ND^+
B_o	15.301(3)	8.2338(6)-B^d
B_1	14.664(4)	7.983(6)
10^4D_o	15.78 (6)	4.60 (1)-D^d
10^4D_1	14.40(13)	5.0 (2)
α_e	0.637(5)	0.251(6)
B_e	15.620(4)	8.359(3)
Y_o	5.11 (2)	9.56 (1)
Y_1		8.99 (1)
A_o	78.2 (3)	78.72 (8)
A_1		71.8 (1)

Table 4.13: Ratios of the rotational constants for $^2\Pi$

Ratio	Experimental Value	Theoretical Value
B_e^D/B_e	0.5351 (2)	0.5339
α_e^D/α_e	0.394 (10)	0.390
D_o^D/D_o	0.2915	0.2851(D_e^D/D_e)

4.7 Band origins and vibrational constants.

In bands with $\Delta\Lambda=\pm1$ it is convenient to determine the band origins from the intense Q branches. For $^2\Sigma^+-^2\Pi$ we have

$$Q_{1,2}(J) = \nu_o + F'_{1,2}(J) - F''_{1d,2d}(J) \qquad (4.29)$$

Defining $F''(J)$ and $\Delta\nu_{cd}(J)$ by

$$F''_i(J) = \tfrac{1}{2}(F''_{ic}(J)+F''_{id}(J)) \qquad (4.30)$$

$$\Delta\nu_{icd}(J)=F''_{ic}(J)-F''_{id}(J) \qquad (4.31)$$

we obtain

$$\nu_o=\tfrac{1}{2}(Q_1(J)+Q_2(J))-\tfrac{1}{2}(F'_1(J)+F'_2(J))+\tfrac{1}{2}(F''_1(J)+F''_2(J))-\tfrac{1}{4}(\Delta\nu_{1cd}(J)+\Delta\nu_{2cd}(J)) \qquad (4.32)$$

For $^2\Sigma^- - ^2\Pi$ the expressions become

$$Q_{1,2}(J)=\nu_o+F'_{1,2}(J)-F''_{1c,2c}(J) \qquad (4.33)$$

$$\nu_o=\tfrac{1}{2}(Q_1(J)+Q_2(J))-\tfrac{1}{2}(F'_1(J)+F'_2(J))+\tfrac{1}{2}(F''_1(J)+F''_2(J))+\tfrac{1}{4}(\Delta\nu_{1cd}(J)+\Delta\nu_{2cd}(J)) \qquad (4.34)$$

In $^2\Delta - ^2\Pi$ bands the Λ-doubling of the lower state may be eliminated by taking the average of all four Q branches:

$$\nu_o=\tfrac{1}{4}(Q_{1cd}(J)+Q_{1dc}(J)+Q_{2cd}(J)+Q_{2dc}(J))-\tfrac{1}{2}(F'_1(J)+F'_2(J))+\tfrac{1}{2}(F''_1(J)+F''_2(J)) \qquad (4.35).$$

The expressions in F(J) were calculated from the rotational constants using equations (4.1), (4.2), (4.12) and (4.19). Values of ν_o were found for each band, using the low values of J. In some cases only two or three values could be used because of the perturbations in $^2\Pi$; for bands with NH^+ $^2\Pi(1)$ it was necessary to use values of J in the range $7\frac{1}{2}$ to $12\frac{1}{2}$. The results are presented in tables 4.14(NH^+) and 4.15(ND^+), those for $^2\Sigma^+ - ^2\Pi$ being in the form of a Deslandres array.

Table 4.14: Band origins for NH^+, in cm^{-1}

$^2\Sigma^+ - ^2\Pi$

v' \ v''	0		1
0	34537.68 (2)		
	2004.95		
1	36542.63 (2)	2915.48 (8)	33627.15 (8)
	1857.39		1857.45
2	38400.02 (2)	2915.42 (10)	35484.60(10)
			1720.43
3			37205.03(16)

$^2\Sigma^- - ^2\Pi$

(0,0)- 21543.88 (2)

(0,1)- 18628.25 (7)

$^2\Delta - ^2\Pi$

(0,0)- 22911.98 (2)

Table 4.15: Band origins for ND^+, in cm^{-1}

$^2\Sigma^+ - ^2\Pi$

v' \ v''	0		1
0	34671.99 (1)		
	1495.91		
1	36167.90 (1)		
	1414.71		
2	37582.61 (1)	2144.64 (15)	35437.97 (15)
			1337.75
3			36775.72 (15)

Table 4.15: ND^+ (continued)

$^2\Sigma^- - ^2\Pi$

(0,0)- 21719.45(8)

(0,1)- 19574.71(15)

(1,0)- 22901.91(8)

$^2\Delta - ^2\Pi$

(0,0)-23020.62(8)

From the band origins we obtain the first vibrational quanta for the $^2\Pi$ states of NH^+ and ND^+:

$$\Delta G(\tfrac{1}{2}) = 2915.53 \pm 0.06 \text{ cm}^{-1} \quad (NH^+)$$

$$\Delta G^D(\tfrac{1}{2}) = 2144.69 \pm 0.10 \text{ cm}^{-1} \quad (ND^+).$$

If G(v) is approximated by equation (4.9), then these quanta are given by

$$\Delta G(\tfrac{1}{2}) = \omega_e - 2\omega_e x_e \qquad (4.36)$$

$$\Delta G^D(\tfrac{1}{2}) = \rho\,\omega_e - 2\rho^2 \omega_e x_e \qquad (4.37)$$

On substituting for ρ, the vibrational constants

$$\omega_e = 2988.3 \text{ cm}^{-1}$$

$$\omega_e x_e = 36.4 \text{ cm}^{-1}$$

are obtained for NH^+ $^2\Pi$.

4.8 The ground state of NH^+

As mentioned in chapter 1, Feast (1951) showed that the lowest electronic state of NH^+ could be either $^2\Pi$ or $^4\Sigma^-$. According to the vibrational numbering we have chosen, the ground state is $^2\Pi$ if vh=0; but if vh≠0, then $^4\Sigma^-$ lies lower than $^2\Pi$.

By obtaining and analysing the spectra of ND^+ as well as those of NH^+, it has been possible to measure

a vibrational quantum of $^4\Sigma^-$ for each isotope. Furthermore, the fact that the values of T_e are to a good approximation independent of the isotopic mass enables us to relate the energy levels of the deuteride to those of the hydride.

The most dependable vibrational constants are those for $^2\Sigma^+$(table 4.5). The energies of $^2\Sigma^+(0)$ above the bottom of the potential curve are

$$G(0) = 1061.13\text{cm}^{-1}(NH^+),\ 779.80\text{cm}^{-1}(ND^+).$$

Combination of these values with the band origins for $^2\Sigma^+ - ^2\Pi$ shows that $^2\Pi$ (v=0) of NH^+ is 415.66 cm^{-1} above $^2\Pi$ (v=0) of ND^+. The levels of $^4\Sigma^-$ have been referred to $F_{1c}(\frac{1}{2})$ of $^2\Pi$ (0), and after correcting for this we obtain the vibrational term scheme of Figure 4.9, where the energies are referred to ND^+, $^2\Pi$ (0). $^4\Sigma^-$(vh) is 331.5 cm^{-1} above NH^+ $^2\Pi$ (0) and $^4\Sigma^-$(vd) is 412.4 cm^{-1} above ND^+ $^2\Pi$ (0). In view of the extrapolation of the $^4\Sigma^-$ levels to N_s=0 and the method of calculating the relative positions of the $^2\Pi$ states, the value of G(vh)-G(vd) is estimated as 335 ± 15 cm^{-1}.

If the vibrational energy function G(v) of $^4\Sigma^-$ can be written in the form (4.9), then we have the three equations

$$\omega_e - 2(vh+1)\omega_e x_e = 2536\pm10 \qquad (4.38)$$

$$\rho\omega_e - 2(vd+1)\rho^2\omega_e x_e = 1881.5 \qquad (4.39)$$

$$\omega_e(vh+\tfrac{1}{2} - \rho(vd+\tfrac{1}{2})) - \omega_e x_e((vh+\tfrac{1}{2})^2 - \rho^2(vd+\tfrac{1}{2})^2) = 335\pm15 \qquad (4.40)$$

It is important to realise that approximate relationships between the rotational and vibrational

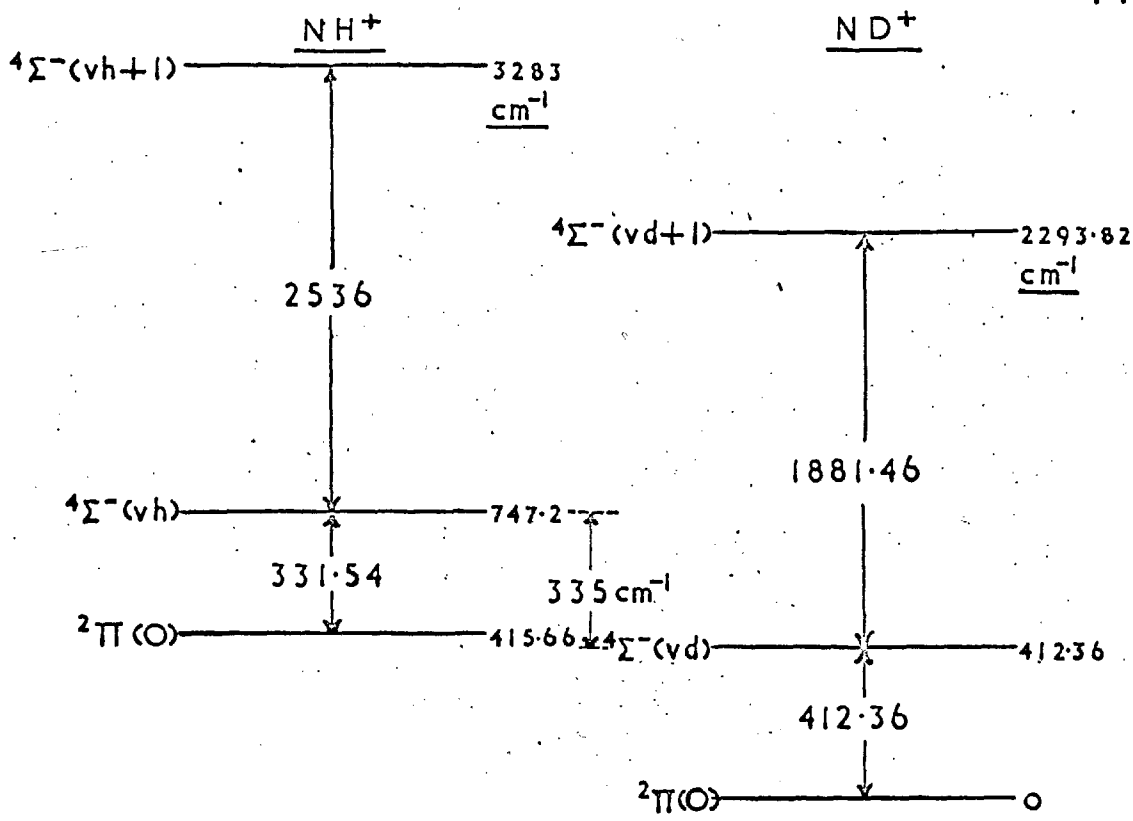

Figure 4.9: Vibrational levels of $^4\Sigma^-$ (not to scale)

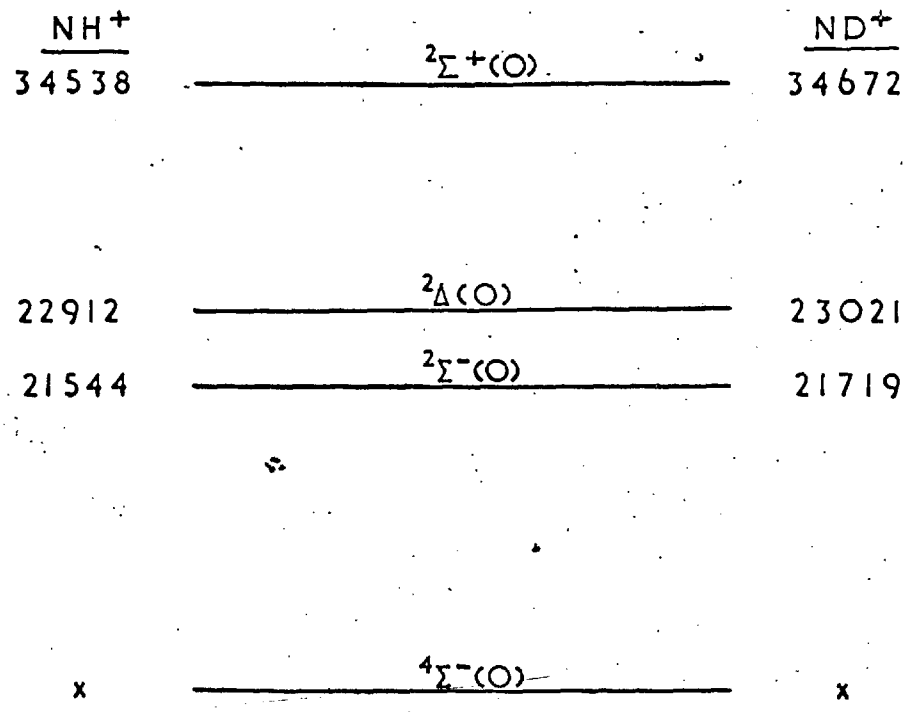

Figure 4.10: Energies above $^2\Pi(O)$, in cm^{-1}

constants, such as (4.11), cannot be used to find the vibrational numbering because they use B_e, and the choice of B_e implies a particular numbering. Again, B_{vd}/B_{vh} equals ρ^2, but this does not necessarily mean that vd=vh, since for $^2\Sigma^+$ B_3^D/B_2 also equals ρ^2. However, we know that ω_e is greater than 2500 cm^{-1}, so that (G(vh)-G(vd)) is relatively small. Therefore vd is equal to or greater than vh, and we examine equations (4.38-40) accordingly.

1) If vh=vd, then vh=vd=0. In this case (4.38) and (4.39) give

$$\omega_e = 2680 \pm 27 \text{ cm}^{-1}$$
$$\omega_e x_e = 72 \pm 19 \text{ cm}^{-1},$$

and the left-hand side of equation (4.40) equals 352 ± 17 cm^{-1}. Therefore vh=vd=0 is a consistent solution with reasonable values for the constants.

2) If vd=vh+1, equations (4.38-40) can be solved to give two roots. Only vh=3 gives reasonable molecular constants from (4.38-39):-

$$\omega_e = 2983 \pm 107 \text{ cm}^{-1}$$
$$\omega_e x_e = 56 \pm 15 \text{ cm}^{-1}.$$

Equation (4.40) now represents $(G(3)-G^D(4))$, for which the above constants give 548 ± 566 cm^{-1}! Thus vh=3, vd=4 is a possible numbering.

3) If vd=vh+2 is substituted in (4.38-40), reasonable constants are obtained only for vh=6. This would mean that G(0) of $^4\Sigma^-$ was some 18000 cm^{-1} below G(0) of $^2\Pi$, which is most unlikely (see below).

We have therefore two possibilities which are consistent with experiment, namely vh=vd=0 and vh=3, vd=4.

Now, the electron configurations of NH^+ are identical with those of CH, so that the lowest configuration is $K(2s\sigma)^2(2p\sigma)^2 2p\pi$, which gives rise to the $^2\Pi_r$ term only (Herzberg, p.341). The first excited configuration is $K(2s\sigma)^2\ 2p\sigma(2p\pi)^2$, which gives $^4\Sigma^-$, $^2\Delta$, $^2\Sigma^+$ and $^2\Sigma^-$. All these states are expected to be stable, so that they must be identified with the states observed in these experiments. The relative spacing of the terms derived from the configuration --- $\sigma\pi^2$ has been predicted using quantum mechanics (Mulliken (1932), p12), with the result that $^2\Delta$ may, to a first approximation, be expected to lie half way between $^2\Sigma^+$ and the mean of $^2\Sigma^-$ and $^4\Sigma^-$.

The energies of the v=0 levels of $^2\Delta$, $^2\Sigma^+$ and $^2\Sigma^-$ relative to $^2\Pi$(v=0) are given in Figure 4.10. If $^4\Sigma^-$ lies at an energy x above $^2\Pi$(0), and x is predicted from the theoretical result given above, we obtain

$$x = +1028\ cm^{-1}(NH^+),\ +1020\ cm^{-1}(ND^+).$$

If vh=0, x=+332 cm^{-1}; and if vh=3, x=-8000 cm^{-1} (approx). Therefore, the available evidence suggests that the <u>v=0</u> level of $^4\Sigma^-$ perturbs NH^+ $^2\Pi$(0), and that $^2\Pi_r$ is the ground state of NH^+, being 332 cm^{-1} below $^4\Sigma^-$.

In accordance with the usual practice, the states will now be named $X^2\Pi$, $A^2\Sigma^-$, $B^2\Delta$, $C^2\Sigma^+$ and $a^4\Sigma^-$.

The constants of $a^4\Sigma^-$, deduced from

perturbations of $X^2\Pi$ and by application of the isotope effect, are presented in table 4.16.

Table 4.16 : Constants of $^4\Sigma^-$, in cm^{-1}

	NH^+	ND^+
B_o	14.72	7.86
B_1	14.26	7.68
α_e	0.46	0.18
$10^4 D_o$	18.9	5.4
ω_e	2680(27)	1959(20)
$\omega_e x_e$	72(19)	39(10)

CHAPTER 5: THE WEAK SINGLET SYSTEMS OF NH AND ND.

The positive-column discharge used in the present work proved to be an intense source not only for the spectra of NH^+, but also for those of NH. As described in chapters 1 and 2, the opportunity was taken to photograph the $d^1\Sigma^+ - c^1\Pi$ and $c^1\Pi - b^1\Sigma^+$ systems of NH and ND at high dispersion, to analyse new bands, and to calculate new and revised molecular constants. In particular, no analyses of the ND systems discussed here have previously been published. For NH, little has previously been added to the work of Lunt, Pearse and Smith (1935a, 1936).

The constants have been determined by the method of least squares, as described in the introduction to chapter 4. The standard deviation of the last significant figure is given in brackets following each constant.

5.1 The $d^1\Sigma^+ - c^1\Pi$ system

The values of the rotational constant B (and hence the inter-nuclear distance) are almost equal for the states d and c, so that according to the Franck-Condon theory of intensity distribution the sequence of bands with v'=v" will be the most intense in the d-c system. This is observed to be so, and the (0,0) and (1,1) bands of NH, and the (0,0), (1,1) and (2,2) bands of ND - all in the wavelength range 2460-2560Å - were photographed in the third order of the 21ft grating with Ilford Zenith plates. Exposures varied from 1 hour for the (0,0) bands to 7½hours for the ND (2,2) band, and the accuracy of the wave numbers

ranges from $\pm 0.03 cm^{-1}$ to $\pm 0.06 cm^{-1}$, depending on the intensity of the band. Lunt et al (1936) photographed the (0,0) band of NH ($\lambda 2530$) on a Hilger E1 quartz spectrograph using exposures of 'from 1 to 2 hours'; with the same spectrograph and the present source, exposures of only 30 seconds were required.

Bands of the v'-v"=1 sequence could not be distinguished from the hydrogen continuum, but at longer wavelengths it was possible, by using exposure times of $7\frac{1}{2}$ hours with the fast Ilford Zenith Astronomical plates, to photograph part of the v'-v"=-1 sequence. The wavelengths of the P and Q band heads are presented in table 5.1; the Q head of the (1,2) band of ND has been predicted by means of combination differences.

Table 5.1: Wavelengths in Å of the band heads of the d-c system.

	NH		ND	
Band	P head	Q head	P head	Q head
(0,0)	2557.245	2530.159	2552.940	2532.382
(0,1)	2683.071	2673.540	2648.229	2640.281
(1,1)	2516.261	2504.169	2526.480	2515.548
(1,2)			2613.396	(2609.02)
(2,2)			2497.195	2491.946

$^1\Sigma^+ - ^1\Pi$ bands have three branches, the first lines of which are shown in Figure 5.1. The branches represent the following energy differences:

$$P(J) = \nu_o + F'_c(J-1) - F''_c(J) \qquad (5.1)$$

$$Q(J) = \nu_o + F'_c(J) - F''_d(J) \qquad (5.2)$$

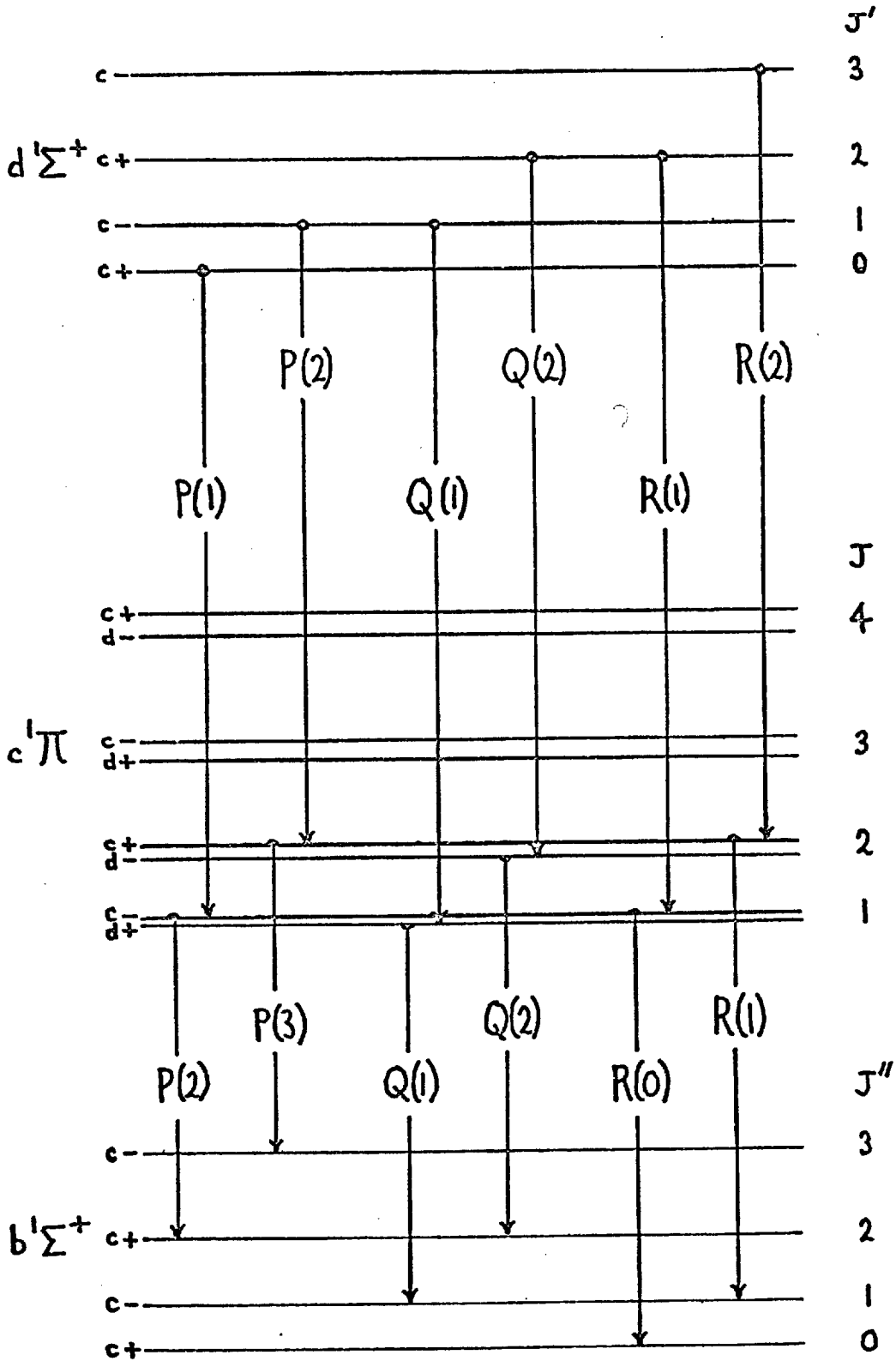

Figure 5.1: First lines for $^1\Sigma^+ - ^1\Pi$ and $^1\Pi - ^1\Sigma^+$

$$R(J) = \nu_0 + F'_c(J+1) - F''_c(J) \qquad (5.3)$$

Most of the structure of the present bands is very open, as shown in Plate 5; the Q branch of the ND (0,0) band, however, contains within a range of 0.5Å no fewer than 20 lines, of which 12 have been resolved. Such a narrow congested region bounded by two sharp edges is characteristic of a Q branch with <u>two</u> heads, and this interpretation may be verified from the enlarged photograph published in Whittaker (1967) and from the Fortrat Diagram of Figure 5.2. In the (0,0) band of NH, the Q branch was not resolved for J less than 9, but the first members may be predicted from the relations

$$Q(J)=P(J+1)+F''_c(J+1)-F''_d(J)=R(J-1)+F''_c(J-1)-F''_d(J) \qquad (5.4)$$

using data for $c^1\Pi$ from Pearse (1933) and Dieke and Blue (1934). The results of such predictions are given in table 5.2, and a Fortrat Diagram is included in Figure 5.2.

<u>Table 5.2</u>: Predicted wave numbers for part of the Q branch of the NH d-c (0,0) band, in cm^{-1}.

J	Q	J	Q
1	39512.38	5	39511.30
2	12.16	6	11.18
3	11.83	7	11.25
4	11.42	8	11.56

It is clear that this branch also has two heads, the second being near J=6. In table 5.1 the value given for the Q head of each (0,0) band refers to the head of longer wavelength.

The (0,1) band of NH at λ2683 overlaps the

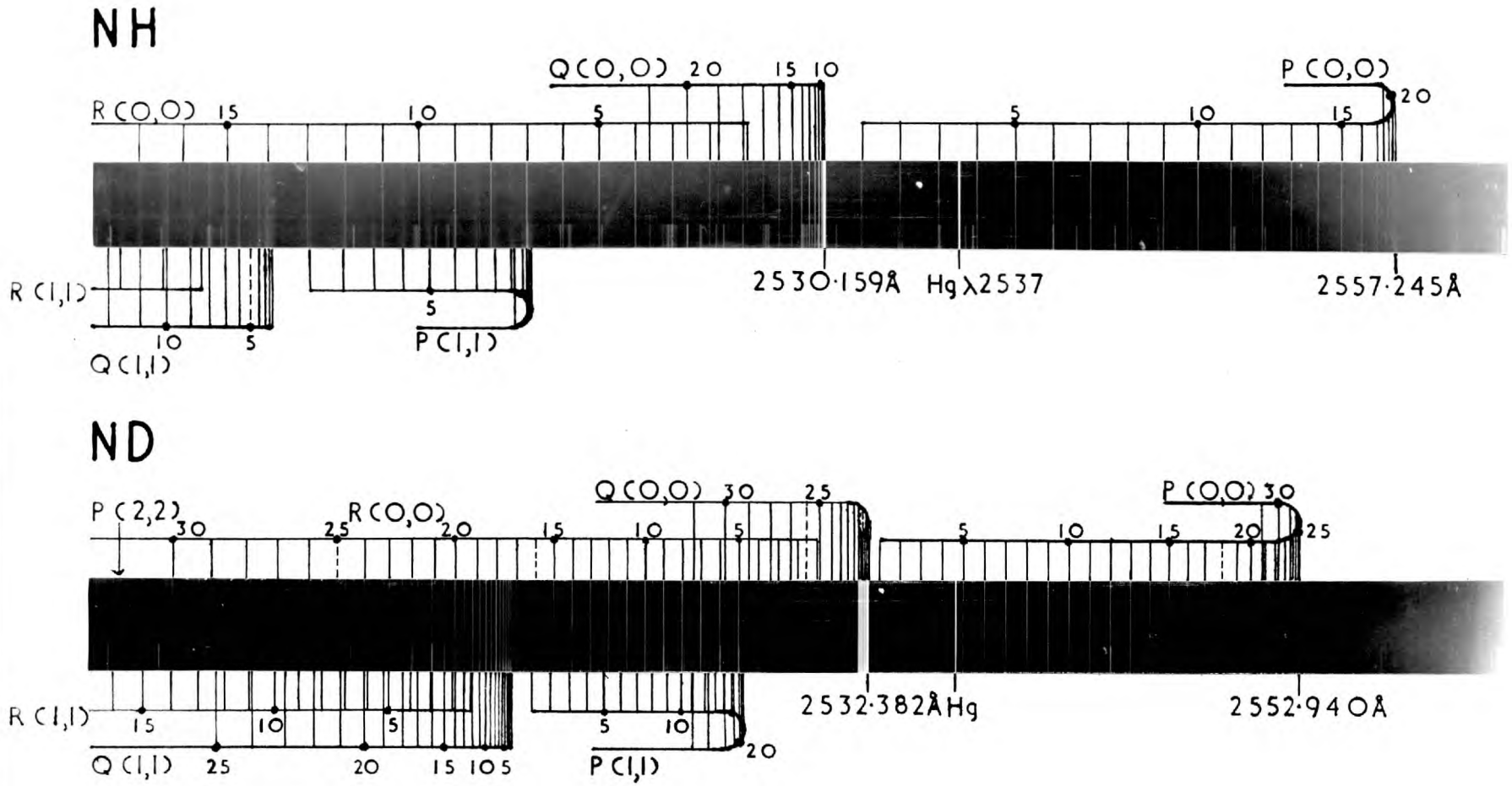

PLATE 5: (0,0) SEQUENCE OF $d'\Sigma^+ - c'\Pi$

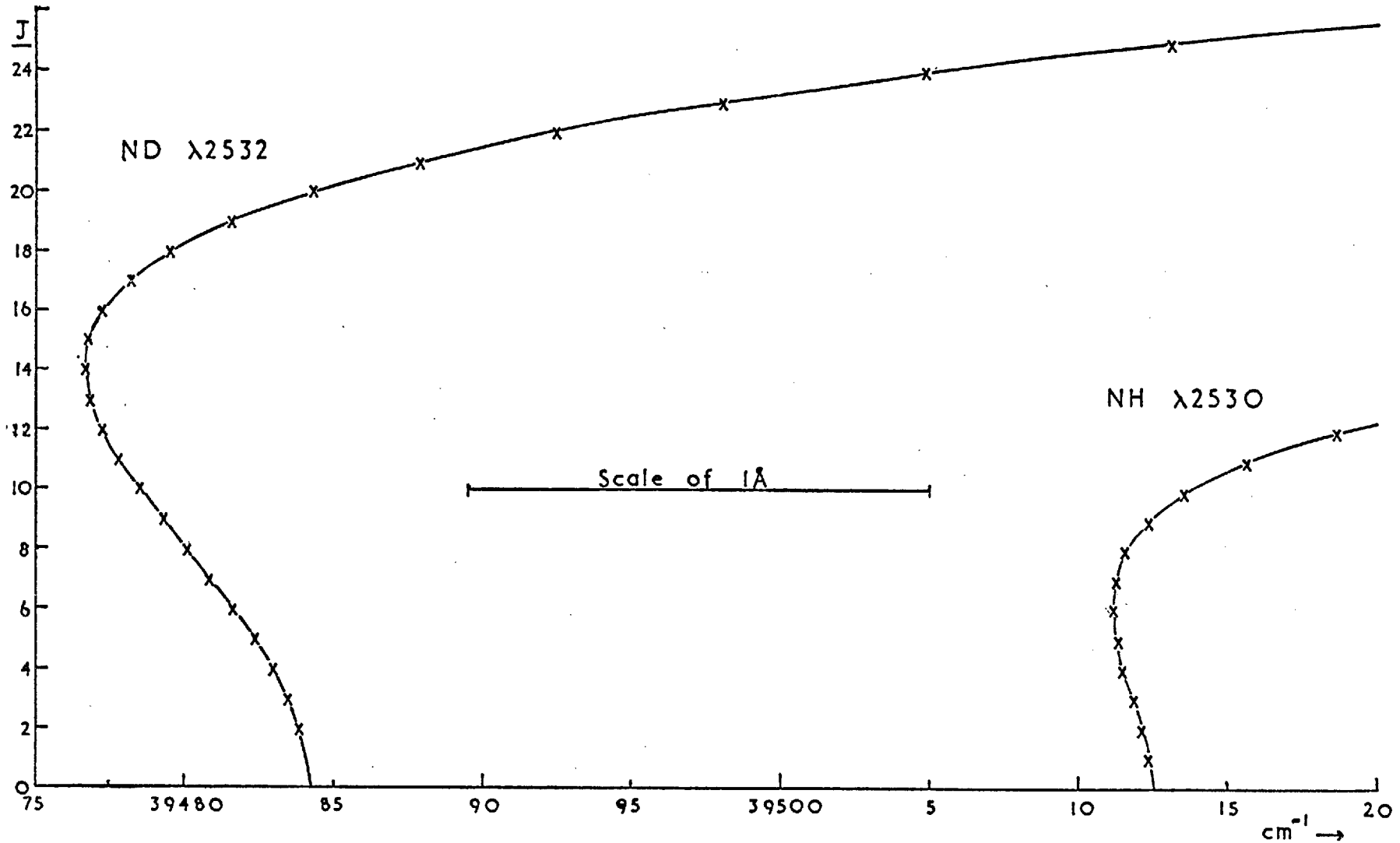

Figure 5.2: Fortrat Diagram of the double-headed Q branches at 2530Å and 2532Å.

(2,0) band of the ultraviolet NH^+ system, but as both bands have a very open structure, this did not hinder the analysis. The numbering of the (0,1) band agrees with that of Narasimham and Krishnamurty (1966), who obtained the band at somewhat lower dispersion (2.6 Å/mm as compared with 0.36 Å/mm) but found only four members of the weak R branch.

The (0,1) band of ND is surprisingly weak; it is apparently less intense than the corresponding band of NH and is of similar intensity to the (1,2) band of ND. It would be interesting to check the intensities quantitatively; all the transitions from J'=17 and J'=26 of ND $d^1\Sigma^+(0)$ and from J'=5 of NH $d^1\Sigma^+(1)$ are abnormally weak, which suggests that accidental predissociations - caused through perturbation by a diffuse state (Herzberg, p. 415) - may occur.

The (1,2) band of ND was overlapped by the nitrogen band at λ 2609 (section 3.1). The wavenumbers of all the observed bands are given in tables 5.4(NH) and 5.5(ND).

Table 5.3 shows some combination differences ($\Delta_2F_c(J)$) for $c^1\Pi$ taken from the (0,0) bands of the three singlet systems of NH and ND. The data for the λ3240 band and the λ3235 band are taken from Dieke and Blue (1934) and Hanson et al (1965), respectively; the figures for the d-c and c-b systems are from the present work.

Table 5.3: Some values of $\Delta_2 F_c(J)$ for $c^1\Pi$ (v=0), in cm^{-1}

	NH bands			ND bands		
	d-c	c-a	c-b	d-c	c-a	c-b
J	λ2530	λ3240	λ4502	λ2532	λ3235	λ4484
2	141.30	141.30	141.38	76.28		76.22
3	197.52	197.40	197.55	106.74	106.68	106.68
4	253.28	253.29	253.27	137.02	136.98	136.94
5	308.58	308.55	308.57	167.19	167.16	167.13
6	363.30	363.20	363.26	197.17	197.25	197.15
7	417.21	417.13	417.27	227.01	227.11	226.98
8	470.46f	470.37	470.43	256.56	256.65	256.58
9	522.62	522.51f	522.68	285.91	285.92	285.88
10	573.78f		573.81	314.90	314.96	314.93

Table 5.4: Wave numbers of the $d^1\Sigma^+ - c^1\Pi$ system of NH, cm^{-1}

	(0,0) band			(1,1) band		
J	P	Q	R	P	Q	R
1	39484.30	39512.30/	39568.75	39894.46	39921.38	
2	455.85	512.30/	596.56	863.84	923.79	40004.30
3	427.45		624.11	846.76	927.44	034.50
4	399.04		651.41	824.96	932.56	
5	370.83	511.33/	678.59	804.84	939.15	098.76
6	342.83		705.50	786.04/	947.35	132.95
7	315.29		732.44	770.20	957.37	168.40
8	288.29		759.19	756.18	969.39	205.72
9	261.98	512.30/	786.04	744.57	983.66	244.82
10	236.57	513.56	813.02	736.04	40000.65	286.26
11	212.26	515.64	840.34	730.80	020.62	330.15
12	189.26	518.64	868.05	729.55	044.09	377.12
13	167.88	522.78	896.53	732.44/	071.68	427.74
14	148.38	528.37	925.81	741.46	104.32	
15	131.10	535.67	956.22			
16	116.44	545.07	988.19			
17	104.83	556.93	40021.80			
18	096.79	571.84	057.88			
19	092.86	590.31	097.12			
20	094.02	613.11	139.31			
21	101.10	641.05				

Table 5.4 (NH) continued

(0,1) band

J	P	Q	R
1	37364.23	37392.47	
2	340.97	397.34	37481.61
3	320.28	404.88/	516.89
4	302.34	414.98	554.70
5	287.28	427.84	595.02
6	275.22	443.61	637.90
7	266.42	462.39	683.45
8	261.12	484.51	732.14/
9	259.66	510.03	783.66
10	262.22/	539.45	838.83
11	269.60	573.14	897.69
12	282.01	611.59	960.72/
13	300.23	655.41	38028.94
14	325.04	705.39	102.31
15	357.76	762.87	

Table 5.5: Wave numbers of the $d^1\Sigma^+ - c^1\Pi$ system of ND, in cm^{-1}

	(0,0) band			(1,1) band		
J	P	Q	R	P	Q	R
1	39469.01	39484.18/	39514.36	39726.22	39740.81	
2	453.59	484.18/	529.19	712.16	741.49	39785.28
3	438.08	483.56	543.79	698.55	742.42	800.85/
4	422.45	482.99	558.25	685.19	743.73	816.56
5	406.77	482.35	572.51	672.27	745.38	832.61
6	391.06	481.62	586.66	659.84	747.43	849.03
7	375.34	480.84	600.62	647.87	749.91	865.76
8	359.65	480.06	614.49	636.40	752.77/	882.86
9	344.06	479.27	628.21	625.54	756.33	900.35
10	328.58	478.49	641.82	615.38	760.36	918.32
11	313.31	477.80	655.42	605.97	765.04	936.82
12	298.23	477.19/	668.98	597.31	770.44	955.87
13	283.45		682.54	589.58	776.61	975.51
14	269.04	476.65/	696.20	582.85	783.70	995.91
15	255.07		709.98	577.29	791.77	40017.19
16	241.59	477.19/	723.90	573.01	800.85/	039.29
17	228.73		738.08	570.13	811.32	062.60
18	216.59		752.77/	568.86	823.14	086.99
19	205.15		767.46	569.21	836.52	112.72
20	194.69		782.84	571.67	851.66/	140.00
21	185.25	487.85	798.82	576.26	868.83	169.18
22	176.93	492.38	815.57	582.9 /	888.31	200.30
23	170.02	497.99	833.18	593.25	910.30	233.87
24	164.45	504.79	851.66/	606.0 /	935.40	269.96
25	160.62	513.10			964.1	
26	158.78		892.42			
27		534.69	915.21			
28	161.38	548.55	939.75			
29	166.56	564.95	966.1			
30	174.87	584.0	994.5			
31	186.56	606.0 /				

Table 5.5 (ND) continued

	(0,1) band			(1,2) band		
J	P	Q	R	P	Q	R
1		37863.48				
2		865.11				
3	37822.28	867.46	37927.78	38279.96	38323.93	
4	810.37	870.82		271.31	329.87/	
5	799.29	874.88	965.10	264.10	337.40/	
6	789.32	879.88	984.83	258.79/	346.40	38447.82
7	780.22	885.77		254.92/	357.05	
8	772.34	892.61		252.96/	369.45	
9	765.30/	900.52	38049.42	252.96/	383.72	
10	759.53	909.52	072.84	254.92/	399.82	
11	755.00	919.52		258.79/	418.12	
12	751.75	930.78	122.74	265.40	438.53	
13	749.85/	943.33		274.29		
14	749.85/	957.10	177.07/	285.93		
15	750.78	972.46	205.77	300.45		
16	753.87	989.48				
17	758.83					
18	765.30/	38028.67				
19	774.93	051.33				
20		076.03				

Table 5.5 (ND) continued

(2,2) band

J	P	Q	R
1	40103.02	40117.18	40145.66
2	090.56	118.87	161.56
3	079.34	121.82	178.04
4	069.19	125.84	196.17
5	060.10	130.74	215.16
6	052.12	136.83	235.10
7	045.46	144.18	256.21
8	040.17	152.63	278.20
9	036.07	162.55	301.73
10	033.63≠	173.80	324.54
11	032.86	186.23	352.63
12	033.63≠	201.31	380.32
13	036.98	217.80	410.0
14	042.31	236.38	
15	050.13	257.35	
16		281.00	
17		307.56	
18		337.7	

5.2 The $c^1\Pi - b^1\Sigma^+$ system

Lunt, Pearse and Smith (1935a) obtained the λ4502 band of NH - the (0,0) band of the c-b system - after an

exposure of 5½ hours in the first order of a 10 ft grating (15000 lines per inch). With the present source exposures of 5 to 15 minutes were required in the second order of a 21ft grating (30000 lines per inch), using Zenith Astronomical plates. The corresponding ND band at λ4484 was obtained under similar conditions and the two bands are reproduced in Plate 6. The measurements of strong lines were consistent to ± 0.01 cm^{-1}, and the wavelengths of the band heads are 4501.977 Å (NH), 4484.463 Å (ND).

The three branches of a $^1\Pi - ^1\Sigma^+$ transition are given by

$$P(J) = \nu_o + F'_c(J-1) - F''_c(J) \qquad (5.5)$$

$$Q(J) = \nu_o + F'_d(J) - F''_c(J) \qquad (5.6)$$

$$R(J) = \nu_o + F'_c(J+1) - F''_c(J) \qquad (5.7)$$

and the first lines are shown in the lower part of Figure 5.1. Sixteen members of the Q and R branches have been found for the λ4502 band, compared with the twelve members listed by Lunt et al. Some of the combination differences for $c^1\Pi(0)$ were given in table 5.3.

In section 2.6, mention was made of a weak hydride band at λ5254 belonging to a singlet system. It was photographed in the first order of the 21ft grating using an exposure of 7½ hours with Ilford Astra 3 plate. The band head is at 5253.98Å - degraded to the red - and analysis shows that it is the (0,1) band of the NH c-b system. The P branch is so weak that only two members were measured, but table 5.6 shows that the values of $\Delta_1 F'_{cd}(J)$ - defined by equation (5.8) - agree with those from the λ4502 band, proving that the upper level is $c^1\Pi(0)$.

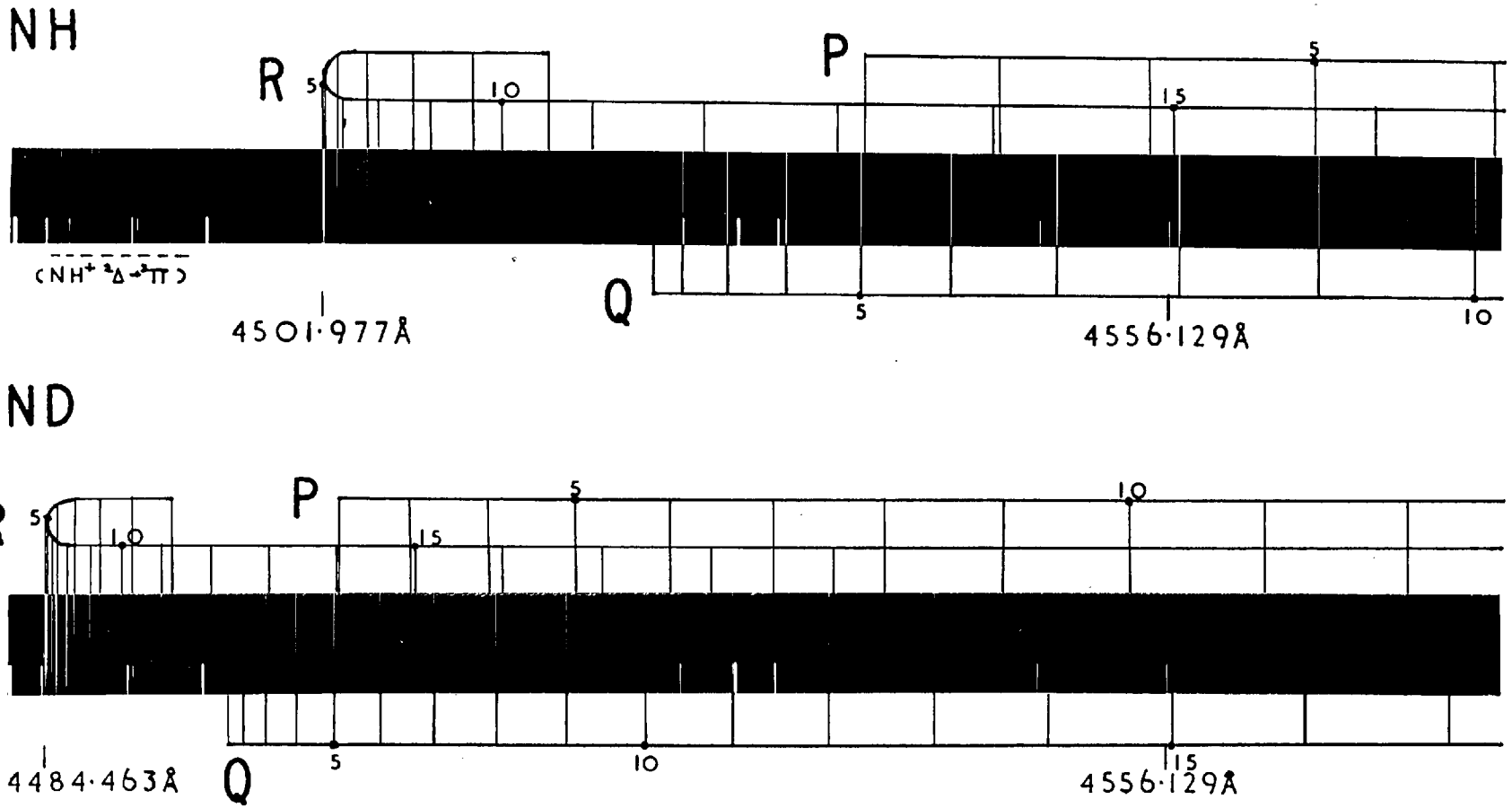

PLATE 6: (0,0) BANDS OF $c'^1\Pi - b'^1\Sigma^+$

$$\Delta_1 F'_{cd}(J) = R(J) - Q(J) = F'_c(J+1) - F'_d(J) \qquad (5.8)$$

Table 5.6: Some values of $\Delta_1 F'_{cd}(J)$ for NH c–b bands

J	λ4502	λ5254	J	λ4502	λ5254
1	56.64	56.63	6	195.95	195.89f
2	84.86	84.86	7	222.97	222.96
3	112.98	112.93	8	249.59	249.59
4	140.86	140.85	9	275.75	275.72
5	168.59	168.49	10	301.37	301.33

Fragments of the ND (0,1) band were found overlapping the (0,1) band of ND^+ $A^2\Sigma^- - X^2\Pi$. The wavenumbers of the c–b bands are given in tables 5.7 (NH) and 5.8 (ND).

Table 5.7: Wave numbers of the $c^1\Pi - b^1\Sigma^+$ system of NH, in cm^{-1}

	(0,0) band			(0,1) band		
J	P	Q	R	P	Q	R
0	-	-	22134.93	-	-	
1	-	22102.05	158.69	-	18897.36	18953.99
2	22036.40	092.92	177.78	18834.17	890.64	975.50
3	21994.59	079.16	192.14		880.53	993.46
4	948.36	060.77	201.63		866.97	19007.82
5	897.66	037.65	206.24		849.90	018.39
6	842.46	009.78	205.72f	661.96	829.28f	025.17
7	782.74	21977.04	200.01		804.94	027.90
8	718.49	939.32	188.91		776.82	026.41
9	649.56	896.49	172.23		744.81	020.53
10	575.94	848.37	149.75		708.68	010.01
11	497.41	794.82	121.25			18994.70
12	413.93	735.63	086.43		623.42	974.16
13	325.28	670.59	045.03		573.86	
14		599.40f	21996.69			
15		521.81	941.06			
16		437.36	877.68			

Table 5.8: Wave numbers of the $c^1\Pi - b^1\Sigma^+$ system of ND, in cm^{-1}

	(0,0) band			(0,1) band	
J	P	Q	R	P	Q
0	-	-	22252.58		
1	-	22234.91	265.43		
2	22199.65	230.12	275.87		
3	177.20	222.93	283.87		
4	152.47	213.32	289.41		
5	125.32	201.26	292.45		
6	095.81	186.76	292.96		
7	063.93	169.78	290.91	19705.47	
8	029.66	150.29	286.24	675.05	19795.61
9	21993.01	128.26	278.89	642.65	777.79
10	953.93	103.69	268.86		757.95
11	912.41	076.47	256.09		735.95
12	868.41	046.62	240.43	533.57/	711.83
13	821.86	014.08	221.93	493.13	685.38
14	772.80	21978.77	200.41		656.63
15	721.16	940.66	175.88		625.56
16	666.84	899.65	148.16		592.02
17		855.64	117.25		
18	550.01	808.60	083.00		
19	487.34	758.45	045.27		
20	421.77/	705.01			
21	353.15	648.22			
22		587.94			

If a diatomic molecule is assumed to be a non-rigid, vibrating symmetric top, then the term values for a singlet state may be written

$$F_v(J) = B_v(J(J+1)-\Lambda^2)-D_vJ^2(J+1)^2+H_vJ^3(J+1)^3 \qquad (5.9)$$

In a $^1\Pi$ state there is also Λ-doubling, which depends on a splitting constant q according to the equation

$$F_c(J)-F_d(J) = q_vJ(J+1) \qquad (5.10)$$

The combination differences are again represented by an equation of the form (4.4):

$$\Delta_2F(J)=(4B-6D+6.75H)(J+\tfrac{1}{2})-(8D-34H)(J+\tfrac{1}{2})^3+12H(J+\tfrac{1}{2})^5 \qquad (5.11).$$

The R and P branches of the d-c and c-b systems were used to find $\Delta_2F_c(J)$ in the usual way, but $\Delta_2F_d(J)$ could be found only by using the Q branches:

$$\Delta_2F_d(J) = \Delta_1F_{cd}(J-1) + \Delta_1F_{dc}(J) \qquad (5.12).$$

In general, data from the c-b system were preferred, since the wavenumber dispersion is higher in the visible than in the ultraviolet and the Q lines of the d-c (0,0) bands were blended at low values of J; but for the highest rotational members of v=0, and for all the members of v=1 and v=2, only the d-c system could be used. The quantities $\Delta_2F(J)/(J+\frac{1}{2})$ were expressed as polynomials in $(J+\frac{1}{2})^2$, differences from blended and very weak lines being omitted. The coefficients of the polynomials yielded the effective rotational constants B^c, B^d etc according to equation (5.11), and B_v, D_v, H_v have usually been taken as $\frac{1}{2}(B_v^c + B_v^d)$, $\frac{1}{2}(D_v^c + D_v^d)$ etc.

In $^1\Sigma \leftrightarrow {}^1\Pi$ bands it is not possible to observe

directly the Λ-type splitting at a particular value of J. However, the quantity $\Delta_1 F_{cd}(J) - \Delta_1 F_{dc}(J)$ gives the sum of the Λ-type splittings in the J and J+1 levels. It follows from (5.10) that

$$\Delta_1 F_{cd}(J) - \Delta_1 F_{dc}(J) = 2q_v(J+1)^2 \qquad (5.13)$$

whence q_v was determined. Since $q_v = B_v^c - B_v^d$ (Herzberg p228), the values of B_1 and B_2 were taken as $(B_v^c - \frac{1}{2}q_v)$. All the rotational constants are given in table 5.9, where the variation of B with v is taken as

$$B_v = B_e - \alpha_e(v+\tfrac{1}{2}) + \gamma_e (v+\tfrac{1}{2})^2 \qquad (5.14)$$

Values for the origins of the bands were found by a least-squares fitting of R(J-1) + P(J) and of Q(J) to polynomials in J^2 and J(J+1) according to the following relations, which are derived from (5.1-3), (5.5-7) and (5.9):

d-c system

$$R(J-1)+P(J) = 2\nu_0 + 2B^{c\prime\prime} + 2(B' - B^{c\prime\prime} - D' + D^{c\prime\prime})J^2 - \qquad (5.15)$$

$$Q(J) = \nu_0 + B^{d\prime\prime} + (B' - B^{d\prime\prime})J(J+1) - \qquad (5.16)$$

c-b system

$$R(J-1)+P(J) = 2\nu_0 - 2B^{c\prime} + 2(B^{c\prime} - B'' - D^{c\prime} + D'')J^2 - \qquad (5.17)$$

$$Q(J) = \nu_0 - B^{d\prime} + (B^{d\prime} - B'')J(J+1) - \qquad (5.18)$$

The results are presented in tables 5.10(NH) and 5.11(ND), those for d-c being in the form of a Deslandres array.

Table 5.9: Rotational constants of $c^1\Pi$, in cm^{-1}.

	NH	ND
B_o	14.1569(7)	7.6326(4)
B_1	12.866(2)	7.1628(6)
B_2		6.610(3)
$10^4 D_o$	22.14(5)	6.09(1)
$10^4 D_1$	27.1(4)	6.75(3)
$10^4 D_2$		9.52(9)
$10^8 H_o$	-25.8(11)	-3.84(11)
$10^8 H_1$	-111(13)	-10.58(31)
$10^3 q_o$	15.55(7)	4.56(4)
$10^3 q_1$	17.7(1)	4.80(4)
$10^3 q_2$		5.1(4)
B_e	14.8024(13)	7.8364(17)
α_e	1.291(2)	0.387(3)
γ_e		-0.0415(16)
B_o^c	14.1659(11)	7.6344(5)
B_o^d	14.1478(10)	7.6307(5)
B_1^c	12.875(2)	7.1652(6)
B_1^d	12.866(5)	7.1608(8)
B_2^c		6.613(3)
B_2^d		6.602(2)
$10^4 D_o^c$	22.22(8)	6.08(2)
$10^4 D_o^d$	22.06(7)	6.10(2)
$10^4 D_1^c$	26.5(3)	6.75(3)
$10^4 D_1^d$	27.6(7)	6.74(4)
$10^4 D_2^c$		9.66(12)
$10^4 D_2^d$		9.38(12)
$10^8 H_o^c$	-24.28(172)	-3.92(15)
$10^8 H_o^d$	-27.41(128)	-3.75(15)
$10^8 H_1^c$	-130(11)	-10.44(35)
$10^8 H_1^d$	-90(24)	-10.72(51)

Table 5.10: Band origins for NH, in cm^{-1}

$d^1\Sigma^+ - c^1\Pi$

v' \ v''	0	1
0	39498.45(2)	37376.95(4)
1		39907.22(4)

$c^1\Pi - b^1\Sigma^+$

(0,0) - 22120.78(1)

(0,1) - 18914.87(1)

Table 5.11: Band origins for ND, in cm^{-1}

$d^1\Sigma^+ - c^1\Pi$

v' \ v''	0	1	2
0	39476.69(4)	37855.51(2)	
1		39733.39(2)	38308.54(6)
2			40109.39(10)

$c^1\Pi - b^1\Sigma^+$

(0,0) - 22244.94(1)

(0,1) - 19873.3(2)

The vibrational constants were derived from the band origins by means of equation (5.19), and the results are given in table 5.12.

$$\Delta G(v+\tfrac{1}{2}) = \omega_e - 2(v+1)\omega_e x_e \qquad (5.19)$$

The constants for ND were obtained from $\Delta G^D(\frac{1}{2})$ and $\Delta G^D(3/2)$, but for NH we have only $\Delta G(\frac{1}{2})$ so that the isotope effect must be used. The constants given for NH represent the average of those obtained using $\Delta G(\frac{1}{2})$ and $\Delta G^D(\frac{1}{2})$ on the one hand, and those predicted directly from ω_e^D, $\omega_e x_e^D$ on the other.

Table 5.12: Vibrational constants of $c^1\Pi$, in cm^{-1}

	NH	ND
$\Delta G(\frac{1}{2})$	2121.50(4)	1621.18(4)
$\Delta G(3/2)$		1424.85(6)
ω_e	2484.9(25)	1817.51(8)
$\omega_e x_e$	182.1(17)	98.17(4)

Table 5.13 shows the ratios of the rotational constants for ND and NH, D_o and H_o being used as approximations to D_e and H_e. The agreement with theory is not good, but it is instructive to calculate "revised" values of B_e and α_e - denoted as $B_e(rev)$, $\alpha_e(rev)$ - on the assumption that $\gamma_e = \gamma_e^D/\rho^4$ (see equation (5.14) and table 1.1). We then have $\gamma_e = -0.146$, $\alpha_e(rev) = 0.999$, $B_e(rev) = 14.693$, and the "revised" ratios of table 5.13, which are close to the theoretical values. It is suggested that $\alpha_e(rev)$ and $B_e(rev)$ are more reliable than the corresponding values in table 5.9.

Table 5.13: Ratios of the rotational constants for $c^1\Pi$

Ratio	Experimental value	'Revised' value	Theoretical value
B_e^D/B_e	0.5294(1)	0.5333	0.5339
D_o^D/D_o	0.2751(8)		0.2851-D_e
H_o^D/H_o	0.149(8)		0.152-H_e
γ_e^D/γ_e	0.300(2)	0.387	0.390

5.4 Constants for the $^1\Sigma^+$ states

$^1\Sigma^+$ states have c levels only (section 1.1.2), and the rotational constants for $d^1\Sigma^+(v=0,1,2)$ and $b^1\Sigma^+(0)$ were determined from equation (5.11) in the usual way. Since the assignments for the (0,1) bands of the c-b system are incomplete, the rotational constants for $b^1\Sigma^+(1)$ and the values of $\Delta G''(\frac{1}{2})$ and $\Delta G^D{}''(\frac{1}{2})$ were found by using the method of Jenkins and McKellar as described in Chapter 4 (equations (4.5-6) and (4.28)):

$$M''(J) = \Delta G''(\tfrac{1}{2}) + (B_1''-B_0'')J(J+1) - (D_1''-D_0'')J^2(J+1)^2 + \quad (5.20)$$
$$= Q_{0,0}(J) - Q_{0,1}(J) \text{ etc.}$$

The vibrational constants for $b^1\Sigma^+$ were obtained from $\Delta G(\frac{1}{2})$ and $\Delta G^D(\frac{1}{2})$ by means of the isotope relations. The vibrational constants for $d^1\Sigma^+$ were derived from the band origins of the d-c system in the same way as for $c^1\Pi$.

Table 5.14: Band constants for $^1\Sigma^+$ states, in cm^{-1}

	NH		ND	
	$b^1\Sigma^+$	$d^1\Sigma^+$	$b^1\Sigma^+$	$d^1\Sigma^+$
B_o	16.4301(9)	14.0918(6)	8.8280(4)	7.5633(3)
B_1	15.8252(9)	13.458(3)	8.5897(9)	7.3178(4)
B_2				7.090(6)
10^4D_o	16.39(7)	16.66(4)	4.60(1)	4.75(1)
10^4D_1	16.10(7)	16.1(2)	4.52(3)	4.73(2)
10^4D_2				5.3(4)
10^8H_o		11.1(7)		1.73(8)
10^8H_1				2.28(2)
B_e	16.7326(9)	14.409(2)	8.9472(6)	7.693(3)
α_e	0.6049(3)	0.634(3)	0.2383(8)	0.263(6)
γ_e				0.009(3)
10^4D_e	16.54(7)		4.64(2)	
$10^4\beta_e$	-0.29(2)		-0.084(26)	
$\Delta G(\frac{1}{2})$	3205.89(1)	2530.27(6)	2371.81(6)	1877.88(3)
$\Delta G(3/2)$				1800.85(12)
ω_e	3354.69	2676.6(12)	2451.26	1954.91(12)
$\omega_e x_e$	74.40	72.9(8)	39.72	38.52(6)

All the constants are given in table 5.14, and the ratios of the rotational constants are compared in table 5.15. Most of the ratios agree satisfactorily with theory, and the outstanding exception - α_e^D/α_e for the d state - may be revised on the assumption that $\gamma_e = \gamma_e^D/\rho^4$. We then have γ_e=0.032, α_e(rev)=0.698 and α_e^D/α_e(rev) = 0.377, which is sufficiently close to the theoretical value to demonstrate that more values of B_v

are needed.

Table 5.15: Ratios of the rotational constants for $^1\Sigma^+$ states.

Ratio	Experimental value		Theoretical value
	$b^1\Sigma^+$ state	$d^1\Sigma^+$ state	
B_e^D/B_e	0.53472(5)	0.5339(2)	0.53392
D_e^D/D_e	0.281(2)	0.2851(9)-D_o	0.2851
H_o^D/H_o		0.156(12)	0.152-H_e
γ_e^D/γ_e	0.394(2)	0.415(2)	0.390
β_e^D/β_e	0.29(9)		0.208

CHAPTER 6: CONCLUSIONS

6.1 The source

As discovered by C. B. Sharma (1959), a heavy-current positive-column discharge through helium containing traces of nitrogen and hydrogen is an intense source for the emission spectra of NH and NH^+. The partial pressures of the gases can be varied so as to favour the intensity of NH and NH^+ bands relative to those of N_2 and H_2. Since no quantitative work on the discharge parameters has been attempted, any interpretation of the excitation mechanism is largely speculative.

The presence of an excess of helium is known to favour the observation of ionized radicals, and this may be due at least in part to the high ionization potential (24.6 eV) of the helium atom. Once an ionized radical has been formed, it is unlikely to remove an electron from a helium atom, and may well be prevented from discharging itself on the walls of the tube by the abundance of helium atoms present. The absence of NH^+ when argon was used would then be explained by the lower ionization potential (15.8 eV) of the inert gas. It was not possible to used neon (ionization potential 21.6 eV) in these experiments because of the cost.

There is no spectroscopic evidence for NH_2 or NH_3 in the discharge, so the formation of NH^+ may be through the ionization of NH by electron impact. The ionization potential of NH - 13.10 eV (Wilkinson (1963)) -

is only some 3 eV more than the excitation potential of the $d^1\Sigma^+$ state; and the d-c system of NH appears strongly when NH^+ is present.

6.2 NH

The band constants for the $b^1\Sigma^+$, $c^1\Pi$ and $d^1\Sigma^+$ states of NH, derived in part from comparison with ND, were given in tables 5.9, 5.12 and 5.14. It is not possible to compare these with corresponding values in PH, since for PH only the $A^3\Pi - X^3\Sigma^-$ system is known. Kleman (1953) compared the NH-type molecules with those of the CH- and BH-type, and suggested that the $^1\Pi$ state is unstable in PH so that no singlet transitions can be observed at normal wavelengths.

If the dissociation energy of $c^1\Pi$ is obtained from a Birge-Sponer extrapolation, then D_o=0.9 eV. Comparison with the observed rotational levels suggests that predissociation by rotation may occur. Indeed, there is evidence for a maximum in the potential curve at an internuclear distance of 1.91Å (r_e=1.105Å). This problem is being investigated further, but it seems that if the maximum exists, D_o(NH $c^1\Pi$) is not greater than 0.5 eV.

The correlation of the observed states of NH with those of the 'united atom' (oxygen) and the atomic dissociation products, has been given by Mulliken (1932) and Herzberg(1950). The potential curves of Herzberg (p369) are satisfactory for most purposes, but they are

based on a dissociation energy of 4.2 eV for the ground state, which is 1eV more than that given by Seal and Gaydon (1966).

6.3 NH^+

In NH^+ all the band systems analogous to those in the isoelectronic molecule CH have been observed. By studying also the spectra of ND^+, we have produced strong evidence for $^2\Pi_r$ as the ground state. Good progress has therefore been made with all three problems listed at the end of chapter 1.

The electronic states usually observed in CH-type molecules are $^2\Delta$ and $^2\Pi$, and in table 6.1 the values of the rotational constant B_o and the spin-orbit coupling constant, A_o, are compared.

Table 6.1: Constants for CH-type molecules, in cm^{-1}

	$X^2\Pi_r$		$^2\Delta$	
	B_o	A_o	B_o	A_o
CH	14.1961	27.95	14.5816	(-1)
SiH	7.3905	142.83	7.2837	3.58
GeH	6.6301	892.52	6.2252	10.3
SnH	5.31488	2178.89	4.904	20.41
-	-	-	-	-
NH^+	15.301	78.2	13.5295	-3.54
PH^+	8.385	295.94	6.983	1.38

Data for CH are from Fagerholm (1940), for SiH, GeH and SnH from Klynning et al (1966b, 1966a, 1965), and for PH^+ from Narasimham (1957). The variation in the constants

for the neutral molecules is regular, and NH^+ and PH^+ are similar to CH and SiH as expected. From the spin-splitting of the $^2\Sigma$ states in CH, Gero (1941) obtained γ = + 0.048 cm^{-1}($C^2\Sigma^+$), - 0.0285 cm^{-1} ($B^2\Sigma^-$) while for NH^+ we have γ = + 0.097 cm^{-1} ($C^2\Sigma^+$), -0.100 cm^{-1}($A^2\Sigma^-$). The chief differences between the observed spectra of the two molecules are that in NH^+ the $^2\Sigma^-$ state lies below $^2\Delta$ rather than above it, and $a^4\Sigma^-$ is sufficiently near to $X^2\Pi$ to perturb the rotational levels.

If the electrons of NH^+ are placed in their lowest orbitals, the following electron configurations are obtained:

lowest configuration $(1s\sigma)^2(2s\sigma)^2(2p\sigma)^2(2p\pi)$ - $^2\Pi r$

first excited configuration $(1s\sigma)^2(2s\sigma)^2(2p\sigma)(2p\pi)^2$- $^4\Sigma^-$, $^2\Delta$, $^2\Sigma^+$, $^2\Sigma^-$

second excited configuration $(1s\sigma)^2(2s\sigma)^2(2p\pi)^3$ - $^2\Pi_i$

The five stable states observed correspond to the states of the lowest two configurations. The 'united atom' to which NH^+ approximates at small values of r is O^+, whose three lowest states arise from the electron configuration $1s^2 2s^2 2p^3$. These states are remote from any others and must give rise to all the stable states of NH^+ with low energy. On applying the usual rules (Herzberg p 322) we obtain the following states, in order of increasing energy:

$(O^+)\ ^4S_u \rightarrow\ ^4\Sigma^-$

$(O^+)\ ^2D_u \rightarrow\ ^2\Sigma^-,\ ^2\Pi,\ ^2\Delta$

$(O^+)\ ^2P_u \rightarrow\ ^2\Sigma^+,\ ^2\Pi$.

These states are exactly those of the lowest three electron configurations.

As mentioned in chapter 1, NH^+ can dissociate into either $N^+ + H$ or $N+H^+$, since the ionization potentials of the two atoms are little different. Using the symbol I for ionization potential, we have I(H) = 13.60 eV and I(N) = 14.54 eV, so that

$$I(N) - I(H) = 0.94 \text{ eV} = 7600 \text{ cm}^{-1}.$$

N and N^+ each have one electron configuration of much lower energy than any others. Using the correlation rules of Wigner and Witmer (Herzberg p 315ff), we obtain the following states:

$\underline{N + H^+}$: $^4S_u + {}^1S_g \rightarrow {}^4\Sigma^-$

$^2D_u + {}^1S_g \rightarrow {}^2\Sigma^-, {}^2\Pi, {}^2\Delta.$

$^2P_u + {}^1S_g \rightarrow {}^2\Sigma^+, {}^2\Pi$

$\underline{N^+ + H}$: $^3P_g + {}^2S_g \rightarrow {}^2\Pi, {}^4\Pi, {}^2\Sigma^-, {}^4\Sigma^-$

$^1D_g + {}^2S_g \rightarrow {}^2\Sigma^+, {}^2\Pi, {}^2\Delta$

$^1S_g + {}^2S_g \rightarrow {}^2\Sigma^+.$

The correlations with the observed states are shown in Figure 6.1. Each state of the united atom is linked with the lowest pair of dissociation products which could, when brought together, form the molecular species concerned. In this way 'crossing' of the potential curves for states of the same species is avoided.

The potential curves, U(r), of Figure 6.1 are Morse functions, given by equations (6.1-2).

$$U(r-r_e) = D_e(1-\exp(-br+br_e))^2 \qquad (6.1)$$

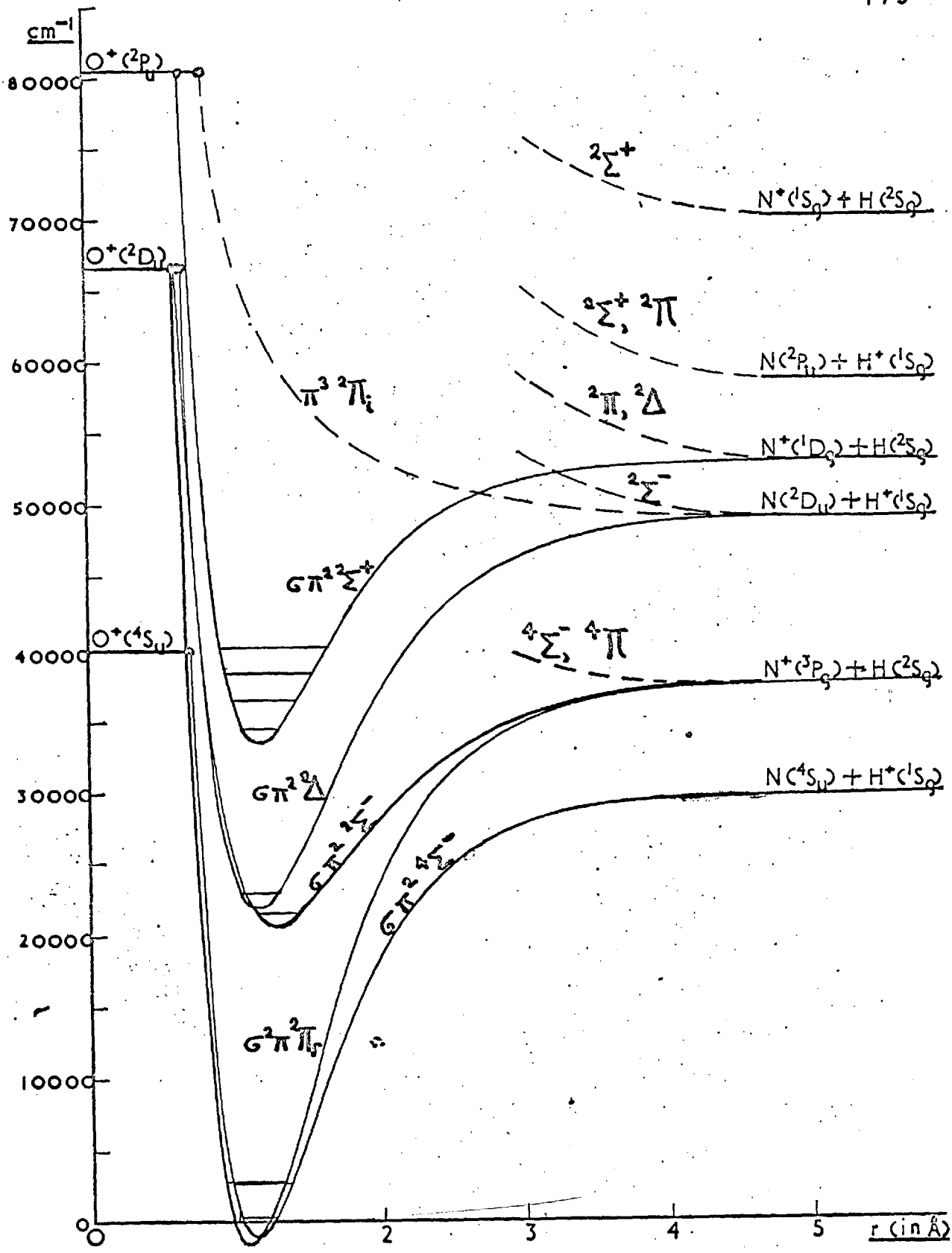

Figure 6.1: Morse potential curves for NH^+

where $b = \left[\frac{2\pi^2 c \mu}{D_e h}\right]^{\frac{1}{2}} \omega_e$ (6.2)

μ is the reduced mass of the molecule and D_e is the dissociation energy of the particular electronic state, measured from the bottom of the potential curve. r_e is found from the relation

$$B_e = \frac{h}{8\pi^2 c \mu r_e^2} \qquad (6.3)$$

and the value of D_e for each state may be found from the separations of the dissociation products and the observed states, provided that D_e for one state is already known. For this purpose the dissociation energy, D_o^o, of the ground state was found from the cycle

$$D_o^o(NH^+) = D_o^o(NH) + I(N) - I(NH) \qquad (6.4).$$

Wilkinson (1963) found $D_o^o(NH^+) = 4.26$eV by using $D_o^o(NH) = 3.76$ eV, $I(NH) = 13.10$ eV (from electron-impact experiments), and $I(H) = 13.60$ eV. We now use $D_o^o(NH) = 3.21$ eV (Seal and Gaydon (1966)) and $I(N)$ rather than $I(H)$, since $^2\Pi_r$ seems to be the ground state. Equation (6.4) then gives

$$D_o^o(NH^+) = 4.65\text{eV} = 37500\ \text{cm}^{-1},$$

from which the values of D_e have been deduced using the data of chapter 4. The positions of the observed vibrational levels are marked in Figure 6.1 and the energies are measured from $^2\Pi(0)$.

The correlation of $X^2\Pi$ with $N^+(^3P_g) + H(^2S_g)$ is confirmed by comparison of the coupling constant derived from the molecule with that derived from the atom. For

normal coupling, the overall width of N^+ (^3P_g), which is derived from a $2s^2 2p^2$ configuration, should be 3A/2. Since $^3P_2 - ^3P_0 = 131.3$ cm^{-1}, we obtain A=87.5 cm^{-1}; while from the molecule $A(^2\Pi) = 78.2$ cm^{-1}. The ratio of the two values is 0.89, in good agreement with the findings of Mulliken (1932, p.37) for hydrides. For CH, Mulliken (1932) predicted that $\pi^3\ ^2\Pi_i$ would be a repulsive state, and this seems likely for NH^+ also, since the transfer of a $2p\sigma$ electron to the $2p\pi$ orbital means that the state should lie some 3eV above $\sigma\pi^2\ ^2\Delta$. There remain eight states arising from possible dissociation products which have not been correlated with the united atom. As very energetic states of O^+ would be needed for this purpose, these states are expected to be unstable.

Since $^2\Pi$ is probably the ground state of NH^+, the $A^2\Sigma^- - X^2\Pi$ and $B^2\Delta - X^2\Pi$ systems may well be found in sources such as the sun and comets, and both systems lie in the most convenient spectral region for astrophysical observation.

ACKNOWLEDGMENTS

I am very grateful to my supervisor, Dr. R. W. B. Pearse, for suggesting the problem, and for his unfailing advice and encouragement. I have also benefited from many discussions with Dr. R. C. M. Learner.

I thank Mr. O. R. Milbank for his skilful work in glass and quartz, and my wife for help in preparing diagrams for the thesis and checking the typescript.

The deuterium was provided by the Atomic Energy Research Establishment, Harwell, through the good offices of Mr. B. L. Tozer and Professor W. R. S. Garton. Financial support was provided by the Science Research Council, in the form of a Research Studentship.

REFERENCES

Almy, G. M. and Horsfall, R.B., Phys. Rev. 51, 491 (1937)

Babcock, H.D., Astrophys. J. 102, 154 (1945)

Chamberlain, J.E., Ph.D Thesis, University of London (1962)

Chauvin, H. and Leach, S., C.R.Acad. Sci. 231, 1482 (1950)

Clarke, F.J.P. and Garton, W.R.S., J.Sci.Instrum. 36, 403 (1959)

Crosswhite, H.M., Spectrum of Iron I, Johns Hopkins Spectroscopic Report No. 13 (1958)

Dieke, G.H. and Blue, R.W., Phys. Rev. 45, 395 (1934)

Dieke, G.H., Phys. Rev. 47, 870 (1935)

Dieke, G.H. and Crosswhite, H.M., J.Q.S.R.T. 2, 97 (1962)

Dixon, R.N., Can. J. Phys. 37, 1171 (1959)

Douglas, A.E., Can. J. Phys. 35, 71 (1957)

Dressler, K. and Ramsay, D.A., Phil. Trans. Roy. Soc. A251, 553 (1959)

Dunham, J.L., Phys. Rev. 41, 721 (1932)

Earls, L.T., Phys. Rev. 48, 423 (1935)

Fagerholm, E., Ark.f Mat., Astr. och Fys. 27A, No.19 (1940)

Feast, M.W., Astrophys. J. 114, 344 (1951)

Florent, R. and Leach, S., J. Phys. Rad. 13, 377 (1952)

Fowler, A. and Gregory, C.C.L., Phil. Trans. Roy. Soc. A218, 351 (1919)

Funke, G.W., Z.Physik 96, 787 (1935)

Funke, G.W., Z.Physik 101, 104 (1936)

Gero, L., Z.Physik 118, 27 (1941)

Gleu, K., Z.Physik 38, 176 (1926)

Guenebaut, M.H., J.Phys. Rad. 16, 140S (1955)

Hanson, H., Kopp, I., Kronekvist, M. and Aslund, N., Ark.Fys. 30, 1 (1965).

Herzberg, G., Spectra of Diatomic Molecules (Van Nostrand), (1950)

Herzberg, G. and Ramsay, D.A., Disc. Farad. Soc. 14, 11 (1953)

Hill, E. and Van Vleck, J.H., Phys. Rev. 32, 250 (1928)

Hori, T., Z. Physik 59, 91 (1929)

Hunter, A. and Pearse, R.W.B., J.Sci. Instrum. 13, 403 (1936)

Jenkins, F.A., J.Opt. Soc. Am. 43, 425 (1953)

Jevons, W., Band Spectra of Diatomic Molecules (Physical Society), (1932)

Kleman, B., Dissertation, Stockholm (1953)

Klynning, L., Lindgren, B. and Aslund, N., Ark. Fys. 30, 141 (1965)

Klynning, L. and Lindgren, B., Ark. Fys. 32, 575 (1966a)

Klynning, L. and Lindgren, B., Ark. Fys. 33, 73 (1966b)

Kopp, I., Kronekvist, M. and Aslund, N., Ark. Fys. 30, 9 (1965)

Kronig, R. de L., Z. Physik 50, 347 (1928)

Lunt, R.W., Pearse, R.W.B. and Smith, E.C.W., Proc. Roy. Soc. A151, 602 (1935a)

Lunt, R.W., Pearse, R.W.B. and Smith, E.C.W., Nature 136, 32 (1935b)

Lunt, R.W., Pearse, R.W.B. and Smith, E.C.W., Proc. Roy. Soc. A155, 173 (1936)

Mulliken, R.S., Rev. Mod. Phys. 2, 60 (1930)

Mulliken, R.S., Rev. Mod. Phys. 3, 89 (1931)

Mulliken, R.S., Rev. Mod. Phys. 4, 1 (1932)

Mulliken, R.S. and Christy, A., Phys. Rev. 38, 87 (1931)

Nakamura, G. and Shidei, T., Jap. J. Phys. 10, 5 (1935)

Narasimham, N.A., Can. J. Phys. 35, 901 (1957)

Narasimham, N.A. and Krishnamurty, G., Proc. Ind. Acad. Sci. A64, 97 (1966)

Pannetier, G., Guenebaut, H. and Gaydon, A.G., C.R. Acad. Sci. 240, 958 (1955)

Pearse, R.W.B., Proc. Roy. Soc. A143, 112 (1933)

Seal, K.E. and Gaydon, A.G., Proc. Phys. Soc. 89, 459 (1966)

Sharma, Chandra Bhan, Ph.D. Thesis, University of London (1959)

Shimauchi, M., Science of Light, 13, 53 (1964)

Shimauchi, M., Science of Light, 15, 161 (1966)

Swings, P., 'Molecular Spectra in Cosmic Sources', ppl45-171 of Astrophysics (ed. Hynck) (McGraw-Hill, 1951)

Whittaker, F.L., Proc. Phys. Soc. 90, 535 (1967)

Wilkinson, P.G., Astrophys. J. 138, 778 (1963)

PROC. PHYS. SOC., 1967, VOL. 90. PRINTED IN GREAT BRITAIN

The $\Delta v = 0$ sequence in the $d\,^1\Sigma^+$–$c\,^1\Pi$ system of NH and ND

F. L. WHITTAKER

Department of Physics, Imperial College, London

MS. received 21*st September* 1966

Abstract. A study of high-dispersion emission spectra of NH and ND in the region 2460–2560 Å yields the following rotational constants for the $d\,^1\Sigma^+$–$c\,^1\Pi$ band system: $B_e' = 14{\cdot}409$(NH), $7{\cdot}693$(ND), $\alpha_e' = 0{\cdot}634$(NH), $0{\cdot}263$(ND), $D_0' = 1{\cdot}666 \times 10^{-3}$(NH), $4{\cdot}75 \times 10^{-4}$(ND), $B_e'' = 14{\cdot}697$(NH), $7{\cdot}841$(ND), $\alpha_e'' = 1{\cdot}015$(NH), $0{\cdot}393$(ND), $D_0'' = 2{\cdot}19 \times 10^{-3}$(NH), $6{\cdot}18 \times 10^{-4}$(ND), all in cm^{-1}. These constants are consistent with the isotope effect. Approximate vibrational constants are also calculated.

1. Introduction

The NH band at 2530 Å was first reported by Hori (1929). His rotational analysis, performed before either the $c\,^1\Pi$–$a\,^1\Delta$ or $c\,^1\Pi$–$b\,^1\Sigma^+$ systems had been analysed, was, however, wrong. Lunt, Pearse and Smith (1936) obtained the same band with a hollow cathode discharge in rapidly streaming ammonia and photographed it using a large quartz spectrograph. Their analysis showed that it was the (0, 0) band of the $d\,^1\Sigma^+$–$c\,^1\Pi$ transition, and they also assigned a few lines to the (1, 1) band. In the present study the (0, 0) and (1, 1) bands of NH and the (0, 0), (1, 1) and (2, 2) bands of ND have been photographed at high dispersion from a positive column discharge through traces of nitrogen and hydrogen (or deuterium) in the presence of helium. The bands lie in the region 2460–2560 Å. This is the first system of ND in which the rotational structure of the levels $v' = 2$ and $v'' = 2$ has been investigated. High-resolution studies of the $c\,^1\Pi$ state in NH and ND have previously been made by Pearse (1933), Dieke and Blue (1934), Shimauchi (1964) and Hanson *et al.* (1965), and data from these papers are used here where appropriate.

2. Experimental details

The spectra were photographed in emission in the third order of a 21 ft concave grating which was blazed for 7500 Å in the first order. The third order, with a reciprocal dispersion of $0{\cdot}37$ Å mm^{-1}, was selected by a prismatic pre-disperser. The full resolution of the spectrograph could not be utilized because of line broadening in the source, the width of strong lines being some $0{\cdot}5$ cm^{-1}. The positive column discharge tube was of the type described by Clarke and Garton (1959) which has a water-cooled quartz capillary (15 cm long and of 4 mm bore) and water-cooled aluminium electrodes. A d.c. generator was used to maintain a current of 2 A through a continuously flowing mixture of helium, nitrogen and hydrogen (or deuterium). The partial pressures of the gases were approximately 90 torr (helium), 1 torr (hydrogen or deuterium) and $0{\cdot}6$ torr (nitrogen). The mineral helium was cleaned by passing it through traps of charcoal

cooled in liquid nitrogen. Of the other gases the nitrogen was of 'oxygen-free' grade, the deuterium was 99·8% pure and the hydrogen was of the usual commercial grade. The only impurity lines were the Hg I line at 2536·52 Å and the C I line at 2478·57 Å. Exposures varied from 1 hour ((0, 0) bands) to $7\frac{1}{2}$ hours (ND (2, 2) band) using Ilford Zenith plates.

The plates were measured on a Zeiss Abbe comparator. Iron arc wavelength standards taken from Crosswhite (1958, Johns Hopkins Spectrosc. Rep. No. 13) were fitted to suitable low-order polynomials by the method of least squares, using an Elliott 803 computer. The accuracy of the resulting vacuum wave numbers is estimated as $\pm 0{\cdot}03\ \mathrm{cm}^{-1}$, except for the weak (2, 2) band of ND where $\pm 0{\cdot}06\ \mathrm{cm}^{-1}$ is more appropriate.

3. Analysis

3.1. *Structure of the bands*

$^1\Sigma^+$–$^1\Pi$ transitions have three branches, given here by

$$\mathrm{P}(J) = \nu_0 + \mathrm{F_c}'(J-1) - \mathrm{F_c}''(J)$$
$$\mathrm{Q}(J) = \nu_0 + \mathrm{F_c}'(J) - \mathrm{F_d}''(J)$$
$$\mathrm{R}(J) = \nu_0 + \mathrm{F_c}'(J+1) - \mathrm{F_c}''(J)$$

where the components of the $^1\Pi$ state are labelled according to the convention of Herzberg (1950). The Λ-type splitting is given to a good approximation by

$$\Delta\nu_{\mathrm{cd}} = q_v J(J+1)$$

where $q_v = B_v^{\mathrm{c}''} - B_v^{\mathrm{d}''}$.

The vacuum wave numbers of the branches are given in table 1 (NH) and table 2 (ND),

Table 1. Wave numbers of the NH d $^1\Sigma^+$–c $^1\Pi$ system in cm^{-1}

	(0, 0) band			(1, 1) band		
J	R	Q	P	R	Q	P
1	39568·75	39512·30†	39484·30		39921·38	39894·46
2	596·56	512·30†	455·85	40004·30	923·79	869·84
3	624·11		427·45	034·50	927·44	846·76
4	651·41		399·04		932·56	824·96
5	678·59		370·83	098·76	939·15	804·84
6	705·50	511·33†	342·83	132·95	947·35	786·04†
7	732·44		315·29	168·40	957·37	770·20
8	759·19		288·29	205·72	969·39	756·18
9	786·04	512·30†	261·98	244·82	983·66	744·57
10	813·02	513·56	236·57	286·26	40000·65	736·04
11	840·34	515·64	212·26	330·15	020·62	730·80
12	868·05	518·64	189·26	377·12	044·09	729·55
13	896·53	522·78	167·88	427·74	071·68	732·44†
14	925·81	528·37	148·38		104·32	741·46
15	956·22	535·67	131·10			
16	988·19	545·07	116·44			
17	40021·80	556·93	104·83			
18	057·88	571·84	096·79			
19	097·12	590·31	092·86			
20	139·31	613·11	094·02			
21		641·05	101·10			

Table 2. Wave numbers of the ND $d\,^1\Sigma^+$–$c\,^1\Pi$ system in cm^{-1}

	(0, 0) band			(1, 1) band		
J	R	Q	P	R	Q	P
1	39514·36	39484·18†	39469·01		39740·81	39726·22
2	529·19	484·18†	453·59	39785·28	741·49	712·16
3	543·79	483·56	438·08	800·85†	742·42	698·55
4	558·25	482·99	422·45	816·56	743·73	685·19
5	572·51	482·35	406·77	832·61	745·38	672·27
6	586·66	481·62	391·06	849·03	747·43	659·84
7	600·62	480·84	375·34	865·76	749·91	647·87
8	614·49	480·06	359·65	882·86	752·77†	636·40
9	628·21	479·27	344·06	900·35	756·33	625·54
10	641·82	478·49	328·58	918·32	760·36	615·38
11	655·42	477·80	313·31	936·82	765·04	605·97
12	668·98	477·19†	298·23	955·87	770·44	597·31
13	682·54		283·45	975·51	776·61	589·58
14	696·20	476·65†	269·04	995·91	783·70	582·85
15	709·98		255·07	40017·19	791·77	577·29
16	723·90	477·19†	241·59	039·29	800·85†	573·01
17	738·08		228·73	062·60	811·32	570·13
18	752·77†		216·59	086·99	823·14	568·86
19	767·46		205·15	112·72	836·52	569·21
20	782·84		194·69	140·00	851·66†	571·67
21	798·82	487·85	185·25	169·18	868·83	576·26
22	815·57	492·38	176·93	200·30	888·31	582·9†
23	833·18	497·99	170·02	233·87	910·30	593·25
24	851·66	504·79	164·45	269·96	935·40	606·0†
25		513·10	160·62		964·1	
26	892·42		158·78			
27	915·21	534·69				
28	939·75	548·55	161·38			
29	966·1	564·95	166·56			
30	994·5	584·0	174·87			
31		606·0†	186·56			

	(2, 2) band		
J	R	Q	P
1	40145·66	40117·18	40103·02
2	161·56	118·87	090·56
3	178·04	121·82	079·34
4	196·17	125·84	069·19
5	215·16	130·74	060·10
6	235·10	136·83	052·12
7	256·21	144·18	045·46
8	278·20	152·63	040·17
9	301·73	162·55	036·07
10	324·54	173·80	033·63
11	352·63	186·23	032·86
12	380·32	201·31	
13	410·0	217·80	036·98
14		236·38	042·31
15		257·35	050·13
16		281·00	
17		307·56	
18		337·7	

blended lines being marked with a dagger. As is clearly seen in the figure (plate), the Q branch of the ND (0, 0) band has two heads, the second being at $J = 14$. In the (0, 0) band of NH the Q branch was not resolved for $J < 9$. Early members of the branch may be predicted from the relations

$$Q(J) = P(J+1) + F_c''(J+1) - F_d''(J) = R(J-1) + F_c''(J-1) - F_d''(J)$$

using data of Pearse (1933) and Dieke and Blue (1934). Averaged results for such predictions are given in table 3, showing that this branch also has two heads, the second being near $J = 6$. Transitions from the levels $J' = 17$ and $J' = 26$ of the $v' = 0$ state in ND are abnormally weak. It is not certain whether this loss of intensity is caused by an accidental predissociation or by a conventional perturbation.

Table 3. Predicted wave numbers for part of the Q branch of the NH(0, 0) band in cm^{-1}

J	1	2	3	4	5	6	7	8
(Q–39500)	12·38	12·16	11·83	11·42	11·30	11·18	11·25	11·56

3.2. *Rotational constants*

The rotational structure of a singlet state is given by

$$F_j(J) = B_v J(J+1) - D_v J^2(J+1)^2 + H_v J^3(J+1)^3 + \Phi_j(J)$$

where j ≡ c or d, corresponding to the Λ-type doubling components. From the empirical data we have the following combination differences:

$$\begin{aligned}
\Delta_2 F'(J) &= R(J) - P(J) \\
\Delta_2 F_c''(J) &= R(J-1) - P(J+1) \\
\Delta_2 F_d''(J) &= Q(J-1) - Q(J+1) + R(J) - P(J).
\end{aligned}$$

The quantities $\Delta_2 F(J)/(J+\frac{1}{2})$ were expressed as polynomials in $(J+\frac{1}{2})^2$ by a least-squares fitting, differences from blended lines and certain very weak lines being omitted. The coefficients from the polynomials yielded the rotational constants B_v', D_v', H_v', $B_v^{c''}$ etc. according to the equation

$$\frac{\Delta_2 F(J)}{J+\frac{1}{2}} = 4B_v - 6D_v + 6{\cdot}75H_v - (8D_v - 34H_v)(J+\tfrac{1}{2})^2 + 12H_v(J+\tfrac{1}{2})^4.$$

The quantity $Q(J) + Q(J+1) - P(J+1) - R(J)$ gives the sum of the Λ-type splittings in the J'' and $J''+1$ levels. Therefore to a good approximation

$$Q(J) + Q(J+1) - P(J+1) - R(J) = 2q_v(J+1)^2$$

whence q_v is determined. For small values of J'' in the $v'' = 0$ level of NH, values of $\Delta\nu_{cd}$ were taken from Shimauchi (1964). If it is assumed that $\Phi_c(J) = -\Phi_d(J)$, then $B_v'' = \frac{1}{2}(B_v^{c''} + B_v^{d''})$ and so on. In this case B_v'' was taken as $B_v^{c''} - \frac{1}{2}q_v$. The rotational constants are given in table 4, where the errors shown are the standard deviations, and the variation of B with v has been taken as

$$B_v = B_e - \alpha_e(v+\tfrac{1}{2}) + \gamma_e(v+\tfrac{1}{2})^2.$$

Table 4. Rotational constants in cm^{-1}

	NH		ND	
	c $^1\Pi$	d $^1\Sigma^+$	c $^1\Pi$	d $^1\Sigma^+$
B_0	14·155 ±0·001	14·0918 ±0·0006	7·6343 ±0·0006	7·5633 ±0·0003
B_1	12·866 ±0·002	13·458 ±0·003	7·1628 ±0·0006	7·3178 ±0·0004
B_2			6·610 ±0·003	7·090 ±0·006
10^4D_0	21·9 ±0·3	16·66 ±0·04	6·18 ±0·03	4·75 ±0·01
10^4D_1	27·1 ±0·4	16·1 ±0·2	6·75 ±0·03	4·73 ±0·02
10^4D_2			9·52 ±0·09	5·3 ±0·4
10^8H_0	−30 ±2	11·1 ±0·7	−3·18 ±0·23	1·73 ±0·08
10^8H_1	−111 ±13		−10·58 ±0·31	2·28 ±0·20
10^3q_0	15·4 ±0·1		4·42 ±0·03	
10^3q_1	17·7 ±0·1		4·80 ±0·04	
10^3q_2			5·1 ±0·4	
B_e	14·800 ±0·002	14·409 ±0·002	7·841 ±0·002	7·693 ±0·003
$10\alpha_e$	12·89 ±0·02	6·34 ±0·03	3·93 ±0·03	2·63 ±0·06
$10^3\gamma_e$			−39 ±2	9 ±3
$B_0{}^c$	14·1627 ±0·0011		7·6365 ±0·0006	
$B_0{}^d$	14·146 ±0·003		7·6331 ±0·0012	
$B_1{}^c$	12·875 ±0·002		7·1652 ±0·0006	
$B_1{}^d$	12·866 ±0·005		7·1608 ±0·0008	
$B_2{}^c$			6·613 ±0·003	
$B_2{}^d$			6·602 ±0·002	
$10^4D_0{}^c$	22·00 ±0·08		6·17 ±0·02	
$10^4D_0{}^d$	21·9 ±0·6		6·19 ±0·05	
$10^4D_1{}^c$	26·5 ±0·3		6·75 ±0·03	
$10^4D_1{}^d$	27·6 ±0·7		6·74 ±0·04	
$10^4D_2{}^c$			9·66 ±0·12	
$10^4D_2{}^d$			9·38 ±0·12	
$10^8H_0{}^c$	−28·8 ±1·5		−3·25 ±0·18	
$10^8H_0{}^d$	−31 ±3		−3·12 ±0·42	
$10^8H_1{}^c$	−130 ±11		−10·44 ±0·35	
$10^8H_1{}^d$	−90 ±24		−10·72 ±0·51	

According to the simple theory of the isotope effect in diatomic molecules, the constants for ND will be related to those for NH by simple multiples of ρ^2, the ratio of the reduced masses of the isotopes. Writing the superscript i for ND,

$$\rho = (\mu/\mu^i)^{1/2} = 0{\cdot}730\,695.$$

A comparison of the experimental and theoretical ratios is given in table 5. D_0 and H_0

Table 5. Ratios of the rotational constants

Ratio	Experimental value		Theoretical value
	c $^1\Pi$ state	d $^1\Sigma^+$ state	
$B_e{}^i/B_e$	0·5298 ±0·0002	0·5339 ±0·0002	0·53392
$D_0{}^i/D_0$	0·282 ±0·004	0·2851 ±0·0009	0·28507
$H_0{}^i/H_0$	0·106 ±0·010	0·156 ±0·012	0·1522
$\alpha_e{}^i/\alpha_e$	0·305 ±0·002	0·415 ±0·002	0·3901

have been used as approximations to D_e and H_e in this instance. Dunham (1932) showed that the departure from the simple isotope effect is in the form of a power series in $B_e{}^2/\omega_e{}^2$. In this case $B_e{}^2/\omega_e{}^2(\mathrm{NH}) \sim 3\times10^{-5}$ and $B_e{}^2/\omega_e{}^2(\mathrm{ND}) \sim 2\times10^{-5}$. The accuracy of the measurements is not sufficient for the higher-order corrections to

be calculated. It is seen that for $B_e^{i\prime}/B_e'$, $D_0^{i\prime}/D_0'$, $H_0^{i\prime}/H_0'$ and $D_0^{i\prime\prime}/D_0''$ the experimental results are in good agreement with theory. For $\alpha_e^{i\prime}/\alpha_e'$, $\alpha_e^{i\prime\prime}/\alpha_e''$ and $B_e^{i\prime\prime}/B_e''$ it is instructive to calculate revised values (denoted by an asterisk) on the assumption that $\gamma_e' = \gamma_e^{i\prime}/\rho^4$ and that $\gamma_e'' = \gamma_e^{i\prime\prime}/\rho^4$. We then have $\gamma_e' = 0{\cdot}032$, $\alpha_e'^* = 0{\cdot}698$, $\gamma_e'' = -0{\cdot}137$, $\alpha_e''^* = 1{\cdot}015$ and $B_e''^* = 14{\cdot}697\ \mathrm{cm}^{-1}$. This gives $B_e^{i\prime\prime}/B_e''^* = 0{\cdot}5335$ and $\alpha_e^{i\prime\prime}/\alpha_e''^* = 0{\cdot}387$ in good agreement with the theory. $\alpha_e^{i\prime}/\alpha_e'^* = 0{\cdot}377$, which is a fair approximation, and even if B_e' is revised on the basis of γ_e' and $\alpha_e'^*$ the ratio $B_e^{i\prime}/B_e'^* = 0{\cdot}5330$ is still satisfactory. It is suggested that $B_e''^*$ and $\alpha_e''^*$ are more reliable than the corresponding values given in table 4. Because of the rapid variation of H_v'' with v, $H_0^{i\prime\prime}/H_0''$ is not a suitable approximation for $H_e^{i\prime\prime}/H_e''$.

3.3. *Vibrational constants*

Values for the origins of the bands were found by a least-squares fitting of $\mathrm{R}(J-1)+\mathrm{P}(J)$ and of $\mathrm{Q}(J)$ to polynomials in J^2 and $J(J+1)$, according to the relations

$$\mathrm{R}(J-1)+\mathrm{P}(J) = 2\nu_0+\{2(B_v'-B_v^{c\prime\prime})-2(D_v'-D_v^{c\prime\prime})\}J^2- \quad (1)$$

$$\mathrm{Q}(J) = \nu_0+(B_v'-B_v^{d\prime\prime})J(J+1)- \ . \quad (2)$$

For the (0, 0) band of NH only equation (1) could be used as the two heads of the Q branch were not resolved. The origins and vibrational constants are presented in table 6.

Table 6. Band origins and vibrational constants in cm^{-1}

	NH	ND
ν_{00}	$39512{\cdot}61 \pm 0{\cdot}02$	$39484{\cdot}32 \pm 0{\cdot}04$
ν_{11}	$39920{\cdot}09 \pm 0{\cdot}04$	$39740{\cdot}55 \pm 0{\cdot}02$
ν_{22}		$40116{\cdot}00 \pm 0{\cdot}10$
ν_e	$39400{\cdot}91 \pm 0{\cdot}09$	
ω_e'	2665 ± 9	1966 ± 7
$\omega_e'x_e'$	71 ± 8	44 ± 5
$\Delta G_{1/2}'$	2522 ± 4	$1877{\cdot}96 \pm 0{\cdot}07$

The vibrational structure of a diatomic molecule is given to a good approximation by

$$\nu_{v'v''} = \nu_e+\omega_e'(v'+\tfrac{1}{2})-\omega_e'x_e'(v'+\tfrac{1}{2})^2-\omega_e''(v''+\tfrac{1}{2})+\omega_e''x_e''(v''+\tfrac{1}{2})^2. \quad (3)$$

Using the superscript i for the constants of ND, we have measurements of ν_{00}^{i}, ν_{11}^{i} and ν_{22}^{i}. Substitution in (3) gives

$$\nu_e = 39\,400{\cdot}91 \pm 0{\cdot}09\ \mathrm{cm}^{-1}$$

$$\omega_e^{i\prime}-\omega_e^{i\prime\prime} = 137{\cdot}0 \pm 0{\cdot}1\ \mathrm{cm}^{-1}$$

$$\omega_e^{i\prime}x_e^{i\prime}-\omega_e^{i\prime\prime}x_e^{i\prime\prime} = -59{\cdot}61 \pm 0{\cdot}06\ \mathrm{cm}^{-1}.$$

In order to find values of $\omega_e^{i\prime}$ and $\omega_e^{i\prime}x_e^{i\prime}$, the vibrational constants of the lower state have been taken from Hanson *et al.* (1965). Their data are themselves based in part on the work of Nakamura and Shidei (1935). Substitution of the $B_e^{i\prime}$ and $D_0^{i\prime}$ values in Kratzer's approximate relation

$$\omega_e^2 = 4B_e^3/D_e \quad (4)$$

yields $\omega_e^{i\prime} \simeq 1958\ \mathrm{cm}^{-1}$ in good agreement with table 6. Further, if the appropriate constants are substituted in Birge's expression (Herzberg 1950, p. 109)

$$H_e = \frac{2D_e}{3\omega_e^2}(12B_e^2-\alpha_e\omega_e) \quad (5)$$

then $H_e \simeq 1{\cdot}6\times10^{-8}$ cm^{-1} compared with the $H_0{}^{i\prime}$ of $(1{\cdot}73\pm0{\cdot}08)\times10^{-8}$ cm^{-1}.

In the case of NH the values of ν_{00} and ν_{11} are again insufficient for an independent determination of the vibrational constants. Assuming that $\nu_e{}^{NH} = \nu_e{}^{ND}$ and substituting ν_{00} and ν_{11} in (3), we have

$$\omega_e{}' - \omega_e{}'' = 162{\cdot}0\pm0{\cdot}3 \text{ cm}^{-1}$$

$$\omega_e{}'x_e{}' - \omega_e{}''x_e{}'' = -122{\cdot}7\pm0{\cdot}7 \text{ cm}^{-1}.$$

The values $\omega_e{}'' = 2503\pm9$ cm^{-1} and $\omega_e{}''x_e{}'' = 194\pm8$ cm^{-1} (from Hanson *et al.*) were used in finding $\omega_e{}'$ and $\omega_e{}'x_e{}'$. Values of $\Delta G_{1/2}{}^{i\prime}$ and $\Delta G_{1/2}{}'$ were found from

$$\Delta G_{1/2}{}^{i\prime} = \nu_{11}{}^{i} - \nu_{00}{}^{i} + \Delta G_{1/2}{}^{i\prime\prime}$$

and

$$\Delta G_{1/2}{}' = \nu_{11} - \nu_{00} + \Delta G_{1/2}{}''$$

again using data from Hanson *et al.* Values for the ratios $(\omega_e{}^{i\prime} - \omega_e{}^{i\prime\prime})/(\omega_e{}' - \omega_e{}'')$ and $(\omega_e{}^{i\prime}x_e{}^{i\prime} - \omega_e{}^{i\prime\prime}x_e{}^{i\prime\prime})/(\omega_e{}'x_e{}' - \omega_e{}''x_e{}'')$ are 0·8457 and 0·4858, as compared with 0·7307(ρ) and 0·5339(ρ^2) on the simple isotope theory.

For the NH $d\,^1\Sigma^+$ state, equation (4) gives $\omega_e{}' \simeq 2680$ cm^{-1} and (5) gives $H_e{}' \simeq 1{\cdot}00\times10^{-7}$ cm^{-1}, both values agreeing well with experiment.

For the $c\,^1\Pi$ state Kratzer's relation gives $\omega_e{}^{i\prime\prime} \simeq 1766$ cm^{-1} and $\omega_e{}'' = 2433$ cm^{-1}, while Hanson *et al.* give 1829 ± 7 cm^{-1} and 2503 ± 9 cm^{-1} respectively. The discrepancy may be attributed to the substitution of $D_0{}''$ for $D_e{}''$ in (4).

For the same state (and using $\omega_e{}^{i\prime\prime} = 1829$ cm^{-1}, $\omega_e{}'' = 2503$ cm^{-1}) Birge's relation gives $H_e{}^{i\prime\prime} = 2{\cdot}34\times10^{-9}$ cm^{-1} and $H_e{}'' = 1{\cdot}20\times10^{-8}$ cm^{-1}. These values contrast sharply with the experimental ones for $H_0{}^{i\prime\prime}(-3{\cdot}18\times10^{-8}$ cm$^{-1})$ and $H_0{}''(-3\times10^{-7}$ cm$^{-1})$. However, if we assume that

$$H_v{}'' = H_e{}'' + \gamma_1(v+\tfrac{1}{2})$$

then the experimental values give $H_e{}^{i\prime\prime} = +(5\pm3)\times10^{-9}$ cm^{-1} and

$$H_e{}'' = +(10\pm7)\times10^{-8} \text{ cm}^{-1}$$

which are of the right order. This indicates why $H_0{}^{i\prime\prime}$ and $H_0{}''$ may not be substituted for $H_e{}^{i\prime\prime}$ and $H_e{}''$ in the rotational isotope effect.

Acknowledgments

I thank Dr. R. W. B. Pearse for his supervision and encouragement, Dr. R. C. M. Learner for helpful discussion and the Atomic Energy Research Establishment, Harwell, for providing the deuterium. The work was done during the tenure of a Research Studentship from the Science Research Council.

References

Clarke, F. J. P., and Garton, W. R. S., 1959, *J. Sci. Instrum.*, **36**, 403–9.
Dieke, G. H., and Blue, R. W., 1934, *Phys. Rev.*, **45**, 395–400.
Dunham, J. L., 1932, *Phys. Rev.*, **41**, 721–31.
Hanson, H., Kopp, I., Kronekvist, M., and Aslund, N., 1965, *Ark. Fys.*, **30**, 1–8.
Herzberg, G., 1950, *Spectra of Diatomic Molecules* (New York: Van Nostrand).
Hori, T., 1929, *Z. Phys.*, **59**, 91–101.
Lunt, R. W., Pearse, R. W. B., and Smith, E. C. W., 1936, *Proc. Roy. Soc.* A, **155**, 173–82.
Nakamura, G., and Shidei, T., 1935, *Jap. J. Phys.*, **10**, 5–10.
Pearse, R. W. B., 1933, *Proc. Roy. Soc.* A, **143**, 112–23.
Shimauchi, M., 1964, *Science of Light, Tokyo*, **13**, 53–63.

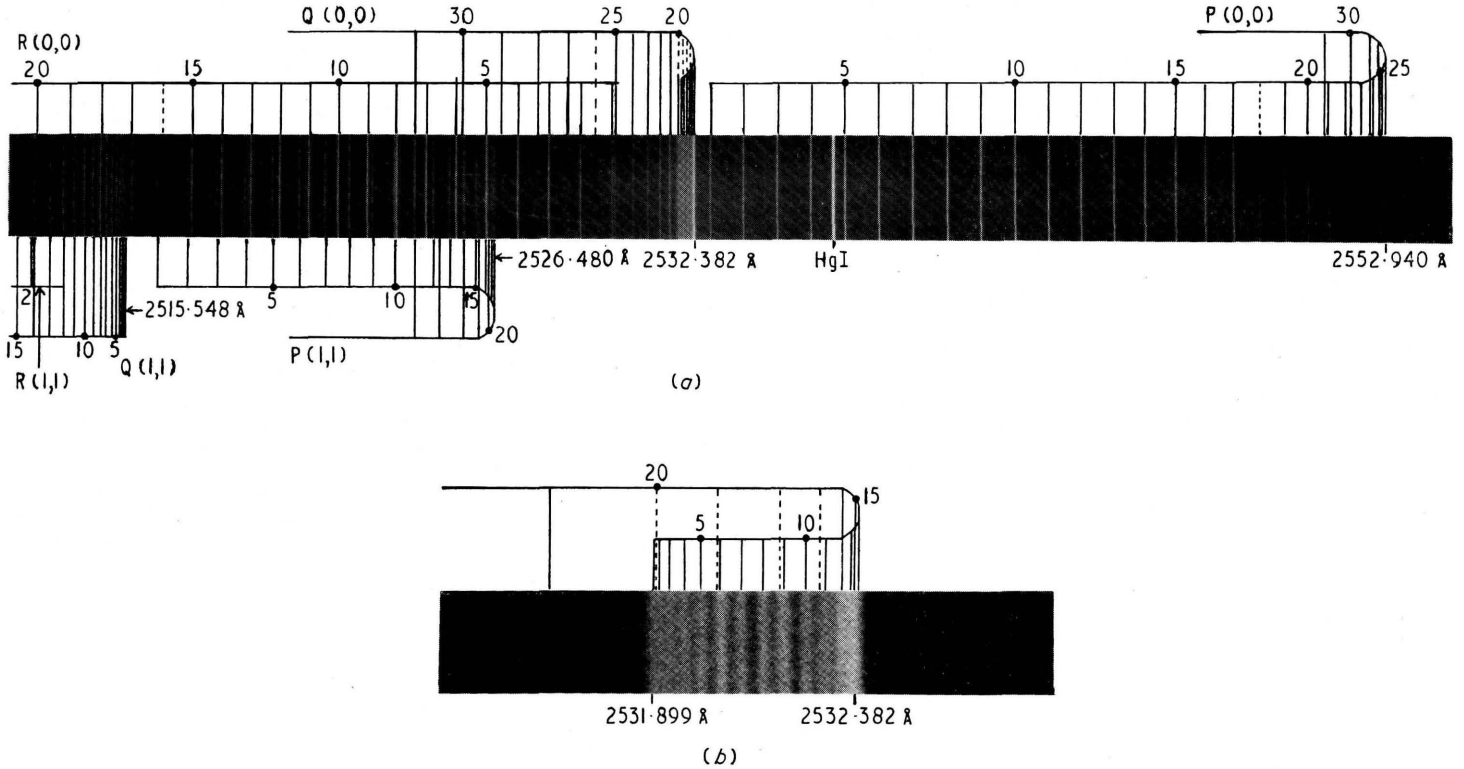

The d $^1\Sigma^+$–c $^1\Pi$ system of ND: (*a*) the heads of the (0, 0) and (1, 1) bands; (*b*) the two heads of the (0, 0) Q branch.